DISK-ADAPTIVE REDUNDANCY: tailoring data redundancy to disk-reliability heterogeneity in cluster storage systems

Saurabh Kadekodi

CMU-CS-20-142

December 2020

School of Computer Science
Carnegie Mellon University
Pittsburgh, PA 15213

Submitted in partial fulfillment of the requirements for the degree of Doctor of Philosophy.

This research was sponsored by the National Science Foundation under grant number CNS-1956271, the Department of Energy under grant number DESC0015234, the Department of Energy/National Nuclear Security Administration under grant number DE-AC52-06NA25396, Google, and Intel.

Keywords: reliability, durability, fault-tolerance, redundancy, distributed storage systems, cluster storage systems, disks, HDD, erasure code, replication, heterogeneity

To all those who think that they aren’t good enough.

Abstract

Large-scale cluster storage systems contain hundreds-of-thousands of hard disk drives in their primary storage tier. Since the clusters are not built all at once, there is significant heterogeneity among the disks in terms of their capacity, make/model, firmware, etc. Redundancy settings for data reliability are generally configured in a "one-scheme-fits-all" manner assuming that this heterogeneous disk population has homogeneous reliability characteristics. In reality we observe that different disk groups fail differently, causing clusters to have significantly high disk-reliability heterogeneity. This dissertation paves the way for exploiting disk reliability heterogeneity to tailor redundancy settings to different disk groups for cost-effective, and arguably safer redundancy in large-scale cluster storage systems.

Our first contribution is an in-depth data-driven analysis of disk reliability of over 5.3 million disks across over 60 makes/models in three large production environments (Google, NetApp and Backblaze). We observe that the strongest disks can be over an order of magnitude more reliable than the weakest disks in the same storage cluster. This makes today's static redundancy schemes selection either insufficient, or wasteful, or both. We identify and quantify the opportunity of achieving lower storage cost along with increased data protection by means of disk-adaptive redundancy.

Our next contribution is designing the heterogeneity-aware redundancy tuner (HeART), an online tuning tool that guides selection of different redundancy settings for long-term data reliability, based on observed reliability properties of each disk group. By processing disk failure data over time, HeART identifies the boundaries and steady-state failure rate for each deployed disk group by make/model. Using this information, HeART suggests the most space-efficient redundancy option allowed that will achieve the specified target data reliability. HeART is evaluated using longitudinal disk failure logs from a large production cluster with over 100K disks. Guided by HeART, the cluster could meet target data reliability levels with much fewer disks than one-scheme-for-all approaches: 11–16% fewer compared to erasure codes like 10-of-14 or 6-of-9 and up to 33% fewer compared to 3-way replication.

While HeART promises substantial space-savings, it is rendered unusable in production settings of real-world clusters, because the IO load of transitions between redundancy schemes overwhelms the storage infrastructure (termed *transition overload*). Analysis on Google's cluster traces shows transition overload consuming 100% of the cluster IO bandwidth for weeks together, making transition overload a show-stopper for practical disk-adaptive redundancy. Building on the insights drawn from our data-driven analysis, Pacemaker is the next contribution of this dissertation; a low-overhead disk-adaptive redundancy orchestrator that realizes HeART's dream in practice. Pacemaker mitigates transition overload by (1) proactively organizing data layouts to make future transitions efficient, (2) initiating transitions proactively in a manner that avoids urgency while not compromising on space-savings, and (3) designing more IO efficient redundancy transitioning mechanisms. Evaluation of Pacemaker with traces from four large (110K–450K disks) production clusters (three from Google and one from Backblaze) shows that the transition IO requirement decreases to never needing more than 5% cluster IO bandwidth (only 0.2–0.4% on average). Pacemaker achieves this while providing overall space-savings of 14–20% (compared to using a static 6-of-9 scheme) and never leaving data under-protected.

The final contribution of this dissertation is the design and implementation of disk-adaptive redundancy techniques from Pacemaker in the widely used Hadoop Distributed File System (HDFS). This prototype re-purposes HDFS's existing architectural components for disk-adaptive redundancy, and successfully leverages the robustness and maturity of the existing code. Moreover, the components that are re-purposed are fundamental to any distributed storage system's architecture, and thus, this prototype also serves as a guideline for future systems that wish to support disk-adaptive redundancy.

Acknowledgments

My time at CMU has been highly rewarding primarily because of my advisors. I have been extremely lucky to have had three fantastic advisors – Prof. Garth Gibson, Prof. Greg Ganger and Prof. Rashmi Vinayak. Throughout these years I was constantly amazed at their ability to convert my ordinary observations and confused conversations into crisp and precise questions which eventually led to the right answers. I spent my first three years learning the ropes of research under Garth's capable (and exciting) tutelage. I was apprehensive and anxious about switching to a new advisor in my fourth year, but to Greg's credit he put me at ease right away. Rashmi's addition as my co-advisor only strengthened our team. The highlights of my Ph.D. are definitely the high-energy and intellectually stimulating meetings that I had with my advisors each week. From Garth's confidence in my research abilities, to Greg's thoughtful and compassionate mentorship, and finally Rashmi's perfectionist attitude have left a lasting impression on me. A large part of the researcher, mentor and student that I am, and will be, is because of them. I sincerely thank them for their time, encouragement, effort and support throughout my Ph.D.

Many thanks to my industry collaborators and mentors – Larry Greenfield, Arif Merchant and Keith Smith who have been extremely influential in letting me work at their organizations and trusting me with analyzing their data. Much of this thesis would not have materialized without their curiosity, support, and curiosity. Special thanks to my committee member Prof. Remzi-Arpaci Dusseau for always encouraging me and providing me with a much-needed listening ear and invaluable advice, be it at hallway conversations during conferences or during causal university visits.

I would like to thank my amazing peers at the Parallel Data Lab and TheSys Lab. Special thanks to Francisco Maturana who has been a wonderful collaborator. His mathematical and analytical expertise has been crucial in the successful publications that have come from this research. I would also like to thank Juncheng Yang, Chirag Nagpal and Suhas Jayaram for their support and contribution to this research. The wonderful company of Rajat Kateja made my working hours much more enjoyable. In addition to my wonderful peers and collaborators, I also would like to thank the MS and MCDS students whom I have had the privilege of mentoring throughout my Ph.D., and from whom I have learnt a lot.

Special thanks are due to the PDL staff. Chad Dougherty, Jason Boles, Mitch Fraznos and Chuck Cranor have been available at any time of the day or night to ensure that I am not blocked by technical issues or equipment unavailability. I also want to thank Karen Lindenfelser and Joan Digney who have organized PDL events flawlessly, and have helped numerous students, including me, in interfacing with the right people. They also serve as a reminder that good people make a good organization, and not just domain experts. The same compliment is deserved by the amazing staff of the Computer Science Department. They have been protectors and champions of us Ph.D. students, especially Deb Cavlovich.

My non-academic CMU family comprises of my friends from Indian Graduate Student Association, especially the "Peace Band" who kept me sane through the ups-and-downs of Ph.D. life. I would like to thank Choitali, Archu, Ajay, Deepanjana, Ishani, Prithvi, Satwik, Hridya, Sudharshan, Tushar, Dipan, Arnab, Abhishikta, Dhivya, Abhilasha, Shounak, Nikita, Oguz, Tejas, Harsha, Alina, Shruti, Priya, Avani and Aditya for fueling my life with music, theater, debates, and most of all, lovely companionship.

I am indebted to Siddharth Singh and Purvasha Chakravarti who have provided me with unconditional love, affection, discussions and food. They have boosted my confidence at every step of the way, for which I am extremely grateful. In the same spirit I wish to thank Vaishnavh Nagarajan who has been a pillar of support through my lowest phases. Vaishnavh's maturity as a person, and as a researcher is something I can only hope to achieve. I would like to thank Arushi Vyas for brightening my days with her enthusiasm and optimism, and bringing out the dancer in me through Zumba. Special appreciation for Abhishek for providing excellent coffee and laughing loudest at my jokes; Anuva for her caring company, amazing food and Marathi banter; for Devdutta and Annesha who have never said no to accompanying me on my whimsical travels. I will cherish the time I was housemates with Harshad Shirwadkar, who has been providing the perfect combination of musical and technical company for over 15 years. In similar ways, I cannot forget the inspiring Indian classical music sessions that I had with Rithisha Padmanabh and Devansh Zurale.

Apart from CMU there has been a network of friends in US and in India who have directly, or indirectly played an important role in helping me achieve this milestone. I would like to thank my friends from PICT - Aditya, Bhagyashree, Piyush, Shardul, Mihir, Sonia, Rishi, Pramod, Shubhangi, Ketaki, Chirayu, Pranay, Ameya, Sanat, Sayali, Prashant, Anuj, Mugdha, Shrikanth, Neha Mundada, Pavneet, Pranali, Harshad Keskar, Neha Mande, Parag and Shivambika for all that you have taught me through numerous fun-filled conversations and activities. I want to specially thank Sanyogita Ranade, Manan Dedhia and Atreyee Maiti who have been the strongest supporters that anyone can ask for. I have benefited tremendously from Sanyogita's unwavering support and unconditional love. During my collaboration with NetApp ATG in Boston, Sanyogita and Manan graciously hosted me for over a month. A sincere thank you for making my experience in Boston a memorable one. I cannot forget the encouragement of Sumit Malani. He has been a pillar of strength through various ups-and-downs and his unshakeable belief in me drives me to do better with every opportunity.

While I had a support system that took care of me during my Ph.D., I cannot discount the contribution of so many of my previous mentors and well-wishers who have made it possible for me to undertake this journey. Special thanks to Prof. Sunil Shende, who went out of his way to educate a bunch of naive students, both in mathematics and in navigating graduate studies. Prof. Peter Dinda from Northwestern also devoted a lot of time and effort during my Masters, and encouraged me to pursue a Ph.D. Before my Masters I was employed at Soft Corner.

Being there definitely boosted my confidence and the familial culture at Soft Corner is one that I will always cherish and try to reproduce at every organization that I am a part of. At Soft Corner I would particularly like to mention Shrikanth Narayanan, Sanyogita Ranade, Ravi Damle, Vaiju Damle, Sanjeev Dharap, and my parents Arun and Meenal for always encouraging me to take on challenges and venture on unexplored paths. Ability of a company to take risks, and building for the sake of learning are my two most important takeaways from Soft Corner.

Among my extended family - Anjali Nerlekar (Anjali aatya), my aunt, is the first person I am very close to, who had done a Ph.D. Her personal and professional pursuits have been inspiring in so many ways, and I am certain they will continue to do so in the future. She and her family Shashank, Mukul and Aseem have been a solid support system throughout my graduate studies. In a similar way, I have got unwavering support to pursue my dreams from my extended family - Sonal maasi, Ameeta maasi, Atul maasa, Vinay kaka, Nikhil, Juhi, Saloni, Neha, Kedar, Motimummy and Dadidada. I would also like to thank Deepa, Siddharth, Megha, Andrew, Aditi, Rajnikant uncle and Jyoti aunty for adding fun, joy and discussions to my life.

I am at a loss for words of how to thank my closest companion and my academic partner-in-crime Shweta Jain. You shook me out of my comfort zone and put me on the path of academic exploration. Your contribution to my success is absolutely fundamental. Despite the distance, the arguments, the crying, if I had to choose anyone to go on an academic journey with, it will always be you.

Finally, at the core of my complex and long support system is my family - Arun, Meenal and Rohan. My parents, Arun and Meenal have been unimaginably supportive throughout this arduous journey. They made sure that my energy and focus was devoted to my Ph.D. Being computer professionals, it is my goodfortune (and probably their misfortune) that I can discuss my research with them. My work ethic is a direct consequence of having observed them over the years. My brother Rohan has been the strongest source of stability throughout my Ph.D. From entertaining research discussions, to discussing personal problems, to now becoming my academic collaborator Rohan's presence has always been instrumental, but more so during my Ph.D.

A heart-felt thank you to everyone that I have mentioned (which is by no means a complete list). You have played a pivotal role in my Ph.D. adventure, and I wish that such a wonderful support system was available to everyone. To all my well-wishers, I will not let you down, and I hope to support you as you have supported me.

Contents

List of Figures

List of Tables

Chapter 1

Introduction

Cluster storage systems (distributed storage systems within large data centers) are primary components of cloud, Internet service, and data analytics infrastructures. With the explosion of machine learning and rapid rise in big data analytics, data science, edge computing and real-time systems, these cluster storage systems are continuously pressured for storage space. For architects of such large-scale storage systems, a petabyte (PB) of free space translates to a critically low free-space warning. In fact, analysts estimate that 175 zettabytes (1 ZB = 1024 PB) of data will be generated annually by 2025, most of which will be stored in data centers [91]. These astronomical capacity requirements are fueled by an exponential rate-of-growth of data. A 2016 study shows data in YouTube growing exponentially year-over-year from 2006 through 2016 [18]. A 2020 study echoes the incredibly high data ingest rate observation by describing the ingest rate in Google Photos. Over 28 billion photos and videos are uploaded each week, which translates to approximately 50000 photos and videos uploaded every second [13]. Although new data and hot/warm data is now often stored on Flash SSDs, cost considerations will lead to the majority of data continuing to be stored on mechanical disks (HDDs) for the foreseeable future [17, 18, 91].

In order to keep up with data growth, modern storage architectures often scale to huge capacities by combining up to hundreds of thousands of storage devices into a single storage system [34, 96, 110]. At such scales, device failures are common, and yet, data has to remain reliable despite these failures. Data redundancy is the most common method to protect against data loss in the face of failures [31, 34, 46, 77, 96]. While replication is often used to improve performance for hot data, erasure coding has become the norm for cost-effectively storing most data [29, 33, 46].

A primary goal when selecting a data redundancy scheme (e.g., 3-way replication vs 2-way replication, or a wider erasure code vs. a narrower erasure code) is ensuring that it satisfies the data reliability goal. Well-established and often-used equations [72, 103] exist for computing the expected reliability for a redundancy scheme. The most commonly used reliability metric is mean-time-to-data-loss (MTTDL) which is a function of the per-device annualized failure rate (AFR; the commonly used alternative for mean-time-to-failure (MTTF)[1]), the number of devices, and the mean-time-to-repair (MTTR). Redundancy settings are generally chosen as if

[1]AFR is the expected number of device failures in a typical year. AFR is a rate quantity, inversely proportional to MTTF.

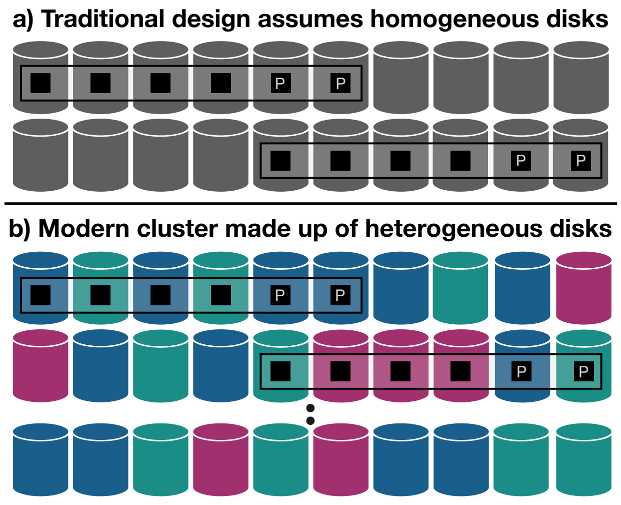
a) Traditional design assumes homogeneous disks
P
P
P
P
b) Modern cluster made up of heterogeneous disks
P
P
P
P
Figure 1.1: Subfigure (a) illustrates the assumption all disks fail similarly. Two 4-of-6 stripes are shown. Subfigure (b) shows the make-up of a modern storage cluster. Each color represents a make/model with a distinct AFR, so the two 4-of-6 stripes may have very different reliability.

all of the devices have the same AFR. This largely holds true for RAID arrays (tens of disks), or even sizable NFS/CIFS file servers, or smaller cluster storage systems (hundreds of disks), which often contain a uniform set of disks deployed all-at-once and removed before wearout. Under this setting all data (see Fig. 1.1a) experiences the same level of data reliability.

Unfortunately, the same reliability math doesn't hold for modern large-scale storage systems because all devices don't have the same AFR. With 100K+ disks deployed over time and per-acquisition optimization of which disks to buy (e.g., lowest-cost-per-byte at each acquisition time), there is a lot of heterogeneity. That is, the constituent devices in such systems are of multiple makes/models and multiple device ages, and AFR values vary as a function of both attributes [48, 56, 73] as is detailed in Chapters 3 and 4. This leads to different MTTDLs which means different levels of reliability.

The MTTDL equations can still be used to guide decisions, as long as a sufficiently high AFR value is used. For example, if the highest AFR value possible for any deployed make/model at any age allowed (before decommissioning) is used, the computed MTTDL will be a lower bound. Unfortunately, the range of possible AFR values in a deployed system is quite large [48, 56, 73, 88] as shown in Chapter 4. For example, in our analysis, as shown in Fig. 4.1, we observe the range to be over an order of magnitude in NetApp, Google and Backblaze logs from double-digit AFRs to low single digit AFRs. Since the overall average is much closer to the lower end of the AFR range, the highest value is a very conservative over-estimate for most of the devices. The resulting MTTDLs are thus loose lower bounds, leading decision-makers to use excessive redundancy.

Nonetheless, we are told by storage administrators of large-scale cluster storage systems that such approaches, and other ad hoc conservative over-protection, are the norm. Such approaches are problematic in two significant ways. First, they result in much higher cost overheads (in the form of more disks with the associated dollar, environmental consequences)

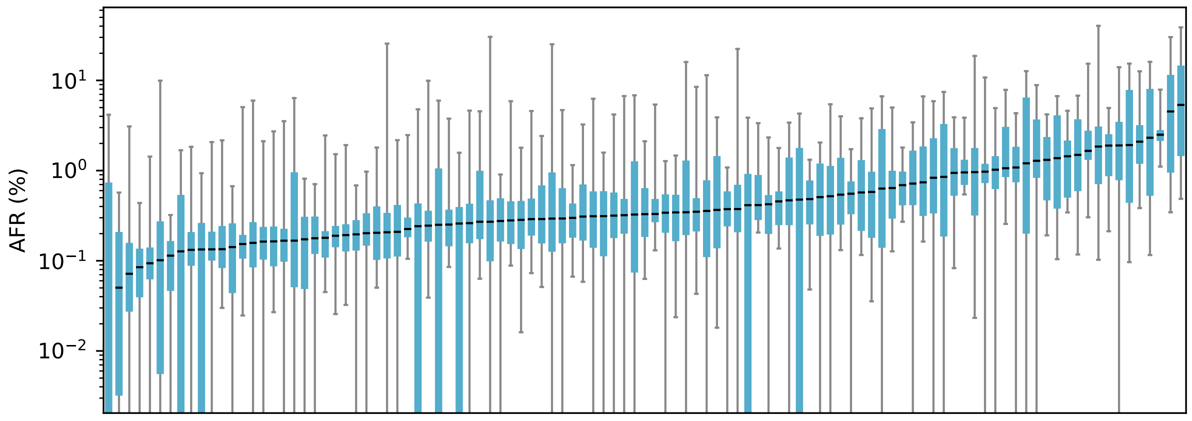

Figure 1.2: AFR heterogeneity observed in over 60 makes/models with a total disk population of over 5.3 million HDDs deployed across Google, NetApp and Backblaze.

than might otherwise be necessary. Second, and more insidious, they are still risky, because it is unclear (until too late) how conservative one needs to be. For example, suppose that the redundancy scheme shown in Fig. 1.1b is designed using the AFR of green disks. Suppose the AFR of purple disks is higher than the green disks, and the AFR of the blue disks is lower than the green disks. Then, the data in the top stripe is over-protected, whereas simultaneously, the data in the bottom stripe is under-protected and at a higher risk of data loss compared to the top stripe despite having the same redundancy scheme.

1.1 Goals

The overarching goal of this thesis is to enable highly-reliable cluster storage system that handles the varying AFRs of different underlying devices, without excessive redundancy or hidden risk of under-protecting data. The system must fulfill the following goals:

- **Always meet data reliability target**: ensure that the redundancy scheme used for data continuously meets the data reliability target irrespective of which subset of disks the data is stored on.
- **Minimize overhead**: keep the IO work associated with adaptive redundancy management from interfering with foreground IO.
- **Maximize space efficiency**: avoid wasting space result from over-protecting data relative to target MTTDL and the specific disk AFRs.

1.2 Contributions

This dissertation makes five primary contributions. The first contribution is to identify the opportunity of performing disk-adaptive redundancy by analyzing the disk-reliability heterogeneity observed in cluster storage systems across disks of different makes/models.

The second contribution is making the case for disk-adaptive redundancy by tailoring data redundancy to the observed disk-reliability heterogeneity. Along with the required analysis, we also evaluate our approach to disk-adaptive redundancy in a data-driven manner by architecting the **Heterogeneity-Aware Redundancy Tuner (HeART)**. HeART is a disk-adaptive redundancy system that replaces ad hoc "one-size-fits-all-devices" approaches to choosing redundancy parameters by dynamically selecting them on the basis of continuously monitoring underlying disk AFR behavior. HeART's online algorithms are based on the disk reliability analysis of a production storage cluster with over 100K disks. HeART could achieve target data reliability levels with fewer disks than traditional approaches: 11–16% fewer compared to erasure codes like 10-of-14 or 6-of-9 and 33% fewer compared to 3-way replication. The design of HeART and associated analyses are described in Chapter 3.

The third contribution is an **in-depth reliability analysis** of over 5 million disks belonging to over 60 makes/models across several clusters belonging to Google, NetApp and Backblaze. This analysis reconfirms the highly varying AFRs across different disk makes/models. In addition we also highlight several important characteristics that directly affect the design of disk-adaptive redundancy systems. Some of the insights were previously unknown, whereas others redefine existing insights to provide a modern, and more comprehensive understanding of disk reliability in modern large-scale storage clusters. The datasets and insights are described in detail in Chapter 4.

While HeART promised substantial space-savings, it is rendered unusable in production settings of real-world clusters, because the IO load of transitions between redundancy schemes overwhelms the storage infrastructure (termed *transition overload*). The fourth contribution is the design of **Pacemaker: a low-overhead disk-adaptive redundancy orchestrator that overcomes transition overload** by (1) proactively organizing data layouts to make future transitions efficient, (2) initiating transitions proactively in a manner that avoids urgency while not compromising on space-savings, and (3) employing innovative IO-friendly transitioning mechanisms to reduce transition IO. Evaluation of Pacemaker with traces from four large (110K–450K disks) production clusters show that the transition IO requirement decreases to never needing more than 5% cluster IO bandwidth (only 0.2–0.4% on average). Pacemaker achieves this while providing overall space-savings of 14–20% and never leaving data underprotected. Chapter 5 describes Pacemaker in detail.

The fifth and final contribution is the **design and implementation of disk-adaptive redundancy in** the popular **Hadoop Distributed File System (HDFS)**. This implementation exercise is meant to show how an existing distributed storage system can be tweaked to support disk-adaptive redundancy. This design re-purposes existing machinery in order to carry out efficient redundancy transitions as outlined in Pacemaker. The re-purposed components are fundamental to any distributed storage system's architecture, and thus, this prototype also serves as a guideline for other systems to support disk-adaptive redundancy. The details of our design are presented in Chapter 6.

We start the rest of the dissertation with Chapter 2 giving the required background and motivating disk-adaptive redundancy. The rest of the dissertation describes the above mentioned contributions in detail.

Chapter 2

Background and motivation

2.1 Overview of cluster storage systems

Large-scale distributed storage systems such as the Google File System [34], Colossus, Amazon S3 [2], Microsoft Azure [19], etc. are composed of multiple cluster storage systems (also called storage clusters). Each cluster is typically divided into multiple storage tiers, each with a distinct purpose, such as the caching tier (also known as the hot tier for short-lived or high-performance data), the primary storage tier (also known as the warm tier where the bulk of the data that is actively in use and has moderate churn resides), the archival tier (also known as the cold tier meant for backups), etc. Large-scale storage clusters can have anywhere between tens to hundreds of thousands of storage devices in their primary storage tier. Furthermore, most clusters in today's large-scale distributed systems are designed in a disaggregated manner, wherein the space on all the storage devices in the same tier is exposed as a single, large addressable storage pool [52]. Data stored in such clusters is stored across a number of storage devices. In most such clusters, clients access any given device directly (via a storage network) or indirectly (via whichever networked storage-node it is attached to) after contacting a logically-separate metadata service that maintains data location and other information While details vary, this basic architecture enables large and time-varying numbers of devices to be used effectively.

2.1.1 Hard disk drives are the primary storage devices

Owing to the economical price-point calculated in terms of dollars-per-terabyte ($/TB), the primary storage tier of most of the large-scale storage clusters today is made up of hard disk drives (HDDs). Throughout this dissertation, any reference to a storage device or a disk implies a reference to a HDD. The storage capacity (space) of commonly used disks ranges from anywhere between 4TB–14TB. The price dynamics are unlikely to change drastically in the foreseeable future, ensuring that the bulk of the bytes in large-scale distributed systems and cloud computing platforms will continue to be stored on HDDs [17, 18].

2.1.2 Disk failures are common

In large-scale storage clusters disk failures happen all the time [34, 85]. In fact, modern distributed storage systems are designed for failures, which means that they treat failures as the norm, and not an exception from the norm [34, 71, 96]. Storage devices exhibit two kinds of failures: *partial failures* and *fail-stops* (complete failures). Partial failures might involve a particular read or write failing because of a sector error or checksum failure. The disk as a whole is still functional, and usually it remaps failed sectors to spare locations in order to continue operation. In the case of fail-stop, the disk stops functioning altogether. This dissertation focuses on data redundancy optimizations for fail-stop failures where all the data from a disk is permanently lost when the disk fails.

2.2 Data reliability is achieved using data redundancy

Data redundancy is the most common approach to protect against permanent data loss amongst continuous disk failures [10, 34, 46, 73, 77, 78, 84]. There are two common ways of performing data redundancy.

2.2.1 Replication

Replication involves creating exact copies of the data on different disks as backup. Usually, data is either duplicated (2-way replicated) or triplicated (3-way replicated). Replication not only makes the data more durable, but also improves its availability since the redundant copies of the data can be used to service reads in parallel.

The degraded mode read algorithm (i.e. the algorithm followed in case one of the disks on which data is stored fails) for replication is very straightforward. The other copies of data are referenced until the lost copy is replenished. There is a background process that continuously monitors if data is under-redundant, and replenishes lost copies using the healthy copies of data that are stored on other disks.

For hot data with certain access patterns, replication may be viewed as the right option for performance, with the replication factor chosen to provide sufficient reliability. But, of course, the cost consequence is a doubling or tripling of the number of disks needed. This makes replication infeasible for majority of the data in modern storage clusters.

2.2.2 Erasure coding

Erasure code is a more space-efficient redundancy mechanism compared to replication. For erasure coding a file, it is first broken into identically sized chunks of data where each chunk is at most a few MBs. Every k chunks of data are then combined with $n-k$ identically sized parity chunks to form an n chunk *stripe*. For the popularly used maximum distance separable (MDS) codes, any k chunks can be used to recover any of the n chunks. In this dissertation we use the notation k-of-n scheme to indicate an erasure code with k data chunks and $n-k$ parity chunks per stripe. k and n are also known as the "dimension" and the "length" of the erasure code. Erasure codes can also be denoted using the (n, k) notation. Both these notations follow the standard notation employed in the coding theory literature. Replication can also be denoted using this notation. For example, 3-replication can be denoted as a 1-of-3 erasure code. Although the description of the notation applies only to "systematic" codes, and most of the erasure codes employed in storage systems are indeed systematic. We will use the k-of-n notation in this dissertation.

The degraded mode read algorithm for erasure coding is more costly and complex compared to that of replication. When a read is requested to a chunk that is missing because the disk on which it was stored has failed, it triggers a process called data reconstruction. Data reconstruction for MDS codes) involves reading any k of the remaining chunks from the stripe that the missing chunk belongs to, after which the missing data is reconstructed using the combination of parity and data chunks that are read. The reconstructed data is then provided to the requesting client. Similar to replication, there is a background monitor process that keeps checking for under-redundant data and issues reconstructions proactively without being triggered by client reads.

It is increasingly common, in large-scale systems, to use erasure-coding (with $k > 1$) for bulk and colder data. With erasure-coding, space efficiency ($\frac{n}{k}$) for tolerating a given number of failures is better. But, additional considerations arise regarding the amount of work involved in recovering from a device failure—since k remaining chunks must be read to reconstruct each lost chunk, too high a k will result in more work than desired and, potentially, full recovery time that is too long. Schemes like 6-of-9 and 10-of-14 have been reported for real deployments [29, 30, 31, 77, 78, 84], and Backblaze reports use of 17-of-20 [11].

2.2.3 Metrics of data reliability

Annualized failure rate (AFR)

Annualized failure rate (AFR) is the standard metric used to describe a disk's fail-stop rate [24]. As the name suggests, it is the expected percentage of disks that will fail-stop in a given year from a population of disks. We calculate AFR using the following formula:

$$AFR\ (\%) = \frac{f_d}{n_1 + n_2 + \ldots + n_d} \times 365 \times 100 \tag{2.1}$$

where f_d is the number of disks failed in d days (a sliding window of typically 30 to 60 days; used to eliminate the jitter observed in instantaneous failure rates) and n_i is the number of disks operational during day i. Next, we will show how the AFR is used in the reliability calculation of a redundancy scheme.

Mean time to data loss (MTTDL)

The standard metric used for reliability of data is *mean time to data loss* (MTTDL). MTTDL is calculated based on two rates – *mean time to failure* (MTTF) and *mean time to repair* (MTTR) [72, 103]. MTTF is a function of the disk's AFR, while the MTTR is the time it takes to reconstruct the lost data from the failed disk. In a large-scale cluster storage system,

$$\begin{tikzcd}
\mathbf{0} \arrow[r, bend left, "n\lambda"] & \mathbf{1} \arrow[l, bend left, "\mu"] \arrow[r, bend left, "(n-1)\lambda"] & \cdots \arrow[l, bend left, "\mu"] \arrow[r, bend left, "(n-k-1)\lambda"] & \textbf{n-k} \arrow[l, bend left, "\mu"] \arrow[r, bend left, "(n-k)\lambda"] & \mathbf{DL}
\end{tikzcd}$$

Figure 2.1: Continuous-time Markov chain used to calculate the MTTDL of a k-of-n erasure coded stripe.

multiple copies of the data exist, that too on distinct disks. Thus, the effort of reconstructing the lost data of a failed disk is shared by numerous disks, which can be so efficient that the time it takes to detect and take action upon a failed disk (approximately 15 minutes [31, 77, 78]) dominates the time taken to reconstruct all of its data [31]. This decouples the MTTR of the disk from its storage capacity. Thus, in large cluster storage systems, the data reliability is only a function of the disk's MTTF (which is a function of its AFR).

When using erasure coding for fault tolerance, MTTDL is calculated at a stripe granularity. A stripe is a set of fixed sized chunks that include both data and parity chunks as explained in Section 2.2.2. Figure 2.1 shows the continuous-time Markov chain that is typically used for calculating the MTTDL of a k-of-n stripe. Each state in the Markov chain represents number of failed chunks in the stripe, starting with **0** and ending with **DL** to denote permanent data loss. Each chunk of a stripe is stored on a separate disk, and for the purpose of calculating the MTTDL, all disks are assumed to fail independent of each other. This simplifies the MTTDL calculation since we can assume that disk failures and repairs are distributed exponentially (in this case with a failure rate of λ). Each arrow to the right indicates failure rate, i.e. $\frac{1}{MTTF}$ whereas each arrow to the left indicates repair rate, i.e. $\frac{1}{MTTR}$. The time to reach from state **0** to state **DL** is the MTTDL, and is usually denoted in tens-of-thousands to millions of hours.

2.3 Characterizing disk reliability over lifetime: the disk bathtub curve

Disk reliability varies over its lifetime as shown in Figure 2.2. When the disk is in its infancy, it suffers from ***infant mortality***. Infant mortality is also referred to as "burn-in" failure rate, and is an increased failure rate usually triggered due to new environment, workload pattern, etc. Eventually the disk AFR plateaus into a low, stable failure rate regime. This regime is called ***useful life***. Infancy lasts 3–5 months whereas useful life lasts 3–4 years. Once the disk is heavily used for approximately 4 years, it suffers from another phase of high AFR similar to infancy. This phase of life is called ***wearout***. When a disk is old enough to be considered to be in its wearout phase, it is usually decommissioned before it fails. This way the data on the disk can be copied over to other disks rather than performing the IO and time-intensive data reconstruction once the disk fails. Moreover, during reconstruction the data is vulnerable to being permanently lost if many such disks fail together. Chapters 3 and 5 contains various AFR curves from the different disk makes/models that we have analyzed to facilitate disk-adaptive redundancy.

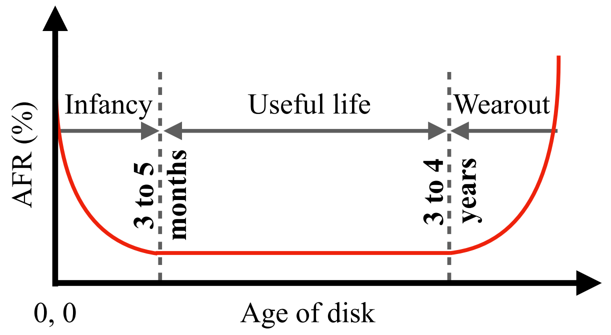

Figure 2.2: The disk hazard curve (also known as the bathtub curve) showing disk reliability over its lifetime.

2.4 Scheme selection problem for scalable storage

Generally, administrators determine the redundancy scheme to be used based on several factors, including cost, performance, and data reliability. For long-term storage, protecting data from loss is a critical constraint. Given the MTTDL and per-make/model AFR and MTTR, the subset of redundancy scheme options that would achieve a target MTTDL can be identified; the final selection can be based on the other considerations. Unfortunately, this simple-sounding approach doesn't work well for large-scale systems. Specifically, the MTTDL equations rely on devices all conforming to the same stationary AFR value and the administrator knowing that value; neither of which are true. Although it may be tempting to use AFR values taken from manufacturer's specifications, studies have shown that failures rates observed in practice often do not match those [85]. More importantly, AFR values vary significantly between makes/models as we will see in Chapters 3–5, and for devices of different ages as described in Section 2.3. Given these two dimensions of AFR heterogeneity, using a single redundancy scheme for all disks, and throughout each disk's life is often wasteful, but can also be dangerous. In order to improve data safety and cost-effectiveness a cluster storage system needs to rethink its "one-scheme-fits-all" redundancy mechanism and employ a more sophisticated approach that takes into account the aforementioned dimensions of AFR hetereogeneity.

Chapter 3

A case for disk-adaptive redundancy

Large cluster storage systems almost always include a heterogeneous mix of storage devices, even when using devices that are all of the same type (e.g., Flash SSDs or mechanical HDDs). Commonly, this heterogeneity arises from incremental deployment combined with per-acquisition optimization of which make/model to acquire (such as targeting the lowest $/TB option available at the time, or requiring the largest capacity disks). As a result, a given cluster storage system can easily include several makes/models, each in substantial quantity. The storage clusters we evaluated had between 3–10 makes/models of disks deployed over a span of a few years. As disks age, or as technology advances, it is common to retire or decommission older disk models and replace them with newer, more advanced variants. Chapter 4 has more details about the composition of the different clusters evaluated in this thesis. Beyond performance and capacity differences, disks can also have substantially different reliabilities.

Despite such differences, the degree of redundancy employed in cluster storage systems for the purpose of long term data reliability (e.g., the degree of replication or erasure code parameters) is generally configured as if all of the devices have the same reliability as described in Section 2.4. Unfortunately, this approach leads to configurations that are overly resource-consuming, overly risky, or a mix of the two. For example, if the redundancy settings are configured to achieve a given data reliability target (e.g., a specific mean-time-to-data-loss: MTTDL) based on the highest AFR of any device make/model, then too much space will be used for redundancy associated with data that is stored fully on lower AFR makes/models. Continuing this example, our evaluations show that the overall wasted capacity can be up to 16% compared to uniform use of erasure code settings stated as being used in real large-scale storage clusters [31, 77, 78, 84] and up to 33% compared to using 3-replication for all data—the direct consequence is increased cost, as more disks are needed. If redundancy settings for all data are based on lower AFRs, on the other hand, then data stored fully on higher-AFR devices is not sufficiently protected to achieve the target MTTDL.

This chapter lays the foundation of performing disk-adaptive redundancy by tailoring redundancy to the observed disk-reliability heterogeneity. We start by first describing the opportunity of performing disk-adaptive redundancy by analyzing disk failure logs of a production cluster storage system with over 100K+ HDDs. This is followed by the design, implementation and evaluation of a disk-adaptive redundancy system called the Heterogeneity-Aware

Make/Model	**Disk group shorthand**	**# of disks**	**Oldest disk age**
Seagate ST4000DM000	S-4	37015	5 yrs
HGST HMS5C4040ALE640	H-4A	8715	4.77 yrs
HGST HMS5C4040BLE640	H-4B	15048	4.2 yrs
Seagate ST8000DM002	S-8C	9885	1.99 yrs
Seagate ST8000NM0055	S-8E	14395	1.2 yrs
Seagate ST12000NM0007	S-12E	21581	8 mts

Table 3.1: The disk groups identified from the Backblaze dataset for reliability heterogeneity analysis. The disk group shorthand above is used to represent the respective makes/models throughout the chapter.

Redundancy Tuner (HeART) on the cluster we analyzed[1].

3.1 Identifying the opportunity

We adopt a data-driven approach to support the case of disk-adaptive redundancy. In this section we make our case by detailing the opportunity of tailoring redundancy to AFR heterogeneity and estimate the space overhead reductions that can be achieved by using disk-adaptive redundancy.

3.1.1 The Backblaze dataset

Our analysis is based on an open source dataset from a data backup organization, Backblaze [10]. This dataset consists of over 5 years of disk reliability statistics from a production cluster storage system with over 100,000 HDDs. Each HDD has a unique serial number, and the first day on which that serial number appears is the *birthday* of that disk and the last day on which a disk is seen is considered its *expiry*. Table 3.1 shows the six make/model disk groups that make up over 90% of the Backblaze deployment, with their population size, the age of their oldest disk, and the shorthand names we will use throughout this dissertation.

We use the standard metric *annualized failure rate (AFR)* to describe a disk's failure behavior [24, 90]. Recall from Section 2.2.3 that AFR is the expected percentage of disk failures in a given year. Note that the AFR calculation is dependent on the number of days a disk was in operation. This can be tricky to estimate from the Backblaze dataset since the "death" of a disk in this dataset may also indicate its decommissioning, which may or may not imply its failure. We argue that, in the case of Backblaze, the date of decommissioning a disk only affects the absolute date at which it would have fail-stopped, but does not affect its *rate of failure*. Backblaze adopts a proactive disk replacement strategy that is driven by monitoring a combination of five S.M.A.R.T. (Self-Monitoring, Analysis and Reporting Technology)

[1]The concept of disk-adaptive redundancy and HeART were published at the USENIX Conference on File and Storage Technologies (FAST), 2019 [48]

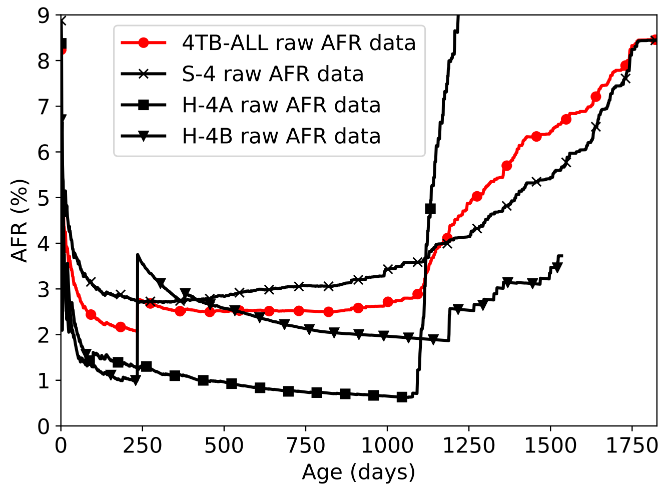

Figure 3.1: AFR comparison between all 4TB disks grouped together and disk groups broken down by make/model. The AFR differences in make/model-based grouping enables disk-adaptive redundancy to perform finer-grained specialization leading to higher benefits.

statistics. Backblaze uses S.M.A.R.T. 5 (Reallocated Sectors Count), S.M.A.R.T. 187 (Reported Uncorrectable Errors), S.M.A.R.T. 188 (Command Timeout), S.M.A.R.T. 197 (Current Pending Sector Count) and S.M.A.R.T. 198 (Uncorrectable Sector Count) as indicators that a disk is about to fail [9]. The increased probability of failure indicated by grown defects in a disk is supported by several previous studies [12, 56, 73, 87]. In fact, Pinheiro et al. [73] show that the critical threshold for several S.M.A.R.T. attributes before their imminent failure is one—that is, the probability of failure of a disk in the next two months increases manifold when any of these S.M.A.R.T. attributes show a value greater than zero. Ma et al. [56] also show the high likelihood of disk failure by monitoring the reallocated sectors count (S.M.A.R.T. attribute 5), which is one of the signals used by Backblaze as a disk replacement indicator. Therefore, we believe that Backblaze's proactive disk replacement rate is a reasonable approximation for the actual disk failure rate.

3.1.2 Disk group formation and varying AFRs

To effectively exploit heterogeneity in AFRs of different disk groups, we need to categorize the disks using some parameter that (1) groups disks with similar AFRs together and (2) has substantially different AFRs across groups. In whichever manner we choose to group the disks, in order to gain statistical confidence in the AFR value, we need to ensure that each disk group has a sizeable population. Our definition of a sizeable population is approximately 10,000 or more disks. This is in line with disk populations considered in previous reliability studies [56, 57, 73]. We identify the following four ways to categorize disks:

- **By make/model**: Economies of scale result in large quantities of disks being purchased from the same vendor. Prior studies have shown that AFR may vary significantly by vintage [26, 56, 73].

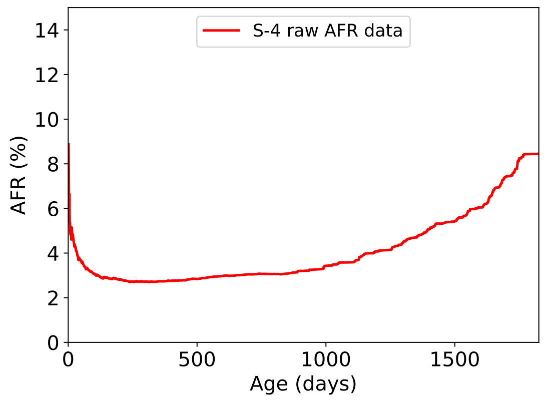

(a) S-4

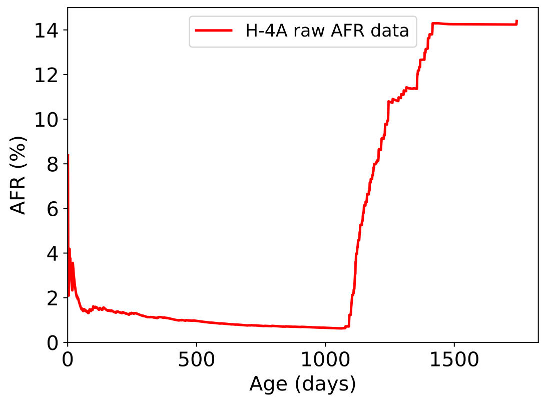

(b) H-4A

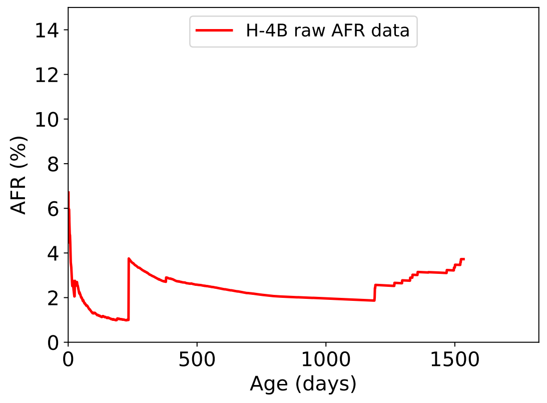

(c) H-4B

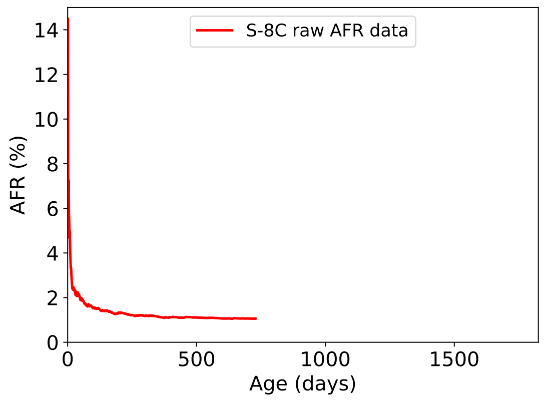

(d) S-8C

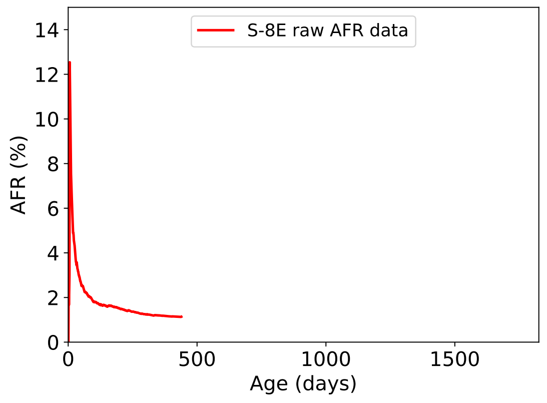

(e) S-8E

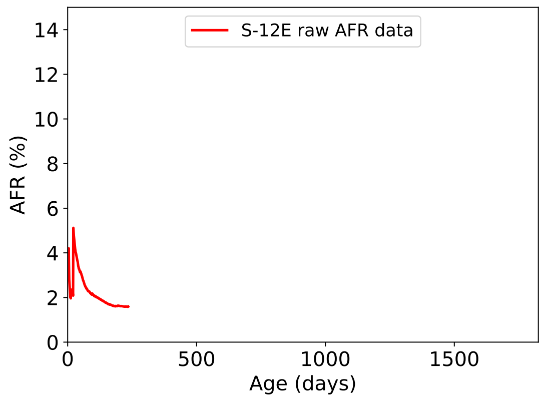

(f) S-12E

Figure 3.2: Cumulative raw AFR versus age (in days) for all six disk groups being analyzed.

- **By capacity**: Grown defects can be a function of disk capacity, thus causing disks of similar capacity to fail at a similar rate.
- **By operational conditions**: Disks that share similar vibration or temperature experiences may cause them to fail similarly. Thus, chassis placement and other operational conditions may influence failure rates.
- **By usage**: Increased space utilization or higher I/O rates may result in different disks showing different failure characteristics.

Unfortunately not all datasets have access to the operational conditions or usage patterns. In the data we analyzed, we only had disk vintage information, and therefore we can only analyze grouping on the basis of make/model or capacity.

Disk groups based on disk capacity

Figure 3.1 shows the AFR by considering all 4TB disks as one disk group (red curve with circular marks) and the AFRs of the three make/models of 4TB disks as individual disk groups (black curves). We see significant differences between AFRs when disks are grouped by make/model, suggesting that grouping by capacity is insufficient.

Disk groups based on disk make/model

Figure 3.2 shows the make/model-based AFR curves for the six disk groups, each with $\approx$10000 HDDs. Incidentally, these makes/models make up more than 90% of the Backblaze dataset. We can observe that there is significant heterogeneity across the different AFR curves across all three phases of the bathtub curve: infancy, useful life and wearout. Between grouping by capacity versus grouping by make/model, it appears that grouping by make/model is the better grouping strategy as it allows for more fine-grained control over exploiting disk-reliability heterogeneity.

Among the disks that show all three phases of a disk's life (Figs. 3.2(a), 3.2(b) and 3.2(c)), S-4 are the oldest disks in the cluster followed by H-4A and then H-4B. The rest of the disks (Figs. 3.2(d), 3.2(e) and 3.2(f)) only show infancy and start of useful life.

3.1.3 Making the case for disk-adaptive redundancy

The goal of disk-adaptive redundancy is to reduce storage overhead by tailoring the redundancy scheme employed to the failure rate of a disk group. The adaptivity comes from explicitly factoring in the disk group-specific AFR values in deciding the appropriate redundancy scheme for each disk group. Based on the canonical bathtub curve (Figure 2.2), and the AFR curves shown in Figure 3.2, we conclude that the safest stage to apply lower redundancy (without the risk of missing their reliability target) during a disk group's lifetime is in its useful life (stable operation period). Despite the AFR in useful life appearing lower than AFRs in infancy and wearout (which might suggest lower opportunity to exploit AFR heterogeneity), it ensures data safety because of the flatness of AFR and lonegevity of the useful life period compared to infancy or wearout. Moreover, it is not immediately clear that tailoring redundancy to infancy and wearout will achieve much benefit because the low cost due to lower

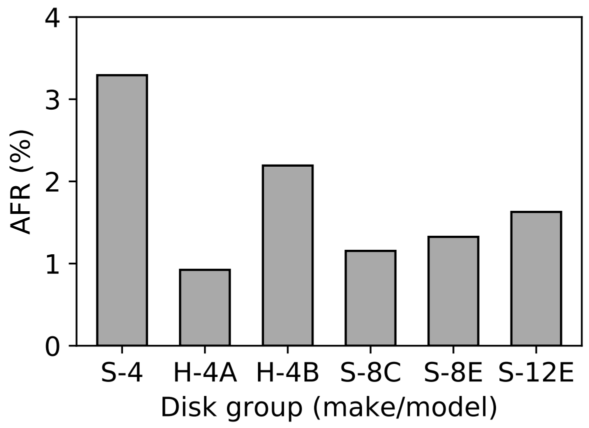

Figure 3.3: Annualized failure rate (AFR) for the six disk groups that make up $>$90% of the 100,000+ HDDs used for the Backblaze backup service [10]. Details of each disk group are given in Table 3.1.

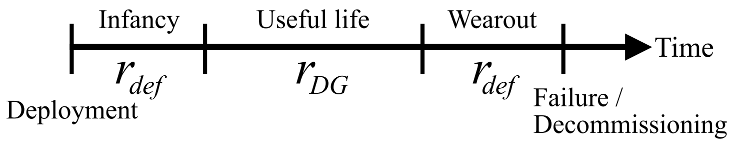

Figure 3.4: An abstract timeline of a disk group from deployment to failure or decommissioning, with the three distinct periods. The notations below the timeline (r_{def} and r_{DG}) denote the redundancy scheme employed during the respective stage.

redundancy is a function of the AFR value and the period of time for which that lower redundancy can be exercised. Since infancy and wearout are short-lived, it does not make sense to risk data safety at the potential of incremental benefit. Figure 3.3 shows the average AFRs during the useful life for the 6 HDD make/model-based disk groups that make up more than 90% of the Backblaze dataset. The highest failure rate is over $3.5\times$ greater than the lowest, and no two are the same.

Figure 3.4 shows the abstract timeline of a disk group, where r denotes the redundancy scheme applied in each stage. Since all cluster storage systems today use some redundancy scheme whose resilience is acceptable to them, we assume that to be the ***default*** redundancy scheme. Since infancy and wearout periods have higher and less stable AFRs compared to useful life, for every disk group, disk-adaptive redundancy should employ the default redundancy scheme for all infancy and wearout periods. This is shown as r_{def} in Figure 3.4. disk-adaptive redundancy suggests lower redundancy than the default scheme only during the useful life period, during which AFR values are relatively stable.

We use the standard metric *mean time to data loss* (MTTDL) for measuring the reliability of data employed in cluster storage systems. As described in Section 2.2.3, MTTDL is proportional to AFR.

When a disk group enters its useful life period, a disk-adaptive redundancy system should choose a redundancy scheme (r_{DG}) that meets the following conditions:

Disk groups		r_{def} **= 10-of-14**		r_{def} **= 6-of-9**		r_{def} **= 1-of-3**	
DG	AFR	r_{DG}	**Cost↓**	r_{DG}	**Cost↓**	r_{DG}	**Cost↓**
S-4	3.29%	10-of-14	**NA**	6-of-9	**NA**	1-of-3	**NA**
H-4A	0.92%	20-of-24	**14%**	12-of-15	**16%**	2-of-4	**33%**

Table 3.2: A sample of the estimated savings achievable via disk-adaptive redundancy. The space reductions obtained on H-4A disks by using redundancy schemes with lower storage overhead while meeting the reliability target set by applying the default redundancy scheme (r_{def}) on S-4 disks.

1. is as reliable as r_{def}, i.e. $MTTDL^{r_{DG}} \geq MTTDL^{r_{def}}$
2. tolerates at least as many failures as r_{def}

According to condition 1 above, we need to set a target MTTDL in order to compare the resilience of different redundancy schemes. Although prior studies have shown MTTDL targets to be as low as 10,000 years [83], in order to ensure that we do not regress on reliability that disks in our dataset can currently offer, we set the target MTTDL to be the MTTDL of the default redundancy scheme applied on the disk group with the highest AFR. S-4 is the disk group with highest useful life AFR in the Backblaze dataset (refer Figure 3.3). Therefore, for every default redundancy scheme, we will use S-4's MTTDL for that scheme as the target MTTDL.

Multiple redundancy schemes can achieve the same or similar MTTDL values. These schemes can differ in their dimension (k) or the number of parity chunks per stripe ($n - k$) or both. It is well known that, generally speaking, schemes with a higher dimension (wide schemes) can provide the same MTTDL with lower space overhead compared to narrower schemes as described in Section 2.2.2 and Section 2.2.3. However, wide schemes consume significantly higher cluster bandwidth for reconstruction, since many more disks have to be accessed when performing reconstruction of failed data [46, 77, 78, 84]. The cluster bandwidth consumed during reconstruction is a major concern in erasure-coded storage systems. This has been highlighted in several works in the past [46, 77, 78, 84] and is consistent with our discussions with cluster storage system administrators. We, therefore, limit our cost reduction analysis to schemes with at most 2× the dimension (i.e., parameter k) of the default redundancy scheme. This is a limit we have set based on our communication administrators of large-scale cluster storage systems.

Table 3.2 shows space-savings for one disk group (H-4A) as an example. We will first highlight the space reduction when erasure coding schemes are used as the default, focusing on the 10-of-14 and 6-of-9 schemes known to have been used in large data centers [31, 77, 78, 84]. For 10-of-14 as the default scheme, the MTTDL difference between H-4A and S-4 disks is over $580\times$. Thus, we can choose a weaker redundancy scheme (a scheme with lower storage overhead $\frac{n}{k}$), so long as conditions 1 and 2 above are fulfilled. In fact, the high AFR differences allow us to use the longest allowed optimized scheme (2× the dimension of the default redundancy scheme) for H-4A disks, i.e. 20-of-24 leading to a useful life space reduction of 14%. Similarly, when using 6-of-9 as the default scheme, the MTTDL difference between H-4A and S-4 is over $160\times$. This again allows us to choose the longest scheme for H-4A when $r_{def} = 6$-of-9, i.e. 12-of-15, providing a space reduction of 16%.

For $r_{def} = 3$-replication (recall that, under the n-of-k notation introduced in Section 2.2.2, 3-replication is denoted as the 1-of-3 erasure code), we can tune the redundancy on H-4A disks to 2-of-4 to respect our $2\times$ default stripe dimension limit and still achieve an MTTDL that is approximately $11\times$ that of S-4's MTTDL. Using a 2-of-4 scheme leads to a 33% reduction in disk space.

Large internet services companies try very hard to minimize free space (as low as 5%, according to some administrators) in order to minimize capital and operating costs. We are told that space-savings translate directly into reduced numbers of disks needed, and even modest space-savings (e.g., 10%) would build a solid case for tailoring redundancy schemes to heterogeneous disk AFRs.

We note that much of the reduction in storage overhead arises from allowing schemes up to $2\times$ in dimension (i.e., parameter k). However, simply employing an erasure code with twice the dimension for all data is not generally a suitable solution. First, the AFR for certain disk groups might be high enough to make schemes with $2\times$ dimension not acceptable causing them to miss the target reliability. Second, and more broadly, the reconstruction overheads can be unacceptable. For popular schemes employed in practice, the amount of cluster bandwidth required for reconstruction is proportional to $k\times$AFR, where k is the dimension of the scheme. The stable and lower AFR during a disk group's useful life period allows the IO generated for reconstruction to be contained even if wider schemes are employed, which is another reason why disk-adaptive redundancy optimizes redundancy schemes *only* during a disk group's useful life. Using wider schemes on data stored on disk groups in their infancy and wearout stages would exacerbate the cluster bandwidth consumption for reconstruction due to higher failure rates in these stages.

This leads us to the design of a disk-adaptive redundancy system that can dynamically tailor the data redundancy to the observed disk failure rates. Online (real-time) use of observed disk reliability requires careful design. disk-adaptive redundancy uses robust statistical approaches to identify not only a useful life AFR estimate for each disk group, but also the transitions between deployment stages: infancy$\rightarrow$useful life$\rightarrow$wearout, as in bathtub curve visualizations. The next section describes the challenges, design and architecture of the first disk-adaptive redundancy system *HeART: the Heterogeneity-Aware Redundancy Tuner.*

3.2 The Heterogeneity-Aware Redundancy Tuner (HeART)

HeART is an online tool for guiding exploitation of reliability heterogeneity among disks to reduce the space overhead (and hence the cost) of data reliability HeART uses failure data observed over time to empirically quantify each disk group's reliability characteristics and determine minimum-capacity redundancy settings that achieve specified target data reliability levels. This section describes the challenges, design and implementation of HeART. We also quantify the cost reductions achieved by HeART for the Backblaze dataset.

3.2.1 Challenges

There are several challenges in practically exploiting the opportunity presented in Section 3.1.

Challenge 1: Function online and be quick

In making our case for HeART, we made use of the complete failure information (e.g., the full bathtub curve) for the disk groups. This helped in clearly identifying the 3 stages of a disk group's lifetime and AFR values in each of the stages. In practice, however, AFR values for disk groups deployed in cluster storage systems can only be known in an online fashion (i.e., as a continuous stream of reliability data, as it is observed). Furthermore, the crux of the cost reduction from HeART comes from quickly tuning the redundancy scheme as soon as we are confident of a disk group having entered its useful life period. Thus, our first challenge in building HeART is that it needs to function in an online fashion taking a continuous stream of disk health data as input and quickly react to the changes in the failure rate.

Challenge 2: Be accurate

It is important to correctly identify the three different stages of the bathtub curve for each disk group (recall Figure 2.2). If we are hasty in declaring the end of the infancy period or lax in identifying end of useful life, we might not meet the reliability target because of having tailored the redundancy to a relatively low failure rate during the useful life period. In contrast, if we are too lax about declaring end of infancy or too hasty in declaring onset of the wearout stage, the opportunity of cost reduction will diminish.

Challenge 3: Filter-out anomalies

Events such as power outages, natural disasters or human error can cause large numbers of disks to fail at once It is important to distinguish between an accidental rise in AFR due to such anomalous events versus the rise in AFR due to onset of the wearout stage. Our third challenge is to perform AFR anomaly detection to avoid prematurely declaring end of useful life, consequently reducing the window of opportunity for cost reduction. At the same time, HeART needs to exercise caution so as to not treat a genuine rise in AFR as an anomaly, which risks not meeting reliability targets.

3.2.2 HeART architecture

Figure 3.5 shows the primary components of HeART. HeART assumes the existence of a disk health monitoring/logging mechanism already in place, which is common in large-scale cluster storage deployments. From the time of deployment till the end of infancy, the default redundancy scheme (r_{def}) is used to protect the data stored on a disk group. Periodically, disk health data for each disk group is passed through an *anomaly detector*. Following an anomaly check, the cumulative AFR of every disk group is passed through a *change point detector*, which checks if a transition to different phase of life has occurred. Once the change point detector announces start of the useful life period, HeART suggests a new redundancy mechanism for

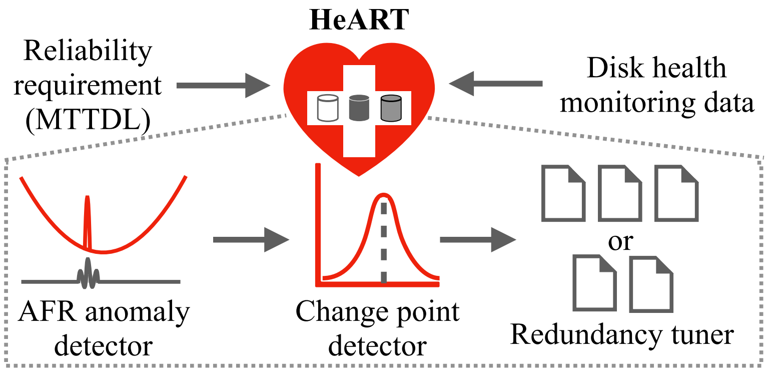

Figure 3.5: Schematic diagram of HeART. Components include an anomaly detector, an online change point detector, and a redundancy tuner.

the useful life of the disk group (r_{DG}). It computes a ***determined useful life AFR*** (AFR$_{DG}$), which is the AFR at the end of infancy padded with a tunable buffer, and uses it to calculate $MTTDL^{r_{DG}}$ for different redundancy scheme (r_{DG}) options. The buffer is introduced to tolerate the fluctuation of AFR during the useful life period (see Section 3.3.3). HeART keeps checking for anomalies and change points throughout the useful life period. When the change point detector marks the end of useful life, HeART raises an alert to reset the redundancy scheme to r_{def} to handle the increased AFR during wearout, as was handled in the absence of HeART.[2]

The remainder of this section describes our approach to addressing the above mentioned challenges. We leverage established tools and algorithms from online services and time-series analysis literature. While other options may perform even better, our evaluations indicate that these established tools are effective. We show the efficacy of HeART using the Backblaze dataset in Section 3.3.

3.2.3 Online anomaly detection

Incidents like losing power to a rack of disks, a natural disaster, or an accident, can cause a large number of failures resulting in a sudden rise in AFR. Such bulk failures can easily exceed the limits of any reasonable redundancy scheme, so administrators seek to mitigate them by defining appropriate failure domains and spreading data+redundancy across the failure domains [77, 78]. Such failures are not reflective of the true rise in AFR because of wearout, and therefore HeART considers these incidents as anomalies. It is important to note that the benefits we extract from exploiting the reliability heterogeneity are proportional to the length of the useful life period, and therefore prematurely announcing wearout stage due to an anomaly would significantly diminish achievable gains.

We use the H-4B disks as a motivating example for anomaly detection (shown in Figure 3.7). The raw AFR curve (red curve) shows that just after a few days into its useful life, there are large spikes in the AFR curve for drives that are about 235 days old (point A) and

[2]We note that the current architecture of HeART determines one useful life AFR for all disks belonging to a disk group and does not handle changes in the intra-disk-group reliability distribution over time.

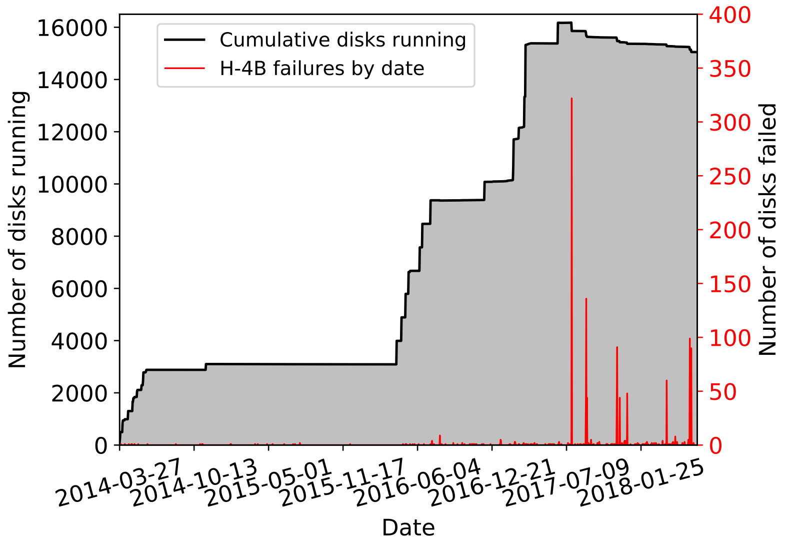

Figure 3.6: Total number of disks and number of disk failures by date for H-4B disks. The step-wise jumps in the black curve represent incremental deployments. The largest red spike represents the disks that failed on July 23, 2017, causing anomalies A and B in Figure 3.7.

380 days old (point B). Further along, we observe three more spikes that are in succession for disks that are about 1200 days old (points C, D and E). The failures corresponding to points A and B are all caused because of 322 drives failing on one particular date. Here, failure of disks of two different ages correspond to a failure event on the same day because these disks were deployed on different dates. Figure 3.6 shows the total number of disks running and the per-day number of disk failures of H-4B as a function of the date. The left y-axis shows the cumulative disks of H-4B running on each day. The steps in the black curve show the incremental deployments of H-4B disks. The right y-axis shows the number of H-4B disks failing on each day (red curve). The tallest red spike in Figure 3.6 corresponds to points **A** and **B** from Figure 3.7. Points C, D and E occurred because of disks failing on different days.

In the absence of anomaly detection, HeART would have incorrectly concluded that the disk group's wearout stage began as early as point A.

3.2.4 Online change point detection

We refer to a transition in the AFR curve of a disk group as a *change point*. There are two major change points for each disk group: end of infant mortality stage and the onset of the wearout stage. This subsection describes our methods of identifying the two change points.

Onset of useful life period. HeART uses prior studies about infant mortality in HDDs along with change point detection to decide a disk group's end of infancy. Prior studies performed on the Google and EMC disk fleets [56, 73] have shown that infant mortality lasts for approximately one quarter. Therefore, in order to be conservative, HeART exempts the first quarter from being assessed for end of infant mortality. Since disk reliability data is collected periodically, each time data is collected after the first 90 days, we run change point

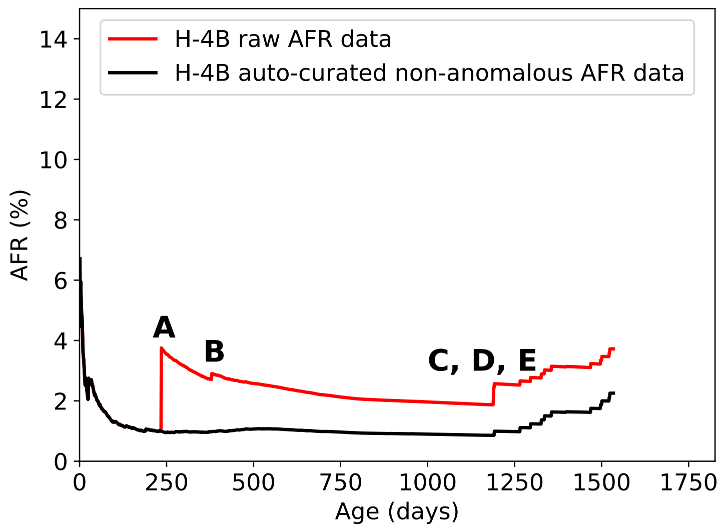

Figure 3.7: Raw and HeART-curated AFR curves for the H-4B disk group. Five spikes in AFR (points A–E), which correspond to four (anomalous) bulk failure events, are automatically filtered out by HeART.

detection on the AFR curve generated by a sliding window of the past 30 days. HeART declares end of infancy if the last change point marked by the detector is over 30 days old, and the failure rate during the last 30 days is relatively constant. More precisely, HeART declares end of infancy when the difference between the observed maximum and minimum AFR values in at least 30 days past the last change point is less than a certain threshold T_{flat}. T_{flat} is the threshold for *flatness* and is a tunable parameter in HeART. Sensitivity to T_{flat} is evaluated in Section 3.3.3. Note that HeART takes a conservative approach in declaring the onset of the useful life period of a disk group in order to increase confidence about reducing redundancy for data stored on that disk group.

In order to evaluate the accuracy of HeART's online change point detection approach, we compare the HeART-determined length of infancy with the true length of infancy (calculated using the lifetime AFR curve for every disk group, which is not possible in production, since it would require knowing the future). In particular, the true length of infancy of each disk group that we choose to compare with is lowest cumulative AFR plus the AFR buffer ($AFR_{DG_{min}} + a$) that is observed by each disk group in its entire lifetime. The disk group's infancy would have definitely ended before this point, and its disks would have safely ventured into their useful lives. Table 3.3 compares the number of days taken by each disk group to reach infant mortality using online change point detection and the true length of infancy. Although it might appear at first that HeART's online change point detector is undershooting the change points in disk groups S-4, H-4A and S-8C, making data residing on those disks unsafe, it is important to note that the true infancy is considering the lowest AFR $+a$ during a disk group's lifetime. HeART sets the useful life AFR to a value that is comfortably higher than $AFR_{DG_{min}} + a$, as shown in the evaluation in Figure 3.8 and explained in Section 3.3.2. Furthermore, HeART allows cluster storage admins to increase the value of a according to

DG	$AFR_{DG_{min}} + a$	Age until $AFR_{DG_{min}} + a$	HeART-determined infancy
S-4	3%	91 days	90 days
H-4A	0.82%	91 days	90 days
H-4B	1.18%	90 days	91 days
S-8C	1.25%	90 days	92 days
S-8E	1.33%	94 days	90 days
S-12E	1.79%	101 days	106 days

Table 3.3: Comparison between length of infant mortality calculated statically (i.e. number of days $>= 90$ needed to reach $AFR_{DG_{min}} + a$ for each disk group, where a is a tunable AFR buffer added on top of the observed AFR at the end of infancy; set by default to 25% of the observed AFR) versus length of infant mortality calculated by online change point detection.

their respective safety standards, which makes HeART choose a higher (and thus safer) AFR for useful life. On the other hand, overshooting the start of useful life is completely safe. It only affects the benefits we can reap (that too by an insignificant amount even if the end of infancy overshoots the actual end of infancy by a few weeks), but does not affect correctness, i.e. does not have an effect on the probability of data loss.

End of useful life period. Unlike the safety net present despite being lax in detecting end of infancy, being lax in declaring the end of useful life period (i.e., onset of wearout) can risk in HeART not meeting the intended reliability target. Hence, HeART takes a conservative approach and marks the end of useful life for the first AFR observed that is greater than the determined useful life AFR. Since HeART checks for anomalous AFR fluctuations before checking for change points, if the anomaly detection phase does not filter out an increase in AFR, HeART assumes it to be a true increase in AFR. Thus, here too HeART takes a conservative approach and errs on the side of exiting the useful life period early and reverting to the default redundancy scheme. Although the H-4A graph in Figure 3.2(b) appears to show a sudden, huge rise in AFR, we believe that it is an artifact of Backblaze's recording of decommissioned disks as failed, based on the device removal pattern seen in the failure data. Data from more sources are needed to confirm this hypothesis. If some disks do exhibit such transitions, then strategies for predicting failures (and wearout onset), such as by using S.M.A.R.T. statistics [6, 57, 114, 120], will be needed to use any but the most conservative redundancy schemes.

3.3 Evaluating the HeART

This section describes implementation details of various components that make up HeART and presents an evaluation of HeART on the Backblaze dataset.

3.3.1 Implementation of the components

Our current implementation of HeART leverages existing, standard algorithms for anomaly detection and change point detection. Employing more sophisticated algorithms might lead to even better results.

Anomaly detector: For anomaly detection, our current implementation of HeART uses the RRCF algorithm [4] exposed by Amazon's data analytics service offering called Kinesis [3].[3] A Kinesis application running the RRCF algoritm keeps polling a Kinesis data stream for new data. As soon as the disk health monitoring system makes the reliability data available, it is uploaded to the Kinesis data stream. The Kinesis application pulls the data from the data stream, runs the anomaly detection on the data, and produces the output also as a stream. The output contains an anomaly scores produced by the RRCF algorithm. Potential anomalies identified by RRCF have a higher anomaly score than data that the algorithm considers non-anomalous. RRCF generates the anomaly score based on how different the new data is compared to the recent past. For consistency with change point detection, we set the window size of the recent past to be one month. If the anomaly score is above a certain threshold, HeART considers that snapshot of reliability data as anomalous. RRCF advises to only consider the highest anomaly scores as true anomalies [4]. The anomaly score threshold is a tunable parameter in HeART. Lowering the score makes HeART more sensitive to fluctuations in AFRs.

Change point detector: Our current implementation of HeART uses a standard window-based change point detection algorithm, which compares the discrepancy between adjacent *sliding windows* within the AFR curve to determine if a change point has been encountered. In particular, we employ the *Ruptures* library for online change point detection [104, 105]. We set the sliding window size to one month, because AFRs at a lower granularity than a month are jittery.

3.3.2 Evaluation on the Backblaze dataset

Identifying useful life period

Figure 3.8 shows the results from HeART running on all 6 disk groups of the Backblaze dataset. HeART accurately identifies the infancy, useful life and wearout stages of the S-4, H-4A and H-4B disk groups shown in Figs. 3.8(a), 3.8(b) and 3.8(c), respectively. For the S-8C, S-8E and S-12E disk groups (Figs. 3.8(d), 3.8(e) and 3.8(f)), HeART identifies the end of infancy and correctly shows that they are still in their useful life. The width of the shaded region of each disk group highlights the "savings region", i.e. the useful life period determined by HeART for which HeART potentially suggests a lower redundancy scheme. The height of the shaded region in Figure 3.8 denotes the AFR values protected by the useful life AFR value determined by HeART for that disk group.

It is important to note that even though Figure 3.8 shows cumulative AFR behavior, HeART performs anomaly detection and online change point detection on AFRs calculated using monthly sliding windows. Thus, not only is the cumulative AFR always inside the

[3]We use Amazon's anomaly-detection-as-a-service so as to avoid re-implementing a state-of-the-art algorithm.

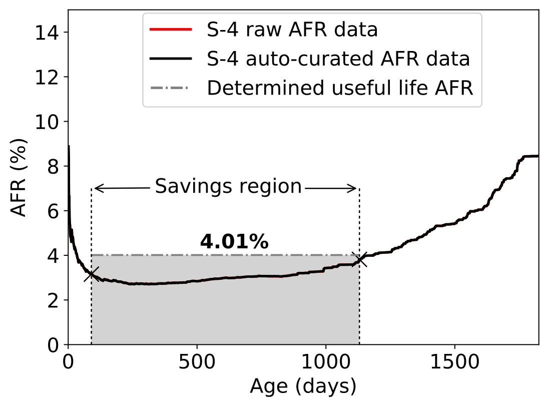

(a) S-4 with HeART-determined AFR

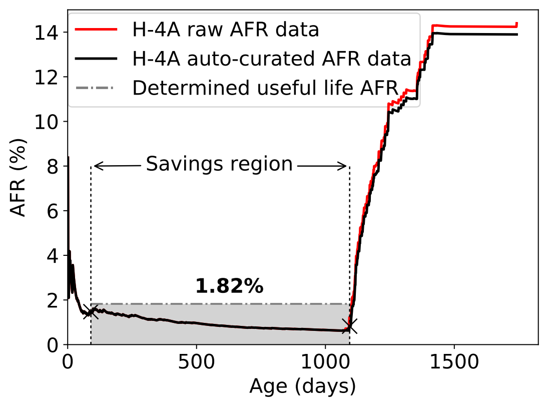

(b) H-4A with HeART-determined AFR

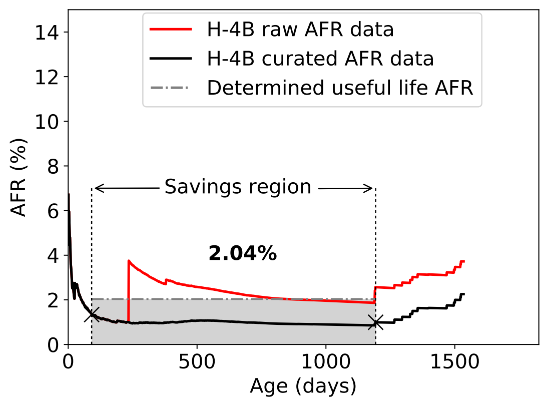

(c) H-4B with HeART-determined AFR

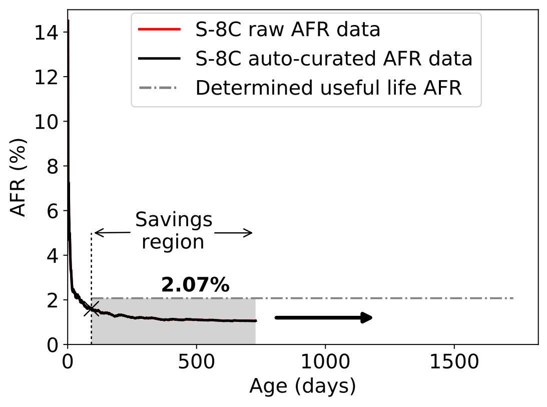

(d) S-9C with HeART-determined AFR

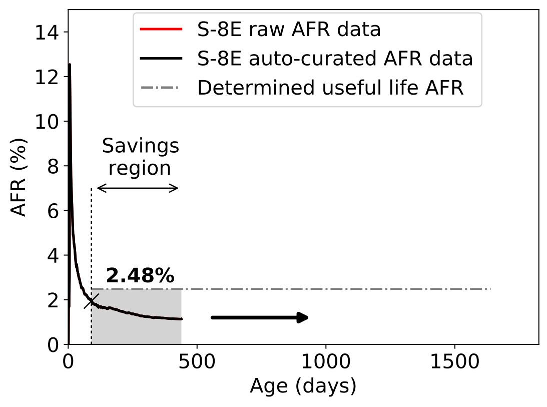

(e) S-8E with HeART-determined AFR

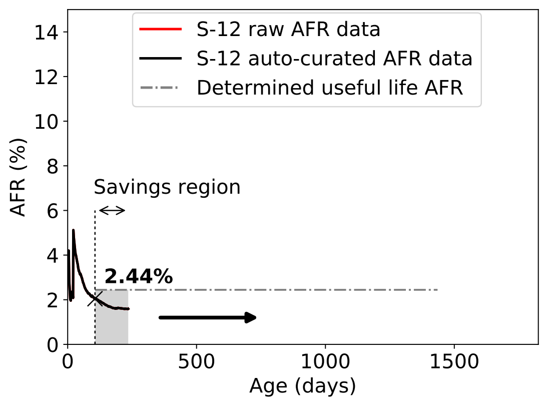

(f) S-12 with HeART-determined AFR

Figure 3.8: HeART in action on all disk groups, showing successful identification of infant mortality, useful life and wearout periods as well as automatic removal of anomalies.

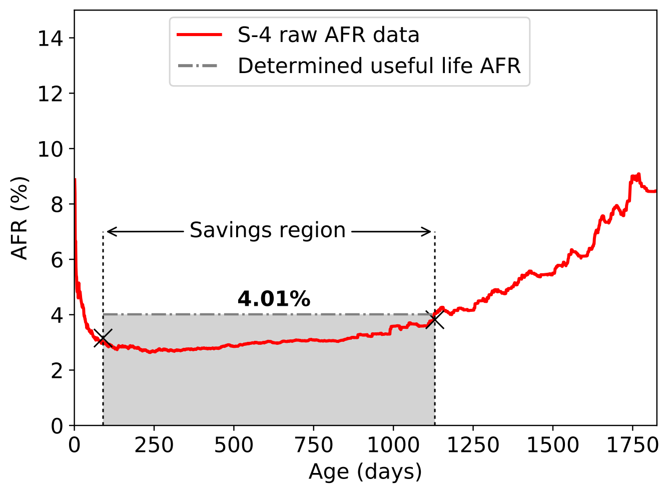

Figure 3.9: AFR of the S-4 disk group using a sliding window of 30 days. The determined useful life AFR value by HeART is conservative enough to subsume even the 30-day AFR values which vary more than the cumulative AFRs.

shaded region, but the instantaneous failure rate for any 30-day period is also less than the determined AFR value. In fact, the first rise in the instantaneous failure rate is what determines the end of the useful life period. Figure 3.9 shows the instantaneous failure rate of S-4 disks being lower than the determined useful life AFR value throughout the useful life period.

In contrast to S-4 (Figure 3.8(a)), the H-4A (Figure 3.8(b)) and H-4B (Figure 3.8(c)) disk groups have a sudden occurrence of their respective wearout stages. The quick reactivity requirement explained in Section 3.2.1 comes into effect for these disk groups. How quickly HeART reacts to changes in the AFR is determined by how quickly failure data is provided to HeART. Since Backblaze maintains daily snapshots of disk health, the quickest reaction to an increased failure rate is on the day that the failures occur. In our evaluation, HeART successfully identifies the increased AFR on the very day it was provided with the increased AFR data.

Anomaly detection

As explained in Section 3.2.3, the anomaly detector successfully detects five anomalies in the lifetime of H-4B disks. Additionally, two anomalies are also detected for the H-4A disks. Correctly identifying anomalous events increased the identified useful life period of H-4B disks by over $5\times$. In the absence of anomaly detection, the end of useful life period would have been incorrectly identified at age 235 days (shown by point A in Figure 3.7).

Cost savings per disk group

Table 3.4 summarizes the cost savings of employing disk group specific redundancy in their respective useful lifespans. Disk groups with similar AFRs are grouped together. As discussed in Section 3.1, we restrict the dimension (k) of the optimized schemes to at most $2\times$ that of the default redundancy scheme (r_{def}). In each case of r_{def}, we set the target reliability to the MTTDL achieved by using the highest-AFR disk group, which in the case of Backblaze are the S-4 disks.

It is important to note that the useful life AFRs determined by HeART are higher than the useful life AFRs shown in Figure 3.3. Recall from Section 3.2.2, that HeART adds a (tunable) buffer above the useful life AFR determined at the end of infancy (which is an additional 25% by default). HeART chooses to be conservative in determining a useful life AFR value to ensure that reliability targets are comfortably met and to elongate the length of the useful life period to maximize benefits.

As in Section 3.1, we exemplify the space reduction for erasure coding schemes using 10-of-14 and 6-of-9 schemes, which are known to have been employed in large-scale data centers [31, 77, 78, 84].

First, we evaluate using 10-of-14 as the default redundancy scheme. 10-of-14 has the lowest storage overhead ($1.4\times$) among the default redundancy schemes we evaluate, making it the hardest to find schemes that meet the target MTTDL and reduce overhead even further. Despite these constraints, HeART enables a 14% space reduction for H-4A, H-4B and S-8C disks by suggesting a 20-of-24 scheme and a reduction of 11% for S-8E and S-12E disks by suggesting a 17-of-21 scheme. Recall that the redundancy scheme selection is done by shortlisting schemes that fulfill the two criteria described in Section 3.1.3. From the shortlisted schemes, HeART chooses the scheme with the lowest storage overhead to achieve maximum space-savings.

Next, we measure HeART's performance when using 6-of-9 as the default redundancy scheme. We observe a space reduction of 16% on H-4A, H-4B and S-8C disks by using the maximum allowed 12-of-15 redundancy scheme. For S-8E and S-12E disks, HeART suggests a narrower 10-of-13 scheme compared to the above three disk groups in order to address their relatively higher determined AFR values, leading to a space reduction of 13%.

Finally, we also include the cost reduction for the canonical redundancy scheme, 3-replication, for completeness. We see that HeART enables 33% space reduction for all disk groups. We note that if replication is employed primarily for availability, that data may not be a candidate for tuning redundancy through HeART.

For H-4A, H-4B and S-8C disks, HeART chose the $2\times$ max stripe-length for all three evaluated default redundancy schemes, extracting the maximum cost reduction (as explained in Table 3.2). Even with the maximum allowed stripe length, the MTTDLs for the above disks are approximately $2.5\times$ higher than the target MTTDL value, suggesting further storage cost reductions if one is allowed even wider schemes.

Overall cost reduction

To highlight the overall cost reduction achieved on the Backblaze disk fleet, we show the capacity-weighted cost savings in Figure 3.10. This cost reduction is over the whole lifetime of the disks (including the unoptimized infancy and wearout periods) and for all six disk groups (including the unoptimized S-4 disks). We only show the benefits for the erasure coding schemes we evaluated, leaving out 3-way replication, since erasure codes are the more popular choice for data durability. The overall cost reduction achieved with the maximum

Disk groups		$r_{def} = MTTDL^{10-of-14}_{4.01\% AFR} = 1.46E+21$			
DG	AFR	$MTTDL^{r_{def}}$	r_{DG}	$MTTDL^{r_{DG}}$	**Cost↓**
S-4	4.01%	$1.46E+21$	10-of-14	$1.46E+21$	**NA**
H-4A	1.82%	$7.57E+22$	20-of-24	$3.56E+21$	**14%**
H-4B	2.04%	$4.28E+22$	20-of-24	$2.01E+21$	**14%**
S-8C	2.07%	$3.98E+22$	20-of-24	$1.87E+21$	**14%**
S-8E	2.48%	$1.61E+22$	17-of-21	$1.58E+21$	**11%**
S-12E	2.44%	$1.75E+22$	17-of-21	$1.72E+21$	**11%**

Disk groups		$r_{def} = MTTDL^{6-of-9}_{4.01\% AFR} = 3.31E+16$			
DG	AFR	$MTTDL^{r_{def}}$	r_{DG}	$MTTDL^{r_{DG}}$	**Cost↓**
S-4	4.01%	$3.31E+16$	6-of-9	$3.31E+16$	**NA**
H-4A	1.82%	$7.80E+17$	12-of-15	$7.20E+16$	**16%**
H-4B	2.04%	$4.94E+17$	12-of-15	$4.56E+16$	**16%**
S-8C	2.07%	$4.66E+17$	12-of-15	$4.30E+16$	**16%**
S-8E	2.48%	$2.26E+17$	10-of-13	$3.99E+16$	**13%**
S-12E	2.44%	$2.41E+17$	10-of-13	$4.26E+16$	**13%**

Disk groups		$r_{def} = MTTDL^{1-of-3}_{4.01\% AFR} = 6.36E+12$			
DG	AFR	$MTTDL^{r_{def}}$	r_{DG}	$MTTDL^{r_{DG}}$	**Cost↓**
S-4	4.01%	$6.36E+12$	1-of-3	$6.36E+12$	**NA**
H-4A	1.82%	$6.80E+13$	2-of-4	$1.70E+13$	**33%**
H-4B	2.04%	$4.83E+13$	2-of-4	$1.21E+13$	**33%**
S-8C	2.07%	$4.62E+13$	2-of-4	$1.16E+13$	**33%**
S-8E	2.48%	$2.69E+13$	2-of-4	$6.72E+12$	**33%**
S-12E	2.44%	$2.82E+13$	2-of-4	$7.06E+12$	**33%**

Table 3.4: Disk space saved by HeART by tuning the redundancy in the useful life of a disk group according to the observed disk group-specific AFRs. The units for MTTDLs is years. The cost savings are calculated for 3 default schemes: 10-of-14 on AFR 4.01% disks, 6-of-9 on AFR 4.01% disks and 3-replication (i.e. 1-of-3) on AFR 4.01% disks. Thus, the target reliability is the MTTDL of the respective default redundancy schemes using a 4.01% AFR (the r_{def} table header). The max dimension of the scheme permitted during useful life for each disk group has at most twice the dimension of default redundancy scheme, i.e. 20 data chunks for 10-of-14, 12 data chunks for 6-of-9 and 2 data chunks for 3-replication.

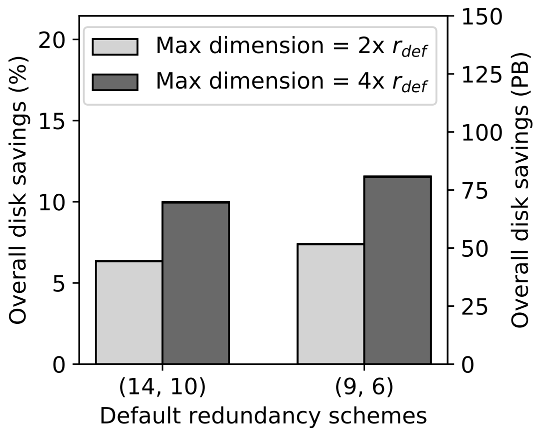

Figure 3.10: Overall space reduction achieved by HeART on the Backblaze dataset over the complete lifetime of every disk group, for erasure codes as the default redundancy mechanism. For a maximum scheme dimension of up to $2 \times r_{def}$, we observe between $6 - 7.5\%$ space reduction and for a maximum scheme dimension of up to $4 \times r_{def}$, we observe between $10 - 12\%$ space reduction, translating to actual space savings of $40 - 80$ PBs.

stripe dimension being $2\times$ the default redundancy scheme is approximately 6% when using 10-of-14 and approximately 7.5% when using 6-of-9 as the default. If we relax the constraint of the maximum stripe dimension to $4\times$ the dimension of the default redundancy scheme, we can expect to achieve between $10 - 12\%$ overall space reduction. These modest percentage savings translate to significant savings in terms of actual storage space in large-scale clusters. For example, as shown on the right-side y-axis in Figure 3.10, savings in storage space for the the Backblaze cluster range between $40 - 80$ PBs.

3.3.3 Sensitivity analysis

There are several configuration parameters that govern the behavior of HeART, of which most are dependent on the ready-made tools we have used for different components of our system (e.g., the threshold for anomaly scores when using RRCF for anomaly detection). There are, however, two fundamental parameters that are independent of which anomaly detector or change point detector is used.

Before going into the details about the two parameters, we note that the modulation of both the parameters only has an effect on the gains that our optimization can yield. *Neither of them affects correctness* of our framework or protection of data in any way. This allows operators of cluster storage systems to start with conservative values, observe the AFR behavior of their disks and accordingly choose apt values to minimize their costs without the risk of missing their reliability target. We next discuss the two parameters.

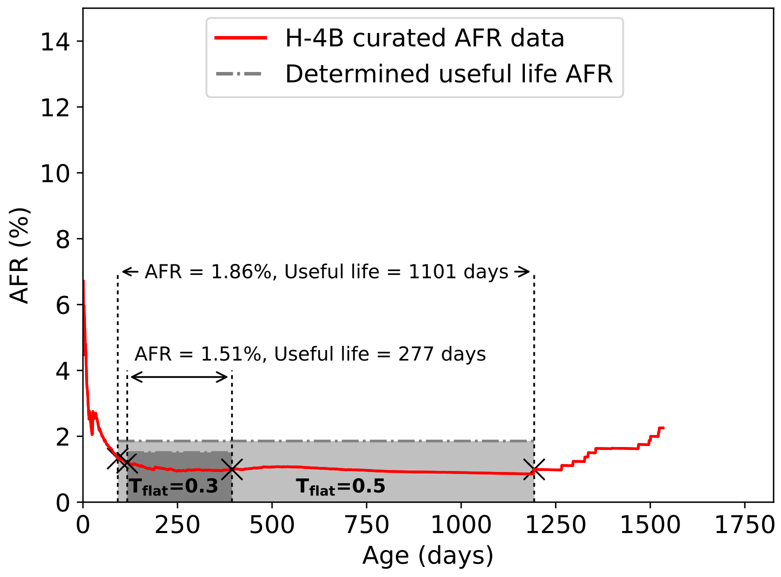

Figure 3.11: The effect of varying T_{flat} (AFR flatness threshold) on the H-4B disk group's AFR curve. Larger T_{flat} implies a higher useful life AFR along with a larger useful life period. The default value for T_{flat} in HeART is 0.5.

Flatness parameter (T_{flat})

T_{flat} is used to deduce the end of the infant mortality period. As mentioned in Section 3.2.4, the end of infancy is defined as the first 30+ day period beyond the change point detected after the first quarter such that the difference between maximum and minimum observed AFR is below the threshold T_{flat}. Thus, T_{flat} essentially determines the flatness in the AFR curve for a given period. Currently, we define T_{flat} to be 0.5. A larger T_{flat} value will reduce the length of infancy until it reaches 90 days, beyond which it will have no effect. A lower T_{flat} will enforce a stricter flatness criteria, typically causing end of infancy to be declared late. Ending infancy sooner potentially causes HeART to choose a larger value as the determined useful life AFR. This, in turn causes HeART to choose a stronger redundancy scheme (with higher space overhead) compared to one that would have been chosen with the determined AFR value derived as a result of a lower T_{flat} value. This reduces the achievable savings within the useful life period of the disk group. As a tradeoff, we get a larger useful life period with a larger T_{flat}, since not only does infancy end sooner, but also the onset of wearout stage is postponed, since the increased useful life AFR now has higher tolerance to AFR variances throughout the useful life.

Figure 3.11 shows the effect of varying T_{flat} on H-4B disks. We show the results for two different values $T_{flat} = 0.3$ and $T_{flat} = 0.5$. When T_{flat} was set to 0.3, we can see HeART declaring end of infancy at close to 100 days. Despite the buffer added to the determined useful life AFR at the end of infancy, the fluctuation in monthly AFRs caused a spike on day 394 to rise above the determined useful life AFR, causing HeART to announce end of useful life. In contrast, when $T_{flat} = 0.5$, infancy was declared to end on day 91, and the determined AFR value was high enough to tolerate the spike on day 394, increasing the useful life period by a significant amount.

Useful life AFR buffer

The AFR buffer is the conservative padding added to the useful life AFR determined at the end of infancy. Currently, the useful life AFR is determined as the AFR value at the end of infancy ***plus an additional buffer***, the tunable AFR buffer parameter. The choice of the buffer value has similar tradeoffs to the flatness parameters discussed above. A high buffer value implies a more conservative approach to setting the determined useful life AFR. This will prolong the useful life period, but restrict the tuning of the redundancy scheme due to the high useful life AFR value determined (and thus reducing benefits). In contrast, setting a low buffer value will shorten the useful life period but allow more cost reductions during the useful life. Operators can set the buffer based on AFR fluctuations observed in their storage systems, which can stem anywhere from workload patterns to operational conditions.

By robustly estimating per-disk-group AFRs and selecting the best redundancy settings for each, HeART avoids the space-inefficiency of one-size-fits-all redundancy schemes. Analysis of failure data for a large-scale production storage cluster shows that using HeART could achieve target data reliabilities with 11–33% fewer disks than popular configurations, offering huge potential cost savings.

While HeART outlines the potential benefits and describes the associated policies and algorithms for performing disk-adaptive redundancy, it refrains from describing the systemic techniques that should be used to carry out redundancy transitions from one scheme to another. We will observe in Chapter 5 that sophisticated mechanisms need to be used to perform disk-adaptive redundancy efficiently. But first, we analyze large production cluster storage systems consisting of millions of disks from three large organizations in Chapter 4. This analysis will prove crucial in informing the design of efficient disk-adaptive redundancy.

Chapter 4

Disk reliability analysis in production environments

We examine disk reliability and deployment characteristics of over 5 million HDDs, covering over 60 makes/models, by analyzing multi-year logs from real-world environments. This chapter presents key insights that inform our understanding of the sources of transition overload (urgent bursts of redundancy transition IO; described in Chapter 5) and challenges/opportunities for a robust disk-adaptive redundancy solution which is described in the next chapter.

4.1 Longitudinal disk reliability datasets

The largest dataset comes from NetApp and contains information about disks deployed in filers (file servers). Each filer reports the health of each disk periodically (typically once a fortnight) using their AutoSupport [51] system. We analyzed the data for a subset of their deployed disks, which included over 50 makes/models and over 4.3 million disks total.

The other datasets come from large storage clusters deployed at Google and the Backblaze Internet backup service. Although the basic disk characteristics (e.g., AFR heterogeneity and the AFR behavior discussed below) are similar to the NetApp dataset, these datasets also capture the evolution and behavior in our target context (large-scale disaggregated storage clusters). The particular Google clusters shown were selected based on their longitudinal data availability, but were not otherwise screened for favorability. Google Cluster1's disk population over three years included ≈350K disks of 7 makes/models. Google Cluster2's population over 2.5 years included ≈450K disks of 4 makes/models. Google Cluster3's population over 3 years included ≈160K disks of 3 makes/models. The Backblaze cluster's population since 2013 has included over 110K disks of 7 makes/models ranging from 4TB to 12TB. A subset of this dataset was also evaluated by HeART as shown in Chapter 3. For each cluster, the multi-year log records (daily) all disk deployment, failure, and decommissioning events from birth of the cluster until the date of the log snapshot.

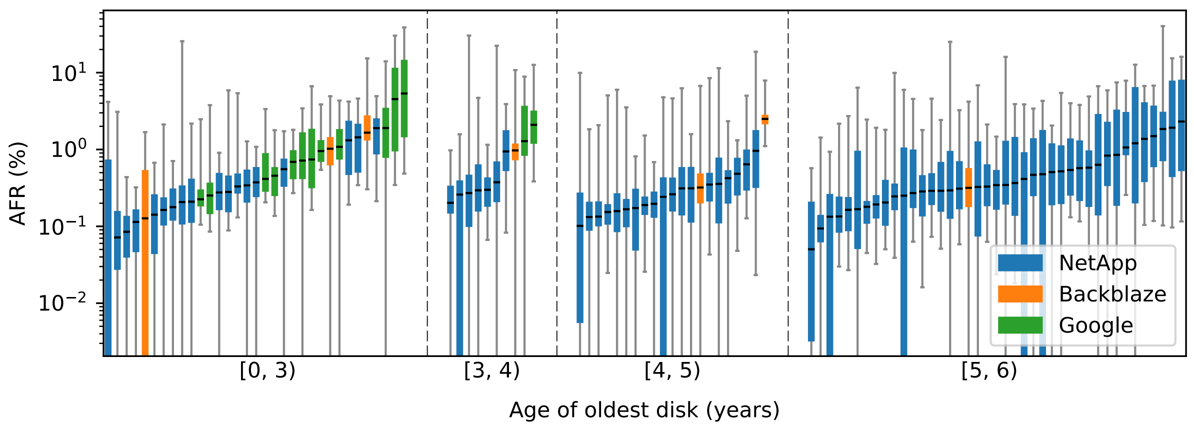

Figure 4.1: AFR spread for over 60 makes/models from NetApp, Google and Backblaze binned by the age of the oldest disk. Each box corresponds to a unique make/model, and at least 10000 disks of each make/model were observed (outlier AFR values omitted).

4.2 Observations and insights

The insight for disk-adaptive redundancy systems

At such large scales space-savings of even 1% affects at least 1000 disks. Thus, optimizations such as disk-adaptive redundancy, which promise close to 20% space-savings directly translate to requiring tens-of-thousands of fewer disks, which dramatically reduces energy and storage costs.

4.2.1 Useful life AFRs are wildly heterogeneous

Figure 4.1 captures the range of AFRs that we observed in our analysis over disks of various ages. The highest useful life AFRs observed are close to two orders of magnitude compared to the lowest useful life AFRs across the 60 makes/models we analyzed across three organizations; NetApp, Google and Backblaze. Analyzed disks consist of both consumer and enterprise grade disks (most disks are enterprise). The proprietary nature of our data prevents us from disclosing the actual make/model or population of each disk type.

The insight for disk-adaptive redundancy systems

The concept of disk-adaptive redundancy rests on exploiting reliability heterogeneity to have different redundancy for different sub-populations of disks. The observation that AFRs across different makes/models differs by orders of magnitude, and that this AFR heterogeneity is ubiquitous suggests that disk-adaptive redundancy is a useful approach that is applicable for most large-scale storage clusters.

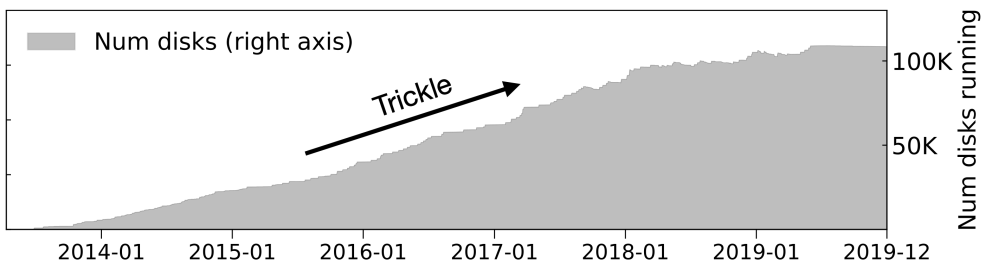

Figure 4.2: Backblaze cluster showing trickle deployments.

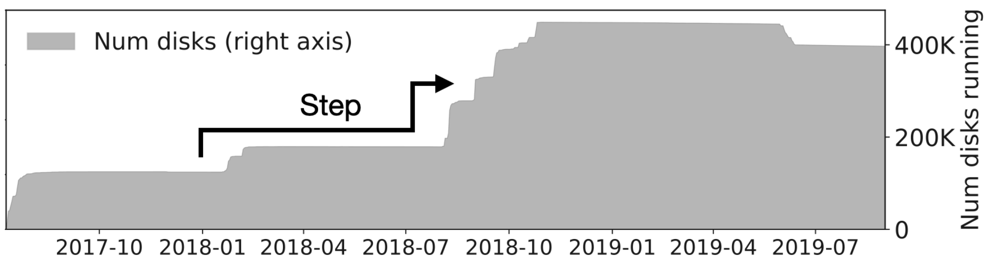

Figure 4.3: Google Cluster2 showing step deployments.

4.2.2 Disks have two distinct deployment patterns

Trickle deployment

Trickle-deployed disks are added to a cluster a-few-at-a-time (by the tens and hundreds), but frequently (weekly or even daily). Trickle-deployed disks may belong to different makes/models. Figure 4.2 shows the Backblaze storage cluster which is entirely trickle-deployed.

Step deployment

Step-deployment introduces many thousands of disks into the cluster "at once" (over a span of a few days), followed by potentially months of no new step-deployments. Disks of a step are typically of the same make/model. Figure 4.3 shows one of the Google clusters that is step-deployed.

Mix of trickle and step deployments

A cluster may be entirely trickle-deployed (like the Backblaze cluster) or entirely step-deployed (like one of the Google clusters), but more often than not, it is usually a mix of the two. Figure 4.4 shows one of the Google clusters that has three of its seven make/models trickle-deployed and the remaining four makes/models step-deployed.

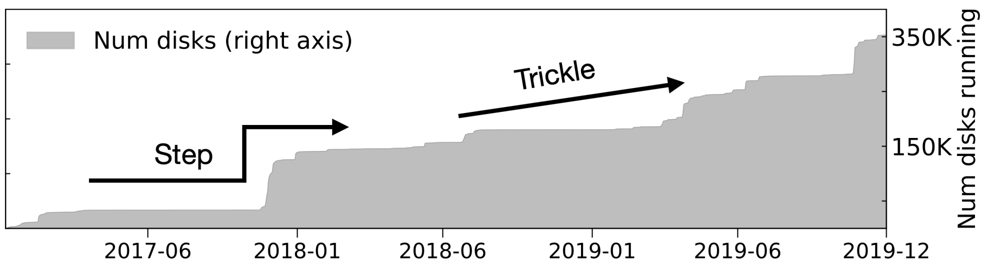

Figure 4.4: Google Cluster1 showing a mix of trickle and step deployments.

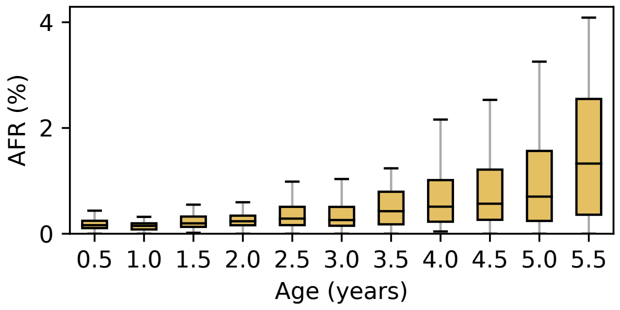

Figure 4.5: Distribution of AFR calculated over consecutive non-overlapping six-month periods for NetApp disks, showing the gradual rise of AFR with age (outliers omitted).

The insight for disk-adaptive redundancy systems

Disk deployment strategies are typically a consequence of disk procurement strategies. On one hand, it might be more cost-effective to purchase disks in bulk (i.e. step), which would then cause them to be deployed in bulk, because they have been purchased already. Whereas, there might be a need of specific disks of a certain capacity which might not have been manufactured, or available in bulk, and therefore are purchased, and deployed as they are made available (i.e trickle). Nevertheless, the nature of disk deployment reflects on how they need to transition to different redundancy schemes. Specifically, since trickle-deployed disks are deployed a-few-at-a-time, and since redundancy transitions are a function of disk age (as explained in Section 3.1.2) trickle-deployed disks transition a-few-at-a-time. In contrast, since step-deployed disks are deployed in bulk, they require transitioning in bulk. Although disk deployment pattern can be chosen in order to benefit disk-adaptive redundancy, in this work we do not recommend or change the deployment pattern, but in fact we design optimizations for transitioning based on the observed deployment pattern (explained in Section 5.3.3).

4.2.3 AFRs rise gradually over time with no clear wearout

The folklore of a single, flat useful life transitioning to a steep wearout phase was not observed in the disk populations we studied. Rather, in general, it was observed that AFR curves rise gradually as a function of disk age. Figure 4.5 shows the gradual rise in AFR over six month periods of disk lifetimes. Each box represents the AFR of disks whose age corresponds to the

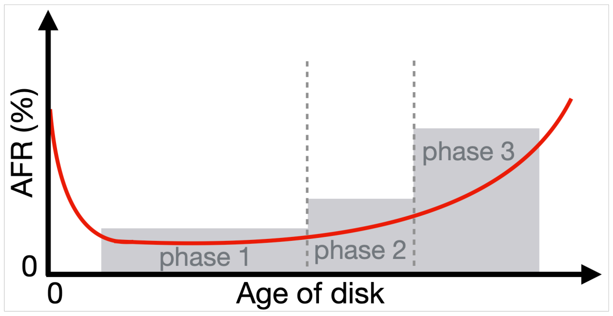

Figure 4.6: A conceptual representation of an AFR curve showing multiple phases of useful life. In contrast with the canonical representation shown in Figure 2.2, the AFR curves observed in real-world cluster storage systems show a non-flat useful life which can be divided into multiple adjacent phases of useful life, each of which can employ a different redundancy scheme.

six-month period denoted along the X axis. AFR curves for individual makes/models (e.g., Figs. 5.3(c) and 5.3(d)) are consistent with this aggregate illustration. Importantly, none of the over 60 makes/models from Google, Backblaze and NetApp displayed sudden onset of wearout[1].

The insight for disk-adaptive redundancy systems

Gradual increases in AFR, rather than a sudden rise in AFR suggests that one could anticipate disks approaching an AFR threshold. This enables disk-adaptive redundancy systems to act proactively, rather than reactively to increase redundancy such that data is never left under-protected.

4.2.4 Useful life could have multiple phases

Figure 4.6 shows a conceptual representation of an AFR curve with multiple useful life phases. Unlike the canonical AFR curve shown in Figure 2.2, the AFR curves observed in real-world deployments (for example Figures 5.3(c), 5.4(b)) show a non-flat, gradually increasing AFR during useful life. Given the gradual rise of AFRs, useful life can be decomposed into multiple, piece-wise constant phases.

Figure 4.7 shows an approximation of the length of useful life when multiple phases are considered. Each box in the figure represents the distribution over different make/models of the approximate length of total useful life (i.e. including all phases). Useful life is approximated by considering the longest period of time which can be decomposed into multiple consecutive phases (number of phases indicated by the bottom X-axis) such that the ratio between the

[1]Figures 3.2(b) and 3.8(b) in Chapter 3 show that AFR rises suddenly during wearout. This is not due to a sudden increase in AFR, but is in fact due to the AFR being calculated by the failed disks counting both failed and decommissioned disks. This is because the Backblaze dataset used in Chapter 3 did not differentiate between failed and decommissioned disks. Since decommissioning events are usually bulk events wherein large batches of disks are discontinued together, it appears as though there is a sudden increase in AFR.

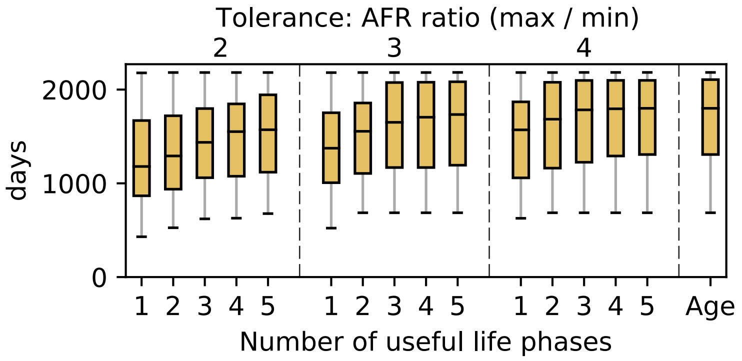

Figure 4.7: Approximation of useful life length for NetApp disks for 1-5 consecutive phases of useful life and three different tolerance levels. Each useful-life phase is approximated by an uninterrupted sequence of days during which AFR remains within the specified (atop graph) ratio between maximum and minimum AFRs. Boxes represent the distribution of the combined length of all phases for different makes/models. The box labeled "age" represents the distribution of the age of the oldest disk for different makes/models, which is an upper bound the length of useful life.

maximum and minimum AFR in each phase is under a given tolerance level (indicated by the top X-axis). The last box indicates the distribution over make/models of the age of the oldest disk, which is an upper bound to the length of useful life. As shown by Figure 4.7, the length of useful life can be significantly extended (for all tolerance levels) by considering more than one phase. Furthermore, the data show that a small number of phases suffice in practice, as the approximate length of useful life changes by little when considering four or more phases.

The insight for disk-adaptive redundancy systems

Having multiple phases of useful life implies potentially multiple redundancy transitions to take adequate advantage of lower redundancy when in phases of life where AFR is low. At the same time, each additional transition has more IO associated with it, and therefore whether to optimize redundancy for each phase of useful life is a trade-off between IO and the resultant space-savings.

4.2.5 Infancy often short-lived

Disks may go through (potentially) multiple rounds of so-called "burn-in" testing. The first tests may happen at the manufacturer's site. There may be additional burn-in tests done at the deployment site allowing most of the infant mortality to be captured before the disk is deployed in production. For the NetApp and Google disks, we see the AFR drop sharply and plateau by 20 days for most of the makes/models. Figures 5.3, 5.4 and 5.5 exhibit this property. In contrast, the Backblaze disks display a slightly longer and higher AFR during infancy, which can be directly attributed to their less aggressive on-site burn-in as shown in the AFR curves from Figure 5.6.

The insight for disk-adaptive redundancy systems

A short-lived infancy implies a larger fraction of the disk lifetime (once it is deployed) to be spent in optimized redundancy, and thus an opportunity for higher space-savings.

Pacemaker's design is heavily influenced from different deployment patterns, gradual onset of wearout and multiple useful life phases to combat an important IO problem called *transition overload* while still maximizing the benefits of disk-adaptive redundancy. This is detailed in the next chapter.

Chapter 5

Combating transition overload in disk-adaptive redundancy systems

Adapting redundancy involves dynamic transitioning of redundancy schemes, because AFRs must be learned from observation of deployed disks and because AFRs change over time due to disk aging. Changing already encoded data from one redundancy scheme to another, for example from an erasure code with parameters k_1-of-n_1 to k_2-of-n_2 can be exorbitantly IO intensive. Although HeART laid the foundation of disk-adaptive redundancy (Chapter 3), its design suffers from overwhelming bursts of urgent transition IO when applied to real-world storage clusters. We refer to this as the ***transition overload*** problem. This chapter introduces *Pacemaker*[1], a new disk-adaptive redundancy orchestration system that exploits insights from the aforementioned analyses from Chapter 4 to realize the dream of safe disk-adaptive redundancy without transition overload.

5.1 Identifying and quantifying transition overload

HeART is designed to perform redundancy transitions as a reaction to AFR changes. Therefore, by the time transition to increase redundancy is issued in response to a rise in AFR, the data is already under-protecte. And it will continue to be under-protected until that transition completes. Simple rate-limiting to reduce urgent bursts of IO would only exacerbate this problem causing data-reliability goals to be violated for even longer. Indeed, as illustrated in Figure 5.1, around 2019-09 data was under-protected for over a month, even though the entire cluster's IO bandwidth (100%) was used solely for redundancy transitions.

5.1.1 Transition overload patterns

Two common transition overload patterns are observed. First is in the case of ***trickle deployments*** described in Section 4.2.2 where disks are added a-few-at-a-time but frequently. A statistically confident AFR observation requires thousands of disks. Thus, by the time it is

[1]Pacemaker was published at the USENIX Symposium on Operating Systems Design and Implementation (OSDI), 2020 [49].

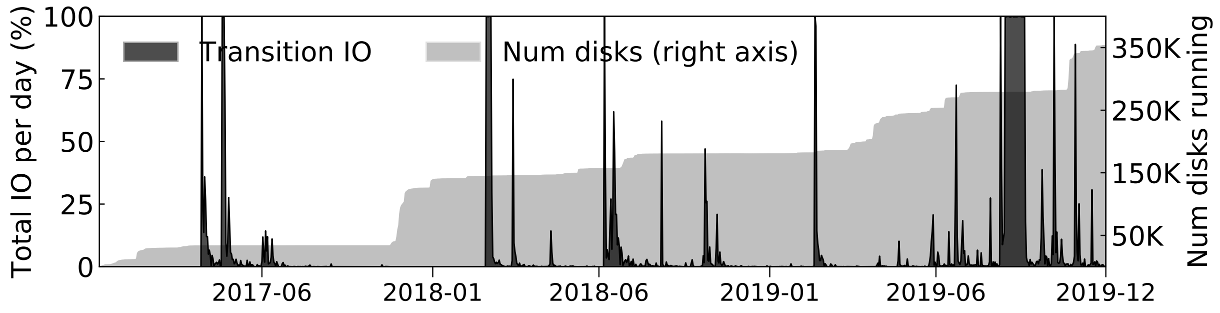

Figure 5.1: Fraction of total cluster IO bandwidth needed to perform HeART-specified transitions on Google Cluster1. HeART would require up to 100% of the cluster bandwidth for extended periods.

known that AFR for a specific make/model and age is too high for the redundancy used, the oldest thousands of that make/model will be past that age. At that point, all of those disks need immediate transition. Second is in the case of ***step deployments*** described in Section 4.2.2 where disks are added in bulk, but occasionally. Steps have sufficient disks for statistically confident AFR estimation. However, when a step reaches an age where the AFR is too high for the redundancy used, *all* disks of the step need immediate transition.

5.1.2 Simple re-encoding cannot reduce transition overload

An enticing solution that might appear to mitigate transition overload is to adapt redundancy schemes only by removing parities in low-AFR regimes and adding parities in high-AFR regimes. While this solution eliminates transition IO when reducing the level of redundancy, it does only marginally better when redundancy needs to be increased, because new parity creation cannot avoid reading all data chunks from each stripe. What makes this worse is that transitions that increase redundancy are time-critical, since delaying them would miss the MTTDL target and leave the data under-protected. Moreover, addition / removal of a parity chunk massively changes the stripe's MTTDL compared to addition / removal of a data chunk. For example, a 6-of-9 MTTDL is $10000\times$ higher than 6-of-8 MTTDL, but is only $1.5\times$ higher than 7-of-10 MTTDL. AFR changes would almost never be large enough to safely remove a parity, given default schemes like 6-of-9, eliminating almost all potential benefits of disk-adaptive redundancy.

5.2 Pacemaker: eliminating transition overload

Pacemaker is an IO efficient redundancy orchestrator for storage clusters that support disk-adaptive redundancy. In this section, first chronicle a disk's lifecycle, introducing the terminology that will be used in the rest of the chapter (defined in Table 5.1). Following this, we will outline the constraint-based approach used by Pacemaker in combating transition overload. Finally, we will identify Pacemaker's key design goals which aid in understanding the details of its architecture in the next section.

Term	*Definition*
Dgroup	Group of disks of the same make/model.
Transition	The act of changing the redundancy scheme.
RDn transition	Transition to a lower level of redundancy.
RUp transition	Transition to a higher level of redundancy.
peak-IO-cap	IO bandwidth cap for transitions.
average-IO-cap	IO bandwidth cap for transitions averaged over the total IO done during a disk's lifetime.
Rgroup	Group of disks using the same redundancy with placement restricted to the group of disks.
Rgroup0	Rgroup using the default one-scheme-fits-all redundancy used in storage clusters today.
Unspecialized disks	Disks that are a part of Rgroup0.
Specialized disks	Disks that are not part of Rgroup0.
Canary disks	First few thousand disks of a trickle-deployed Dgroup used to learn AFR curve.
Tolerated-AFR	Max AFR for which redundancy scheme meets reliability constraint.
Threshold-AFR	The AFR threshold crossing which triggers an RUp transition for step-deployed disks.

Table 5.1: Definitions of Pacemaker's terms.

5.2.1 Disk lifecycle under Pacemaker

Throughout its life, each disk under Pacemaker simultaneously belongs to a *Dgroup* and an *Rgroup*. There are as many Dgroups in a cluster as there are unique disk makes/models. Rgroups on the other hand are a function of redundancy schemes and placement restrictions. Each Rgroup has an associated redundancy scheme, and its data (encoded stripes) must reside completely within that Rgroup's disks. Multiple Rgroups can use the same redundancy scheme, but no stripe may span across Rgroups. The Dgroup of a disk never changes, but a disk may transition through multiple Rgroups during its lifetime. At the time of deployment (or "birth"), the disk belongs to *Rgroup0*, and is termed as an *unspecialized disk*. Disks in Rgroup0 use the default redundancy scheme, i.e. the conservative one-scheme-fits-all scheme used in storage clusters that do not have disk-adaptive redundancy. The redundancy scheme employed for a disk (and hence its Rgroup) changes via *transitions*. The first transition any disk undergoes is an *RDn transition*. A RDn transition changes the disk's Rgroup to one with lower redundancy, i.e. more optimized for space. Whenever the disk departs from Rgroup0, it is termed as a *specialized disk*. Disks depart from Rgroup0 at the end of their infancy. Since infancy is short-lived (Section 4.2.5), Pacemaker only considers one RDn transition for each disk.

The first RDn transition occurs at the start of the disk's useful life, and marks the start of its specialization period. As explained in Section 4.2.4, a disk may experience multiple useful life phases. Pacemaker performs a transition at the start of each useful-life phase. After the first (and only) RDn transition, each subsequent transition is an *RUp transition*. An RUp transition changes the disk's Rgroup to one with higher redundancy, i.e. less optimized for space, but the disk is still considered a specialized disk unless the Rgroup that the disk is being RUp transitioned to is Rgroup0. The space-savings (and thus cost-savings) associated with disk-adaptive redundancy are proportional to the fraction of life the disks remain specialized for.

5.2.2 Key decisions

To adapt redundancy throughout a disk's lifecycle as chronicled above, three key decisions related to transitions must be made

1. ***When should the disks transition?***
2. ***Which Rgroup should the disks transition to?***
3. ***How should the disks transition?***

5.2.3 Constraints

The above decisions need to be taken such that a set of constraints are met. An obvious constraint, central to any storage system, is that of data reliability. The *reliability constraint* mandates that all data must always meet a predefined target MTTDL. Another important constraint is the *failure reconstruction IO constraint*. This constraint bounds the IO spent on data reconstruction of failed disks, which as explained in Section 2.2.3 is proportional to AFR and scheme width. This is why wide schemes cannot be used for all disks all the time, but they can be used for low-AFR regimes of disk lifetimes (as discussed in Section 3.1.3).

Existing approaches to disk-adaptive redundancy make their decisions on the basis of only these constraints [48], but fail to consider the equally important *IO caused by redundancy transitions*. Ignoring this causes the transition overload problem, which proves to be a show-stopper for disk-adaptive redundancy systems. Pacemaker treats transition IO as a first class citizen by taking it into account for each of its three key decisions. As such, Pacemaker enforces carefully designed constraints on transition IO as well.

5.2.4 Designing IO constraints on transitions

Apart from serving foreground IO requests, a storage cluster performs numerous background tasks like scrubbing and load balancing [12, 67, 87]. Redundancy management is also a background task. In current storage clusters, redundancy management tasks predominantly consist of performing data redundancy (e.g. replicating or encoding data) and reconstructing data of failed or otherwise unavailable disks. Disk-adaptive redundancy systems add redundancy transitions to the list of IO-intensive background tasks.

There are two goals for background tasks: Goal 1: they are not too much work, and Goal 2: they interfere as little as possible with foreground IO. Pacemaker applies two IO constraints on background transition tasks to achieve these goals: (1) *average-IO constraint* and (2) *peak-IO*

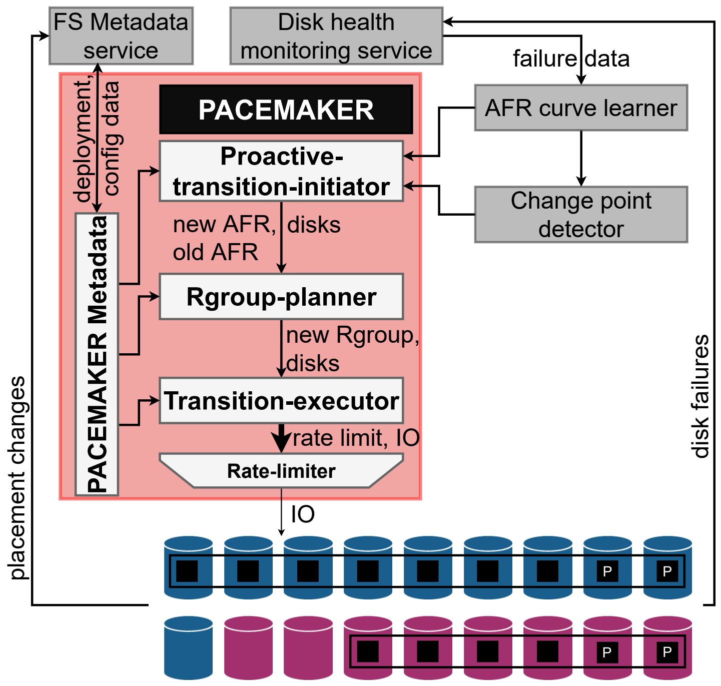

Figure 5.2: Pacemaker architecture.

constraint. The average-IO constraint achieves Goal 1 by allowing storage administrators to specify a cap on the fraction of the IO bandwidth of a disk that can be used for transitions over its lifetime. For example, if a disk can transition in 1 day using 100% of its IO bandwidth, then an average-IO constraint of 1% would mean that the disk will transition at most once every 100 days. The peak-IO constraint achieves Goal 2 by allowing storage administrators to specify the peak rate (defined as the *peak-IO-cap*) at which transitions can occur so as to limit their interference with foreground traffic. Continuing the previous example, if the peak-IO-cap is set at 5%, the disk that would have taken 1 day to transition at 100% IO bandwidth would now take at least 20 days. The average-IO constraint and the peak-IO-cap can be configured based on how busy the cluster is. For example, a cluster designed for data archival would have a lower foreground traffic, compared to a cluster designed for serving ads or recommendations. Thus, low-traffic clusters can set a higher peak-IO-cap resulting in faster transitions and potentially increased space-savings.

Although not explored as a part of this work, the IO constraints can also be specified in a richer manner than just providing single percentage numbers for the average-IO and peak-IO constraints. For example, it is well known that storage clusters suffer from diurnal foreground workload patterns. This allows for specifying the IO constraints such that the redundancy transitions are scheduled with a higher bandwidth during low foreground workload, and with a lower bandwidth during high foreground workload.

5.2.5 Design goals

The key design goals are to answer the three questions related to transitions such that the space-savings are maximized and the following constraints are met: (1) reliability constraint on all data all the time, (2) failure reconstruction IO constraint on all disks all the time, (3) peak-IO constraint on all disks all the time, and (4) average-IO constraint on all disks over time.

5.3 Design of Pacemaker

Figure 5.2 shows the high level architecture of Pacemaker and how it interacts with some other components of a storage cluster. The three main components of Pacemaker correspond to the three key decisions that the system makes as discussed in Section 5.2. The first main component of Pacemaker is the ***proactive-transition-initiator*** (Section 5.3.1), which determines when to transition disks using the AFR curves and the disk deployment information. The information of the transitioning disks and their observed AFR is passed to the ***Rgroup-planner*** (Section 5.3.2), which chooses the Rgroup to which the disks should transition. The Rgroup-planner passes the information of the transitioning disks and the target Rgroup to the ***transition-executor*** (Section 5.3.3). The transition-executor addresses how to transition the disks to the planned Rgroup in the most IO-efficient way.

Additionally, Pacemaker also maintains its own ***metadata*** and a simple ***rate-limiter***. Pacemaker metadata interacts with all of Pacemaker's components and also the storage cluster's metadata service. It maintains various configuration settings of a Pacemaker installation along with the disk deployment information that guides transition decisions. The rate-limiter rate-limits the IO load generated by any transition as per administrator specified limits. Other cluster components external-to-Pacemaker that inform it are the *AFR curve learner* and the *change point detector.* As is evident from their names, these components learn the AFR curve of each Dgroup and identify change points for redundancy transitions. The AFR curve learner receives failure data from the *disk health monitoring service*, which monitors the disk fleet and maintains their vitals.

5.3.1 Proactive-transition-initiator

Proactive-transition-initiator's role is to determine *when to transition the disks.* Below we explain Pacemaker's methodology for making this decision for the two types of transitions (RDn and RUp) and the two types of deployments (step and trickle).

Deciding when to RDn transition a disk

Recall that a disk's first transition is an RDn transition. As soon as proactive-transition-initiator observes (in a statistically accurate manner) that the AFR has decreased sufficiently, and is stable, it performs an RDn transition from the default scheme (i.e., from Rgroup0) employed in infancy to a more space-efficient scheme. This is the only RDn transition in a disk's lifetime.

Deciding when to RUp transition a disk

RUp transitions are performed either when there are too few disks in any Rgroup such that data placement is heavily restricted (which we term *purging an Rgroup*), or when there is a rise in AFR such that the reliability constraint is (going to be) violated. Purging an Rgroup involves RUp transitioning all of its disks to an Rgroup with higher redundancy. This transition isn't an imminent threat to reliability, and therefore can be done in a relaxed manner without violating the reliability constraint as explained in Section 5.3.3.

However, most RUp transitions in a storage cluster are done in response to a rise in AFR. These are challenging with respect to meeting IO constraints due to the associated risk of violating the reliability constraints whenever the AFR rises beyond the AFR tolerated by the redundancy scheme (termed *tolerated-AFR*).

In order to be able to safely rate-limit the IO load due to RUp transitions, Pacemaker takes a *proactive* approach. The key is in determining when to initiate a proactive RUp transition such that the transition can be completed before the AFR crosses the tolerated-AFR, while adhering to the IO and the reliability constraints without compromising much on space-savings. To do so, the proactive-transition-initiator assumes that its transitions will proceed as per the peak-IO constraint, which is ensured by the transition-executor. Pacemaker's methodology for determining when to initiate a proactive RUp transition is tailored differently for trickle versus for step deployments, since they raise different challenges.

Proactive-transition-initiator for trickle-deployed disks

For trickle-deployed disks, Pacemaker considers two category of disks: (1) first disks to be deployed from any particular trickle-deployed Dgroup, and (2) disks from that Dgroup that are deployed later.

Pacemaker labels the first C deployed disks of a Dgroup as *canary* disks, where C is a configurable, high enough number of disks to yield statistically significant AFR observations. For example, based on our disk analyses, we observe that C in low thousands (e.g., 3000) is sufficient. The canary disks of any Dgroup are the first to undergo the various phases of life for that Dgroup, and these observations are used to learn the AFR curve for that Dgroup. The AFR value for the Dgroup at any particular age is not known (with statistical confidence) until all canary disks go past that age. Furthermore, due to the trickle nature of the deployment, the canary disks would themselves have been deployed over weeks if not months. Thus, AFR for the canary disks can be ascertained only in retrospect. Pacemaker never changes the redundancy of the canary disks to avoid them from ever violating the reliability constraint. This does not significantly reduce space-savings, since C is expected to be small relative to the total number of disks of a Dgroup (usually in the tens of thousands).

The disks that are deployed later in any particular Dgroup are easier to handle, since the Dgroup's AFR curve would have been learned by observing the canaries. Thus, the date at which a disk among the later-deployed disks needs to RUp to meet the reliability constraints is known in advance by the proactive-transition-initiator, which it uses to issue proactive RUp transitions.

Although less probable, it might happen that the canaries have an AFR behavior that is different from the disks that follow the canaries because of some failure behavior that was introduced as a function of the disk's manufacturing batch, instead of its make/model. To prevent from making data under-reliable in such scenarios, even though the AFR curve has been learned from the canaries, Pacemaker continuously monitors the AFR curve of all disks in the storage cluster at all times. Any indication that the AFR is rising beyond what can be tolerated for any subset of disks will cause Pacemaker to RUp transition those disks even though it might mean violating its IO constraints.

Proactive-transition-initiator for step-deployed disks

Recall that in a step deployment, most disks of a Dgroup may be deployed within a few days. So, canaries are not a good solution, as they would provide little-to-no advance warning about how the AFR curve's rises would affect most disks.

Pacemaker's approach to handling step-deployments is based on two properties: (1) Step-deployments have a large number of disks deployed together, leading to a statistically accurate AFR estimation; (2) AFR curves based on a large set of disks tend to exhibit gradual, rather than sudden, AFR increases as the disk ages (Section 4.2.3). Pacemaker leverages these two properties to employ a simple *early warning* methodology to predict a forthcoming need to RUp transition a step well in advance. Specifically, Pacemaker sets a threshold, termed *threshold-AFR*, which is a (configurable) fraction of the tolerated-AFR of the current redundancy scheme employed. For step-deployments, when the observed AFR crosses the threshold-AFR, the proactive-transition-initiator initiates a proactive RUp transition.

5.3.2 Rgroup-planner

The Rgroup-planner's role is to determine *which Rgroup should disks transition to.* This involves making two *interdependent* choices: (1) the redundancy scheme to transition into, (2) whether or not to create a new Rgroup.

Choice of the redundancy scheme

At a high level, the Rgroup-planner first uses a set of selection criteria to arrive at a set of viable schemes. It further narrows down the choices by filtering out the schemes that are not worth transitioning to when the transition IO and IO constraints are accounted for.

Selection criteria for viable schemes. Each viable redundancy scheme has to satisfy the following criteria in addition to the reliability constraint:

1. must satisfy the minimum number of simultaneous failures per stripe (i.e., $n - k$).
2. must not exceed the maximum allowed stripe dimension (k).
3. must have its expected failure reconstruction IO (AFR $\times$ k $\times$ disk-capacity) be no higher than was assumed possible for Rgroup0 (since disks in Rgroup0 are expected to have the highest AFR).
4. must have a recovery time in case of failure (MTTR) that does not exceed the maximum MTTR (set by the administrator when selecting the default redundancy scheme

for Rgroup0).

Determining if a scheme is worth transitioning to. Whether the IO cost of transitioning to a scheme is worth it or not and what space-savings can be achieved by that transition is a function of the number of days disks will remain in that scheme (also known as ***disk-days***). This, in turn, depends on (1) when the disks enter the new scheme, and (2) how soon disks will require another transition out of that scheme.

The time it takes for the disks to enter the new scheme is determined by the transition IO and the rate-limit. When the disks will transition out of the target Rgroup is dependent on the future and can only be estimated. For this estimation, the Rgroup-planner needs to estimate the number of days the AFR curve will remain below the threshold that forces a transition out. This needs different strategies for the two deployment patterns (trickle and step).

Recall that Pacemaker knows the AFR curve for trickle-deployed disks (from the canaries) in advance. Recall that step-deployed disks have the property that the AFR curve learned from them is statistically robust and tends to exhibit gradual, as opposed to sudden AFR increases. The Rgroup-planner leverages these properties to estimate the future AFR behavior based on the recent past. Specifically, it takes the slope of the AFR curve in the recent past[2] and uses that to project the AFR curve rise in the future.

The number of disk-days in a scheme for it to be worth transitioning to is dictated by the IO constraints. For example, let us consider a disk running under Pacemaker that requires a transition, and Pacemaker is configured with an average-IO constraint of 1% and a peak-IO-cap of 5%. Suppose the disk requires 1 day to complete its transition at 100% IO bandwidth. With the current settings, Pacemaker will only consider an Rgroup worthy of transitioning to (assuming it is allowed to use all 5% of its IO bandwidth) if at least 80 disk-days are spent after the disk entirely transitions to it (since transitioning to it would take up to 20 days at the allowed 5% IO bandwidth).

From among the viable schemes that are worth transitioning to based on the IO constraints, the Rgroup-planner chooses the one that provides the highest space-savings.

Decision on Rgroup creation.

Rgroups cannot be created arbitrarily. This is because every Rgroup adds ***placement restrictions***, since all chunks of a stripe have to be stored on disks belonging to the same Rgroup. Therefore, Rgroup-planner creates a new Rgroup only when (1) the resulting placement pool created by the new Rgroup is large enough to overcome traditional placement restrictions such as "no two chunks on the same rack[3]", and (2) the space-savings achievable by the chosen redundancy scheme is sufficiently greater than using an existing (less-space-efficient) Rgroup.

The disk deployment pattern also affects Rgroup formation. While the rules for whether to form an Rgroup remain the same for trickle and step-deployed disks, mixing disks deployed differently impacts the transitioning techniques that can be used for eventually transitioning disks out of that Rgroup. This in turn affects how the IO constraints are enforced. Specifically,

[2]Pacemaker uses a 60 day (configurable) sliding window with an Epanechnikov kernel, which gives more weight to AFR changes in the recent past [41].

[3]Inter-cluster fault tolerance remains orthogonal to and unaffected by Pacemaker.

for trickle deployments, creating an Rgroup for each set of transitioning disks would lead to too many small-sized Rgroups. So, for trickle-deployments, the Rgroup-planner creates a new Rgroup for a redundancy scheme if and only if one does not exist already. Creating Rgroups this way will also ensure that enough disks (thousands) will go into it to satisfy placement restrictions. Mixing disks from different trickle-deployments in the same Rgroup does not impact the IO constraints, because Pacemaker optimizes the transition mechanism for few disks transitioning at a time, as is explained in Section 5.3.3. For step-deployments, due to the large fraction of disks that undergo transition together, having disks from multiple steps, or mixing trickle-deployed disks within the same Rgroup, creates adverse interactions (discussed in Section 5.3.3). Hence, the Rgroup-planner creates a new Rgroup for each step-deployment, even if there already exists one or more Rgroups that employ the chosen scheme. Each such Rgroup will contain many thousands of disks to overcome traditional placement restrictions. Per-step Rgroups also extend to the Rgroup with default redundancy schemes, implying a per-step Rgroup0. Despite having clusters with disk populations as high as 450K disks, Pacemaker's restrained Rgroup creation led to no cluster ever having more than 10 Rgroups.

Rules for purging an Rgroup.

An Rgroup may be purged for having too few disks. This can happen when too many of its constituent disks transition to other Rgroups, or they fail, or they are decommissioned leading to difficulty in fulfilling placement restrictions. If the Rgroup to be purged is made up of trickle-deployed disks, the Rgroup-planner will choose to RUp transition disks to an existing Rgroup with higher redundancy while meeting the IO constraints. For step-deployments, purging implies RUp transitioning disks into the more-failure-tolerant RGroup (RGroup0) that may include trickle-deployed disks.

5.3.3 Transition-executor

The transition-executor's role is to determine *how to transition the disks.* This involves choosing (1) the most IO-efficient technique to execute that transition, and (2) how to rate-limit the transition at hand. Once the transition technique is chosen, the transition-executor executes the transition via the rate-limiter as shown in Figure 5.2.

Transition techniques

Suppose the data needs to be conventionally re-encoded from a k_{cur}-of-n_{cur} scheme to a k_{new}-of-n_{new} scheme. The IO cost of conventional re-encoding involves reading–re-encoding–writing all the stripes whose chunks reside on each transitioning disk. This amounts to a read IO of $k_{cur}\times$disk-capacity (assuming almost-full disks), and a write IO of $k_{cur}\times$disk-capacity$\times\frac{n_{new}}{k_{new}}$ for a total IO $> 2 \times k_{cur}\times$disk-capacity for each disk.

In addition to conventional re-encoding, Pacemaker supports two new approaches to changing the redundancy scheme for disks and selects the most efficient option for any given transition. The best option depends on the fraction of the Rgroup being transitioned at once.

Type 1 (Transition by emptying disks). If a small percentage of an Rgroup's disks are being transitioned, it is more efficient to retain the contents of the transitioning disks in that Rgroup rather than re-encoding. Under this technique, the data stored on transitioning disks are simply moved (copied) to other disks within the current Rgroup. This involves reading and writing (elsewhere) the contents of the transitioning disks. Thus, the IO of transitioning via Type 1 is at most $2\times$disk-capacity, independent of scheme parameters, and therefore at least $k_{cur}\times$ cheaper than conventional re-encoding.

Type 1 can be employed whenever there is sufficient free space available to move the contents of the transitioning disks into other disks in the current Rgroup. In the case of trickle-deployments, the steady deployment of a-few-disks-at-a-time ensures that disk space is created in the Rgroup at approximately the same rate as it is removed from the Rgroup because of the transitioning disks. Thus, this is the preferred transition method for trickle-deployed disks. Once the transitioning disks are empty, they can be removed from the current Rgroup and added to the new Rgroup as "new" (empty) disks.

Type 2 (Bulk transition by recalculating parities). If a large fraction of disks in an Rgroup need to transition together, it is more efficient to transition the entire Rgroup rather than only the disks that need a transition at that time. Most cluster storage systems use systematic codes[4] [19, 31, 33, 65], wherein transitioning an entire Rgroup involves only calculating and storing new parities and deleting the old parities. Specifically, the data chunks have to be only read for computing the new parities, but they do not have to be re-written. In contrast, if only a part of the disks are transitioned, some fraction of the data chunks also need to be re-written. Thus, the IO cost for transitioning via Type 2 involves a read IO of $\frac{k_{cur}}{n_{cur}}\times$disk-capacity, and a write IO of only the new parities, which amounts to a total IO of $\frac{n_{new}-k_{new}}{k_{new}} \times \frac{k_{cur}}{n_{cur}}\times$disk-capacity for each disk in the Rgroup. This is at most $2 \times \frac{k_{cur}}{n_{cur}}\times$disk-capacity, which makes it at least $n_{cur}\times$ cheaper than conventional re-encoding.

Selecting the most efficient approach for a transition

For any given transition, the transition-executor selects the most IO-efficient of all the viable approaches. Almost always, trickle-deployed disks use Type 1 because they transition a-few-at-a-time, and step-deployed disks use Type 2 because Rgroup-planner maintains each step in a separate Rgroup.

Choosing how to rate limit a transition

Irrespective of the transitioning techniques, the transition-executor has to resolve the competing concerns of maximizing space-savings and minimizing risk of data loss via fast transitions, and minimizing foreground work interference by slowing down transitions so as to not overwhelm the foreground IO. Arbitrarily slowing down a transition to minimize interference is

[4]In systematic codes, the data chunks are stored in unencoded form. This helps to avoid having to decode for normal (i.e., non-degraded-mode) reads.

only possible when the transition is not in response to a rise in AFR. This is because a rising AFR hints at the data being under-protected if not transitioned to a higher redundancy soon. In Pacemaker, a transition without an AFR rise occurs either when disks are being RDn transitioned at the end of infancy, or when they are being RUp transitioned because the Rgroup they belong to is being purged. For all the other RUp transitions, Pacemaker carefully chooses how to rate limit the transition.

Determining how much bandwidth to allow for a given transition could be difficult, given that other transitions may be in-progress already or may be initiated at any time (we do observe concurrent transitions in our evaluations). So, to ensure that the aggregate IO of all ongoing transitions conforms to the peak-IO-cap cluster-wide, Pacemaker limits each transition to the peak-IO-cap within its Rgroup. For trickle-deployed disks, which share Rgroups, the rate of transition initiations is consistently a small percentage of the shared Rgroup, allowing disk emptying to proceed at well below the peak-IO-cap. For step-deployed disks, this is easy for Pacemaker, since a step only makes one transition at a time and its IO is fully contained in its separate Rgroup. The transition-executor's approach to managing peak-IO on a per-Rgroup basis is also why the proactive-transition-initiator can safely assume a rate-limit of the peak-IO-cap without consulting the transition-executor. If there is a sudden AFR increase that puts data at risk, Pacemaker is designed to ignore its IO constraints to continue meeting the reliability constraint—this safety valve was never needed for any cluster evaluated.

After finalizing the transitioning technique, the transition-executor performs the necessary IO for transitioning disks (read, writes, parity recalculation, etc.). We find that the components required for the transition-executor are already present and adequately modular in existing distributed storage systems. In Section 6, we show how we implement Pacemaker in HDFS with minimal effort.

Note that this design is for the common case where storage clusters are designed for a single dedicated storage service. Multiple distinct distributed storage services independently using the same underlying devices would need to coordinate their use of bandwidth (for their non-transition related load as well) in some way, which is outside the scope of this dissertation.

5.4 Evaluating Pacemaker

Pacemaker-enabled disk-adaptive redundancy using is evaluated on production logs from four large-scale real-world storage clusters, each with hundreds of thousands of disks. This evaluation has four primary takeaways: (1) Pacemaker eliminates transition overload, never using more than 5% of cluster IO bandwidth (0.2–0.4% on average) and always meets target MTTDL, in stark contrast to prior work approaches that do not account for transition IO load; (2) Pacemaker provides more than 97% of idealized-potential space-savings, despite being proactive, reducing disk capacity needed by 14–20% compared to one-size-fits-all; (3) Pacemaker's behavior is not overly sensitive across a range of values for its configurable parameters; (4) Pacemaker copes well with the real-world AFR characteristics explained in Chapter 4. For example, it successfully combines the "multiple useful-life phases" observation with efficient transitioning schemes. This evaluation also shows Pacemaker in action by measuring disk-adaptive redundancy in Pacemaker-enhanced HDFS.

Evaluation methodology.

Pacemaker is simulated chronologically for each of the four cluster logs described in Section 4: three clusters from Google and one from Backblaze. For each simulated date, the simulator changes the cluster composition according to the disk additions, failures and decommissioning events in the log. Pacemaker is provided the log information, as though it were being captured live in the cluster. IO bandwidth needed for each day's redundancy management is computed as the sum of IO for failure reconstruction and transition IO requested by Pacemaker, and is reported as a fraction of the configured cluster IO bandwidth (100MB/sec per disk, by default).

Pacemaker was configured to use a peak-IO-cap of 5%, an average-IO constraint of 1% and a threshold-AFR of 75% of the tolerated-AFR, except for the sensitivity studies in Section 5.4.3. For comparison, we also simulate (1) an idealized disk-adaptive redundancy system in which transitions are instantaneous (requiring no IO) and (2) the prior state-of-the-art approach (HeART) for disk-adaptive redundancy. For all cases, Rgroup0 uses 6-of-9, representing a one-size-fits-all scheme reported in prior literature [31]. The required target MTTDL is then back-calculated using the 6-of-9 default and an assumed tolerated-AFR of 16% for Rgroup0. These configuration defaults were set by consulting storage administrators of clusters we evaluated.

5.4.1 Pacemaker on Google Cluster1 in-depth

Figure 5.3(a) shows the IO generated by Pacemaker (and disk count) over the $\approx$3-year lifetime of Google Cluster1. Over time, the cluster grew to over 350K disks comprising of disks from 7 makes/models (Dgroups) via a mix of trickle and step deployments. Figure 5.3(c) and Figure 5.3(d) show AFR curves of 2 of the 7 Dgroups (obfuscated as G-1 and G-2 for confidentiality) along with how Pacemaker adapted to them at each age. G-1 disks are trickle-deployed whereas G-2 disks are step-deployed. The other 5 Dgroups are omitted due to lack of space. Figure 5.3(b) shows the corresponding space-savings (the white space above the colors).

All disks enter the cluster as unspecialized disks, i.e. Rgroup0 (dark gray region in the Figure 5.3(a) and left gray region of Figs. 5.3(c) and 5.3(d)). Once a Dgroup's AFR reduces sufficiently, Pacemaker RDn transitions them to a specialized Rgroup (light gray area in Figure 5.3(a)). Over their lifetime, disks may transition through multiple RUp transitions over the multiple useful-life phases. Each transition requires IO, which is captured in blue in Figure 5.3(a). For example, the sudden drop in the unspecialized disks, and the blue area around 2018-04 captures the Type 2 transitions caused when over 100K disks RDn transition from Rgroup0 to a specialized Rgroup. The light gray region in Figure 5.3(a) corresponds to the time over which space-savings are obtained, which can be seen in Figure 5.3(b).

Many transitions with no transition overload

Pacemaker successfully bounds all redundancy management IO comfortably under the configured peak-IO-cap throughout the cluster's lifetime. This can be seen via an imaginary horizontal line at 5% (the configured peak-IO-cap) that none of the blue regions goes above.

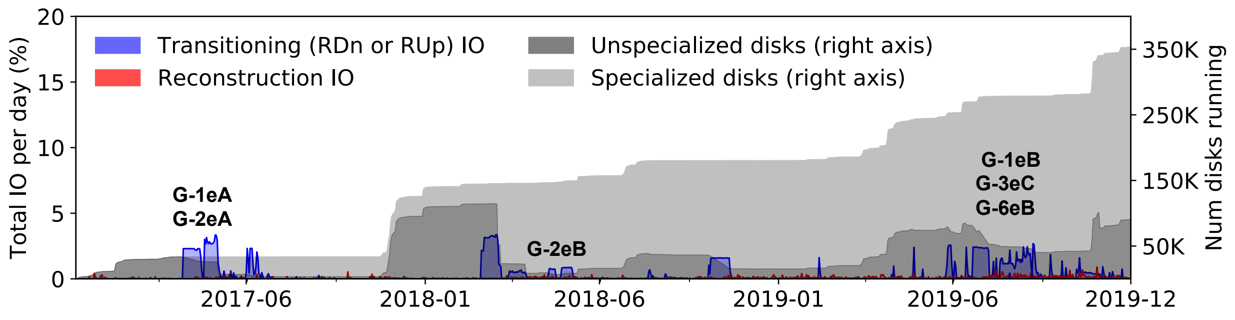

(a) Redundancy management IO due to Pacemaker over its 2.5+ year lifetime broken down by IO type. This is identical to Figure ?? with the left Y-axis only going to 20% to show the detailed IO activity in the cluster.

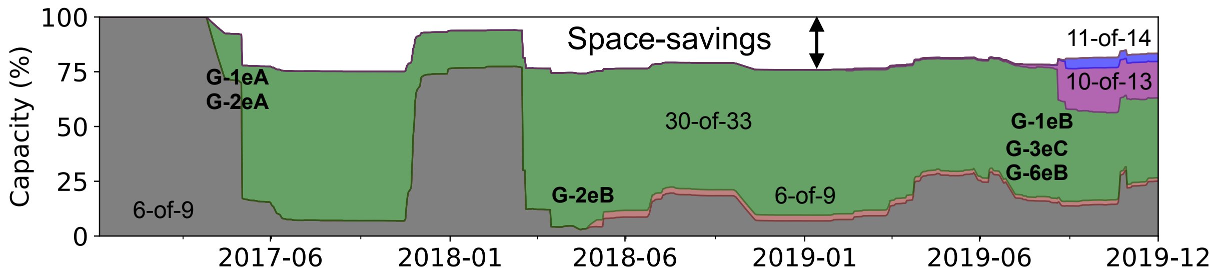

(b) Space-savings due to Pacemaker. Each colored region represents the fraction of cluster capacity that is using a particular redundancy scheme. 6-of-9 is the default redundancy scheme (Rgroup0's).

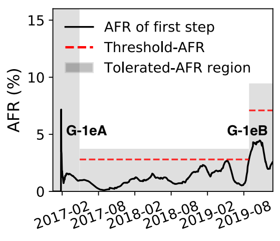

(c) G-1 (step) AFR curve

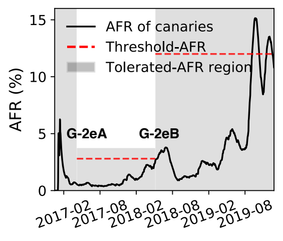

(d) G-2 (trickle) AFR curve

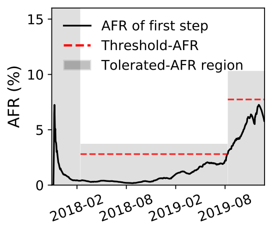

(e) G-6 (step) AFR curve

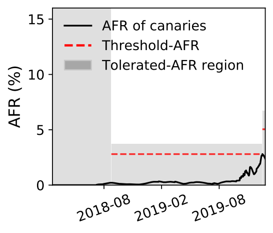

(f) G-4 (trickle) AFR curve

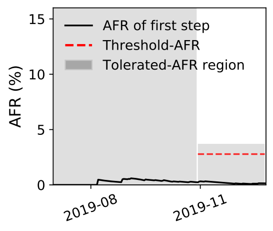

(g) G-8 (step) AFR curve

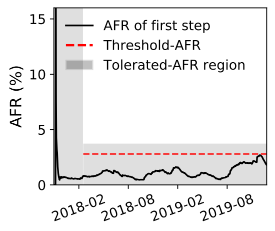

(h) G-5 (step) AFR curve

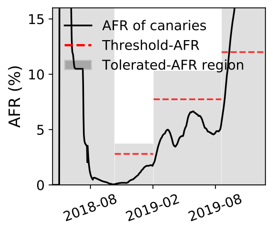

(i) G-3 (trickle) AFR curve

Figure 5.3: Detailed IO analysis and space savings achieved by Pacemaker-enabled adaptive redundancy on Google Cluster1.

Recall that Pacemaker rate-limits the IO within each Rgroup to ensure simultaneous transitions do not violate the cluster's IO cap. Events ***G-1eA*** and ***G-2eA*** are examples of events where both G-1 and G-2 disks (making up almost 100% of the cluster at that time) request transitions at the same time. Despite that, the IO remains bounded below 5%. ***G-3eC*** and ***G-6eB*** also show huge disk populations of G-3 and G-6 Dgroups (AFRs not shown) requesting almost simultaneous RUp transitions, but Pacemaker's design ensures that the peak-IO constraint is never violated. This is in sharp contrast with HeART's frequent transition overload, shown in Figure 5.1.

Disks experience multiple useful-life phases

G-1, G-3, G-6 and G-7 disks experience two phases of useful life each. In Figure 5.3(a), events ***G-1eA*** and ***G-1eB*** mark the two transitions of G-1 disks through its multiple useful lives as shown in Figure 5.3(c). In the absence of multiple useful-life phases, Pacemaker would have RUp transitioned G-1 disks to Rgroup0 in 2019-05, eliminating space-savings for the remainder of their time in the cluster. Section 5.4.3 quantifies the benefit of multiple useful-life phases for all four clusters. While Pacemaker exploits multiple useful-life phases, its IO constraints prevent it from changing redundancy in reaction to all AFR fluctuations (for example, the AFR jitter observed between points G-1eA and G-2-eB for G-1 disks, and between G-2eA and G-2eB disks for G-2 disks). The decomposition of an AFR curve into only a handful of useful-life phases prevents the storage cluster from getting overwhelmed with the IO caused due to redundancy transitions.

MTTDL always at or above target

Along with the AFR curves, Figs. 5.3(c) and 5.3(d) also show the upper bound on the AFR for which the reliability constraint is met (top of the gray region). Pacemaker sufficiently protects all disks throughout their life for all Dgroups across evaluated clusters.

Substantial space-savings achieved

Pacemaker provides 14% average space-savings (Figure 5.3(b)) over the cluster lifetime to date. Except for 2017-01 to 2017-05 and 2017-11 to 2018-03, which correspond to infancy periods for large batches of new empty disks added to the cluster, the entire cluster achieves $\approx$20% space-savings. Note that the apparent reduction in space-savings from 2017-11 to 2018-03 isn't actually reduced space in absolute terms. Since Figure 5.3(b) shows relative space-savings, the over 100K disks deployed around 2017-11, and their infancy period makes the space-savings appear reduced relative to the size of the cluster.

5.4.2 Pacemaker on the other three clusters

Figs. 5.4(a), 5.5(a), 5.6(a) compares the transition IO incurred by Pacemaker to that for HeART [48] for Google Cluster2, Google Cluster3 and Backblaze respectively, along with the corresponding space-savings achieved by Pacemaker. While clusters using HeART would suffer transition overload, the same clusters under Pacemaker always had all their transition

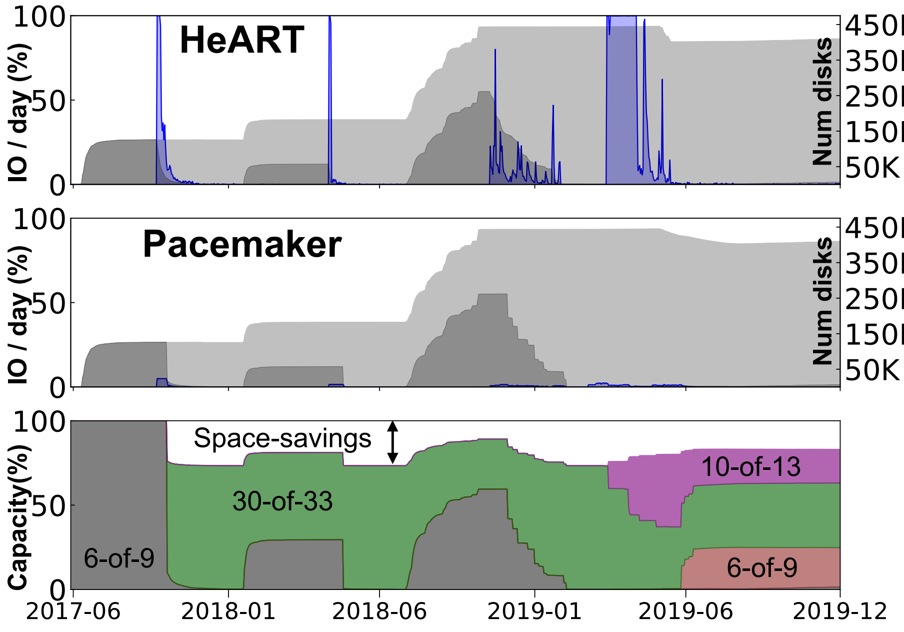

(a) Google Cluster2

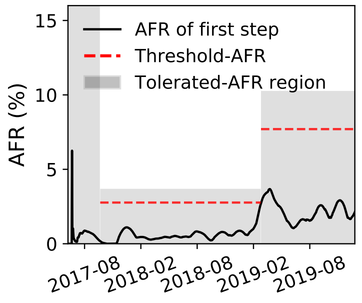

(b) G-1 (step) AFR curve

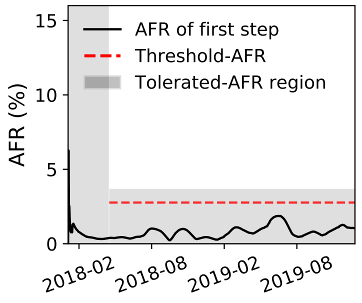

(c) G-5 (step) AFR curve

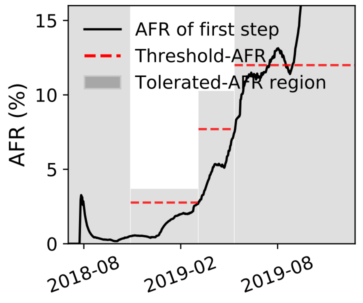

(d) G-3 (step) AFR curve

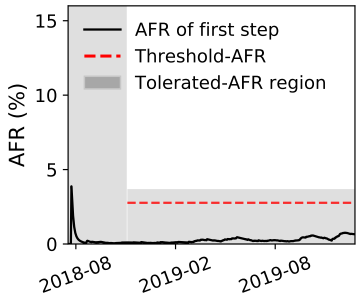

(e) G-4 (step) AFR curve

Figure 5.4: Google Cluster2 transition IO, space-savings and individual Dgroup AFR curves.

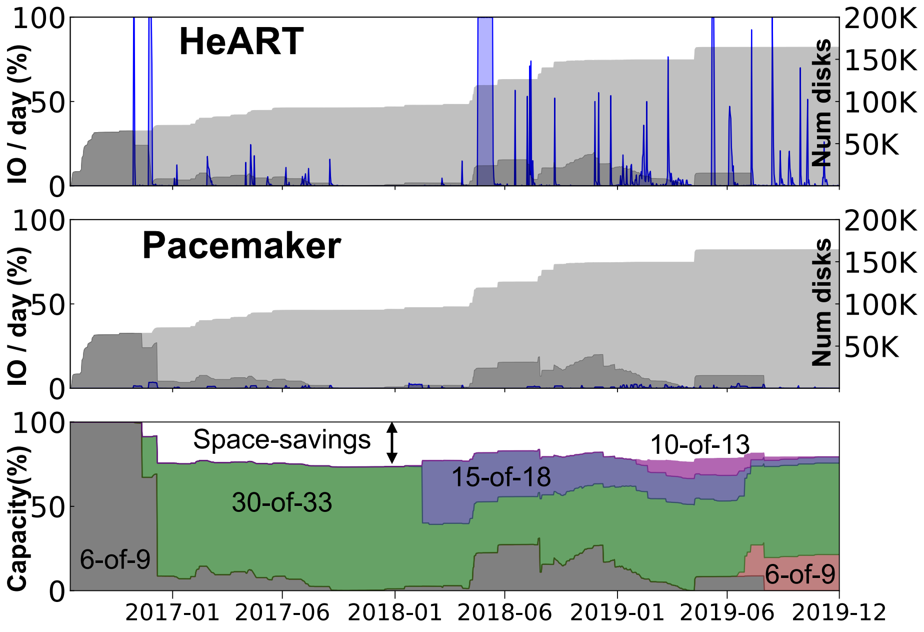

(a) Google Cluster3

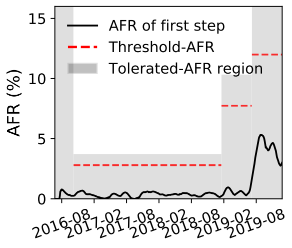

(b) G-2 (step) AFR curve

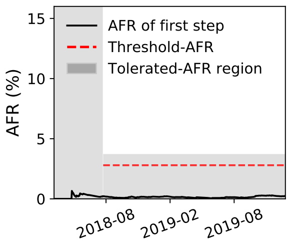

(c) G-4 (step) AFR curve

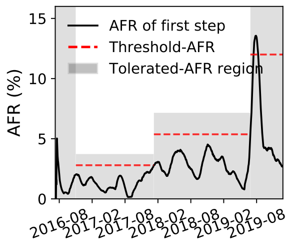

(d) G-1 (step) AFR curve

Figure 5.5: Google Cluster3 transition IO, space-savings and individual Dgroup AFR curves.

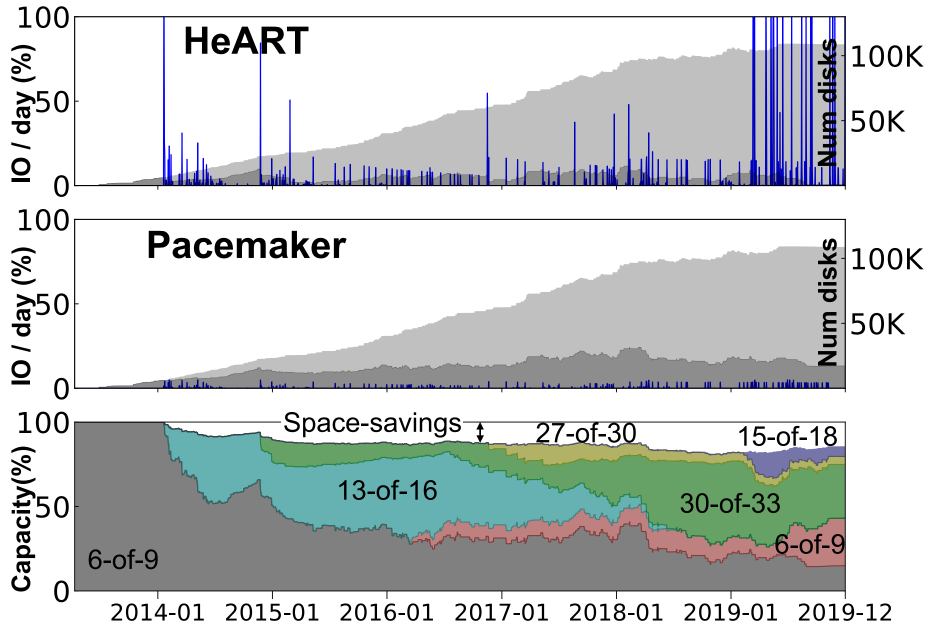

(a) Backblaze Cluster

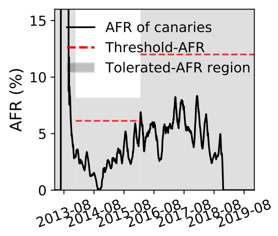

(b) S-4 (trickle)

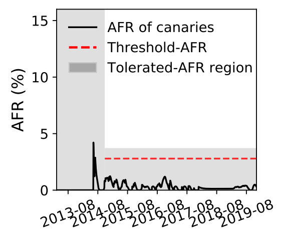

(c) H-4A (trickle)

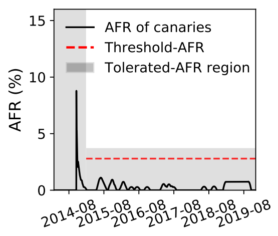

(d) H-4B (trickle)

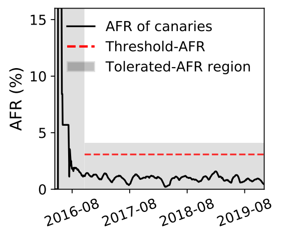

(e) S-8C (trickle)

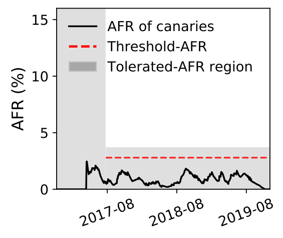

(f) S-8E (trickle)

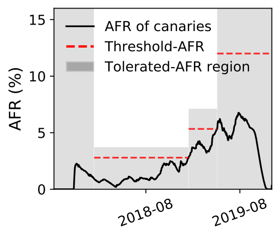

(g) S-12E (trickle)

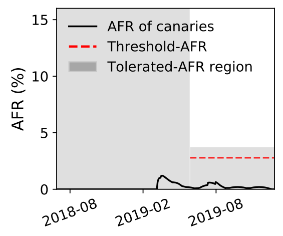

(h) H-12E (trickle)

Figure 5.6: Backblaze cluster transition IO, space-savings and individual Dgroup AFR curves.

IO under the peak-IO-cap of 5%. In fact, on average, only 0.21–0.32% percent of the cluster IO bandwidth was used for transitions. The average space-savings for the three clusters are 14–20%.

Google Cluster2

Figure 5.4(a) shows the transition overload and space-savings in Google Cluster2 and the corresponding space-savings. All Dgroups in Google Cluster2 are step-deployed. Thus, it is not surprising that Figure 5.9 shows that over 98% of the transitions in Cluster2 were Type 2 transitions (bulk parity recalculation). Cluster2's disk population exceeds 450K disks. Even at such large scales, Pacemaker obtains average space-savings of almost 17% and peak space-savings of over 25%. This translates to needing 100K fewer disks.

Google Cluster3

Google Cluster3 (Figure 5.4(a)) is not as large as Cluster1 or Cluster2. At its peak, Cluster3 has a disk population of approximately 200K disks. But, it achieves the highest average space-savings (20%) among clusters evaluated. Like Cluster2, Cluster3 is also mostly step-deployed.

Backblaze Cluster

Backblaze (Figure 5.6(a)) is a completely trickle-deployed cluster. The dark grey region across the bottom of Figure 5.6(a)'s Pacemaker plot shows the persistent presence of canary disks throughout the cluster's lifetime. Unlike the Google clusters, the transition IO of Backblaze does not produce bursts of transition IO that lasts for weeks. Instead, since trickle-deployed disks transition a-few-at-a-time, we see transition work appearing continuously throughout the cluster lifetime of over 6 years. The rise in the transition IO spikes in 2019, for HeART, is because of large capacity 12TB disks replacing 4TB disks. Unsurprisingly, under Pacemaker, most of the transitions are done using Type 1 (transitioning by emptying disks) as shown in Figure 5.9. The average space-savings obtained on Backblaze are 14%.

5.4.3 Sensitivity analyses and ablation studies

Sensitivity to IO constraints

The peak-IO constraint governs Figure 5.7, which shows the percentages of optimal space-savings achieved with Pacemaker for peak-IO-cap settings between 1.5% and 7.5%. A peak-IO-cap of up to 7.5% is used in order to compare with the IO percentage spent for existing background IO activity, such as scrubbing. By scrubbing all data once every 15 days [12], the scrubber uses around 7% IO bandwidth, and is a background work IO level tolerated by today's clusters.

The Y-axis captures how close the space-savings are for the different peak-IO-caps compared to "Optimal savings", i.e. an idealized system with infinitely fast transitions. Pacemaker's default peak-IO-cap (5%) achieves over 97% of the optimal space-savings for each of the four clusters. For peak-IO constraint set to <=2.5%, some RUp transitions in Google

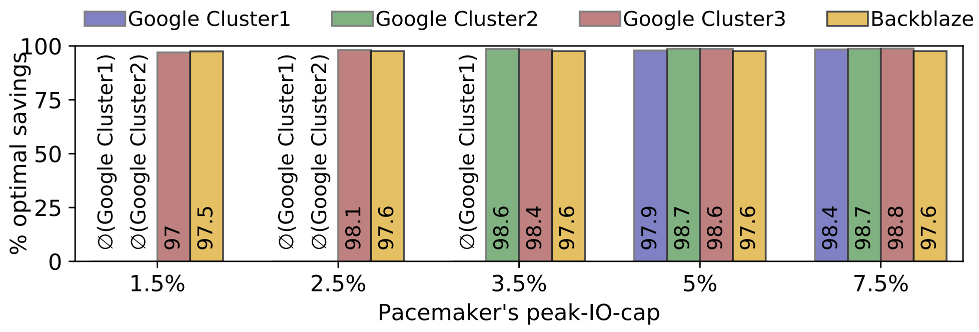

Figure 5.7: Pacemaker's sensitivity to the peak-IO constraint.

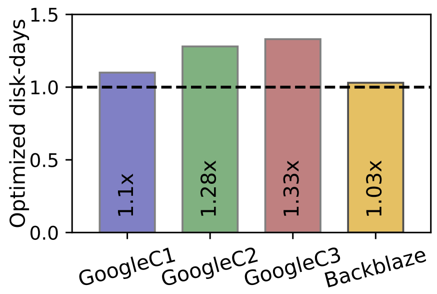

Figure 5.8: Multiple useful-life phases

Cluster1 and Cluster2 become too aggressively rate-limited causing a subsequent AFR rise to violate the peak-IO constraints. We indicate this as a failure, and show it as "ϕ". The same situation happens for Google Cluster1 at 3.5%.

Sensitivity to threshold-AFR

The threshold-AFR determines when proactive RUp transitions of step-deployed disks are initiated. Conceptually, the threshold-AFR governs how risk-averse the admin wants to be. Lowering the threshold would trigger an RUp transition when disks are farther away from the tolerated-AFR (more risk-averse), and vice-versa. We evaluated Pacemaker for threshold-AFRs of 60%, 75% and 90% of the respective Rgroups' tolerated-AFRs. We found that Pacemaker's space-savings is not very sensitive to threshold-AFR, with space-savings only 2% lower at 60% than at 90%. Data remained safe at each of these settings, but would become unsafe with higher values.

Contribution of multiple useful-life phases

Figure 5.8 compares the increased number of disk-days spent in specialized Rgroups because of considering multiple useful-life phases. In the best case, Google Cluster2 spent 33% more disk-days in specialized redundancy, increasing overall space-savings from 16% to 19%. Note that in large-scale storage clusters, even 1% space-savings are considered substantial as it represents thousands of disks.

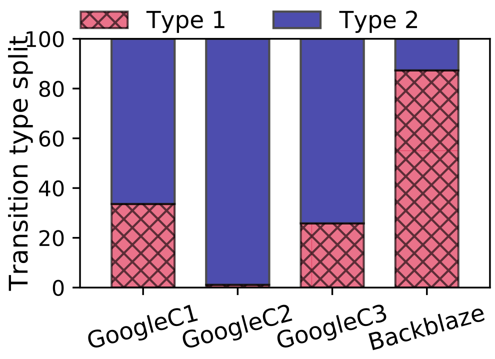

Figure 5.9: Transition type distribution

Contribution of transition types

By proactively keeping step-deployed disks in distinct Rgroups and using specialized transitioning schemes whenever possible, instead of using simple re-encoding for all transitions, Pacemaker reduces total transition IO by 92–96% for the four clusters. Figure 5.9 shows what percentage of transitions were done via Type 1 (disk emptying) vs. Type 2 (bulk parity recalculation). As expected, Google clusters rely more on Type 2 transitions, because most disks are step-deployed. In contrast, the Backblaze cluster is entirely trickle-deployed and hence mostly uses Type 1 transitions. The small percentage of Type 2 transitions in Backblaze occur when Rgroups are purged.

Chapter 3 and Chapter 5 have detailed the design principles and algorithms needed for a disk-adaptive redundancy system. In the next chapter we put these design principles to test by incorporating some of these principles in an existing distributed storage system.

Chapter 6

Realizing disk-adaptive redundancy in practice

In this chapter, we describe the building of a prototype that implements Pacemaker (Chapter 5) in the popularly (and commercially) used Hadoop distributed file system (HDFS) [96]. The intent of this implementation exercise is twofold. First, we describe what changes are required to incorporate disk-adaptive redundancy in an existing distributed storage system. Second (and more broadly), inspired by the insights gained from our implementation exercise, we describe important architectural elements meant to inform the architecture and implementation of future cluster storage systems that aim to natively support disk-adaptive redundancy. We built our prototype using HDFS v3.2.0, which natively supports erasure coding. Our prototype is open-sourced and is available at `https://github.com/thesys-lab/pacemaker-hdfs.git`.[1].

6.1 Background on HDFS architecture

HDFS is a popular open source distributed file system, widely employed in the industry for storing large volumes of data. HDFS draws heavy inspiration from the Google File System (GFS) [34, 96]. has a central metadata server called Namenode (Namenode, akin to the master node in GFS) and a collection of servers containing the data stored in the file system, called Datanodes (Datanode, akin to chunkservers in GFS). Clients interact with the Namenode only to perform operations on file metadata (containing a collection of the Datanodes that store the file data). Clients directly request the data from the Datanodes. Each Datanode stores data on its local drives using a local file system such as Ext4 [20, 58].

[1]We note that this prototype is solely from a functional perspective, and not for production use since it is not optimized from the performance perspective. This is because the performance metrics for practical disk-adaptive redundancy are dependent on large storage clusters with tens of thousands of disks; a setup that is difficult to replicate in an academic context.

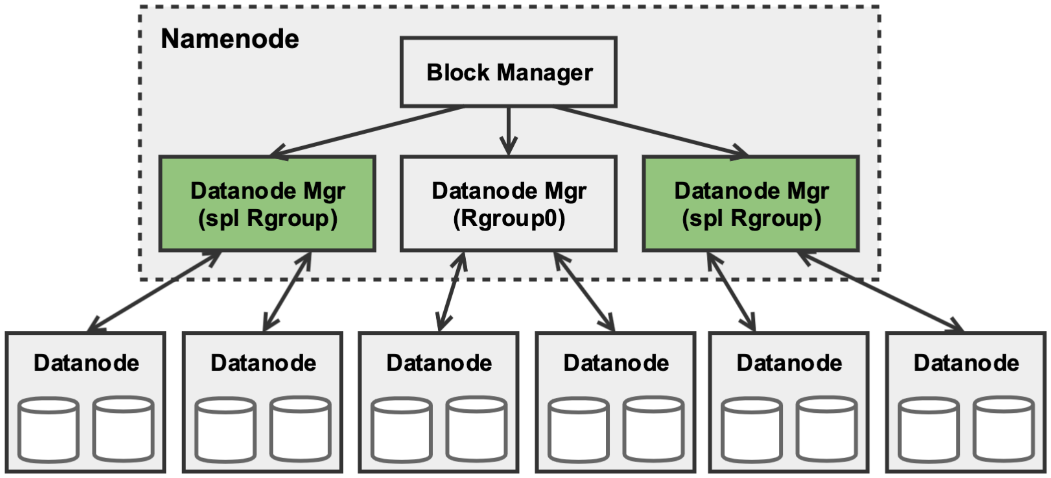

Figure 6.1: Pacemaker-enhanced HDFS architecture.

6.2 Incorporating Pacemaker in HDFS

This section describes how key components of Pacemaker are realized in HDFS. This is meant to be a guideline of the changes required to convert an existing distributed storage system which does not perform disk-adaptive redundancy into one that can perform efficient disk-adaptive redundancy.

6.2.1 Realizing Dgroups in HDFS

This design makes a simplifying assumption that all disks belonging to a Datanode are of the same Dgroup and are deployed together (this could be loosened easily). Under this simplifying assumption, conceptually, an Rgroup would consist of a set of Datanodes that need to be managed independent of other such sets of Datanodes as shown in Fig 6.1.

6.2.2 Realizing Rgroups in HDFS

The Namenode maintains a DatanodeManager, which is a gateway for the Namenode to interact with the Datanodes. The DatanodeManager maintains a list of the Datanodes, along with their usage statistics. The DatanodeManager also contains a HeartBeatManager which handles the periodic keep-alive heartbeats from Datanodes. A natural mechanism to realize Rgroups in HDFS is to have one DatanodeManager per Rgroup. Note that the sets of Datanodes belonging to the different DatanodeManagers are mutually exclusive. Implementing Rgroups with multiple DatanodeManagers has several advantages.

6.2.3 Incorporating the transition-executor in HDFS

Type 1 (transitioning by emptying disks)

An important part of Pacemaker functionality is transitioning Datanodes between Rgroups. Recall from Section 5.3.3 that one of Pacemaker's preferred way of transitioning trickle-deployed disks across Rgroups is by emptying the disks. In HDFS, the planned removal of a Datanode from a HDFS cluster is called decommissioning. Pacemaker equipped HDFS re-uses decommissioning to remove a Datanode from the set of Datanodes managed by one DatanodeManager and then adds it to the set managed by another, effectively transitioning a Datanode from one Rgroup to another.

Type 2 (transitioning by bulk parity re-calculation)

Type 2 transitions are meant to transition the entire Rgroup from one redundancy scheme to another. Type 2 transitions are usually observed when transitioning step-deployed disks as mentioned in Section 5.3.3. Type 2 transitions in Pacemaker equipped HDFS has two parts: add Datanodes in Rgroup A into Rgroup B and change the encoding scheme of files and directories in Rgroup A to that of Rgroup B. There are some challenges in implementing this in HDFS. First, in the currently supported erasure coding version in HDFS (called "Striped"), data blocks are split into smaller "cells". A collection of these cells across HDFS data blocks in different Datanodes form a stripe. This complicates the process of transitioning at the HDFS block level because doing so might affect multiple stripes together causing data inconsistency. Second, transitioning the entire file should reflect as though it happened atomically even though the actual transitioning happens stripe-by-stripe. Third, changing the erasure coding scheme should respect the block placement policy of the target Rgroup. Finally, throughout the transitioning process there should be continued forward progress, i.e. the transitioning and transitioned data should be able to be read by clients at all times.

To overcome those challenges, we come up with the following design. First, we set the cell size to be the HDFS block size. That means the whole block is a single cell, which simplifies the transitioning implementation, which (conceptually) can now happen at the HDFS block level. This is a reasonable assumption, and is only a stop-gap requirement since an erasure coding implementation where an entire HDFS block is an erasure coded block is proposed (as the "Contiguous" method) and is the development pipeline [32]. Second, we create temporary shadow inode using the snapshot feature in HDFS, and perform the transitioning from the original file to the newly created shadow file. This mechanism ensures forward progress by allowing clients to keep reading the previous file throughout the transitioning period. At the end of transitioning, we rename the shadow file to the original file, which ensures the atomicity of the transitioning operation. Third, we only transfer those necessary blocks to form new stripes and respect the requirement of the block placement policy in target Rgroup. That can minimize the data transfer during Type 2 transitions. Fourth, we re-use the existing reconstruction mechanism of the erasure coding module in HDFS to compute new parity blocks according to the erasure coding scheme in the target Rgroup. Finally, we update the metadata in Namenode and delete those blocks are not useful including old parity blocks and the old copy of transferred blocks.

6.2.4 Purging Rgroups

When a Dgroup's Datanode population drops below a threshold, Pacemaker purges the Rgroup and moves the Datanodes to the next most space efficient Rgroup. The Rgroup purging process is conceptually the same as transitioning all Datanodes to another Rgroup as discussed above. A caveat is that because newly introduced Datanodes are empty when they join an Rgroup, bulk Datanode retirement may cause load imbalance. Pacemaker suggests explicitly suggests calling the HDFS load balancer after every retirement (and even periodically if afforded), whose job is to balance the data between data-rich Datanodes to the data-poor Datanodes.

6.2.5 Implementing Pacemaker's IO constraints in HDFS

Handling the average-IO constraint

Recall from Section 5.2.4 that Pacemaker has a average-IO constraint that caps the average IO spent on redundancy transitions over the lifetime of a disk. The average-IO constraint can be easily incorporated into HDFS through the DatanodeManager. Each DatanodeManager maintains per-Datanode metrics such as the amount of IO performed, the load (im)balance, etc. By adding "transition-IO" as another metric that is tracked by the DatanodeManager, we can easily keep track of how much IO is spent over the lifetime of a Datanode (and thus the disks attached to that Datanode).

Handling the peak-IO constraint

The large data movement involved in both Type 1 and Type 2 result in significant use of the network bandwidth. Recall from Section 5.2.4 that Pacemaker's design includes a peak-IO constraint that puts a cap on the rate at which transitions can happen so as to minimize interference with foreground IO traffic, which if not done could negatively affect both throughput and latency.

To implement the peak-IO constraint in Pacemaker equipped HDFS, our design uses the wait-based data transfer throttler, which is originally used in sending and receiving data blocks, journaling, and image transferring. To make use of the throttler in Type 1 and Type 2 transitions, a custom decorator is developed on top of of Javas output stream which has a rate-limiter embedded in it. In Pacemaker equipped HDFS, we wrap the output stream that is used to perform Type 1 and Type 2 transitions by the decorated custom throttler. Finally, given a configured peak-IO cap, the throttled output stream can automatically control the data transfer speed to fulfill the configured bandwidth requirement to meet the peak-IO constraint and ensure predictable performance.

6.2.6 Evaluating Pacemaker equipped HDFS

This section describes basic experiments with the Pacemaker equipped HDFS, focusing on its functioning and operation. Note that Pacemaker is designed for longitudinal disk deployments over several years, a scenario that cannot be reproduced identically in laboratory settings.

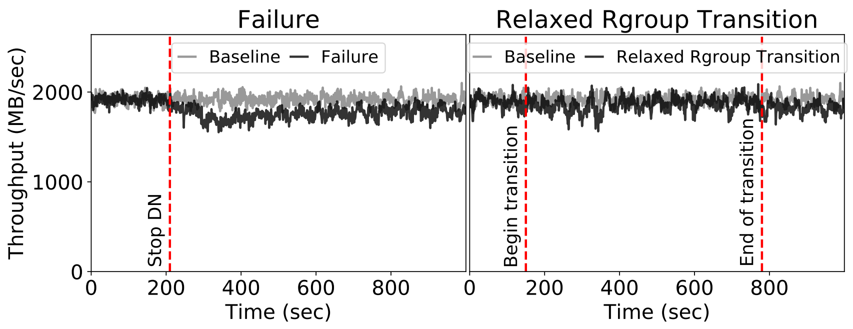

Figure 6.2: DFS-perf reported throughput for baseline, with one Datanode failure and one Rgroup transition.

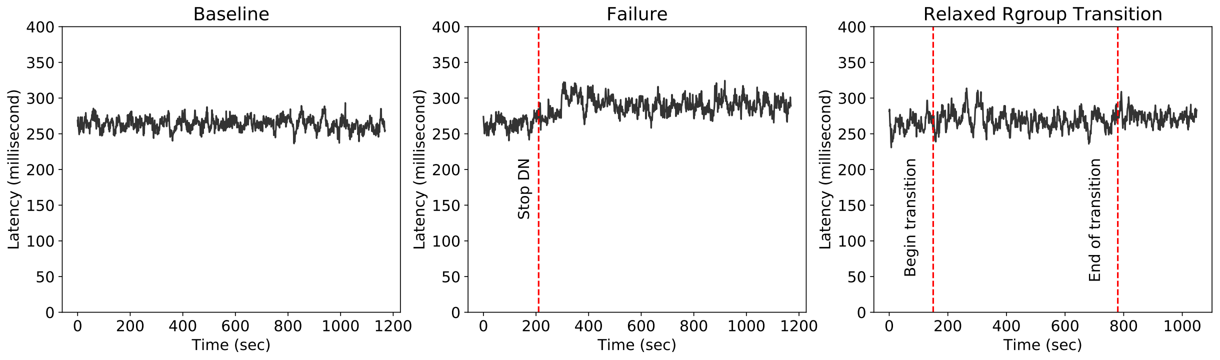

Figure 6.3: DFS-perf reported latency for baseline, with one Datanode failure and one Rgroup transition.

Hence, these HDFS experiments are aimed to display that integrating Pacemaker with an existing storage system is straightforward, rather than on the long-term aspects like overall space-savings or transition IO behavior over cluster lifetime as evaluated via simulation in Chapter 5.

The HDFS experiments run on a PRObE Emulab cluster housed at Carnegie Mellon University [35]. Each machine has a Dual-Core AMD Opteron Processor, 16GB RAM, and Gigabit Ethernet. We use a 21-node cluster running HDFS 3.2.0 with one Namenode and 20 Datanodes. Each Datanode has a 10GB partition on a 10000 RPM HDD for a total cluster size of 200GB. We statically define the cluster to be made up of two Rgroups of ten Datanodes each, one using the 6-of-9 erasure coding scheme and the other using a 7-of-10 scheme. DFS-perf [38], a popular open-source HDFS benchmark is used, after populating the cluster to 60% full. Each DFS-perf client sequentially reads one file over and over again (size=768MB), for a total read size of about 1.75TB over 40 iterations. We use 60 DFS-perf clients, running on 20 nodes separate from the HDFS cluster.

We focus on the behavior of a Datanode as it transitions between Rgroups, compared with baseline HDFS performance (where all Datanodes are healthy) and its behavior while recovering from a failed Datanode. Figure 6.2 shows the client throughput after the setup phase, followed by a noticeable drop in client throughput when a Datanode fails (emulated by stopping the Datanode). This is caused by the reconstruction IO that recreates the data from the failed node. Read latency exhibits similar behavior as shown in Figure 6.3. Eventually, throughput settles at about 5% lower than prior to failure, since now there are 19 Datanodes. The Relaxed Rgroup Transition refers to the customized throttlable output stream that implements the peak-IO constraint as explained in Section 6.2.5. The impact of throttling seen in both throughput and latency when comparing the sudden non-throttled recovery (which is an emulation of sudden transitions shown via the "Failure" plots in Figure 6.2 and Figure 6.3) to the throttled transitions (shown via the "Relaxed Rgroup Transition" plots in the same figures). The gradual reduction of throughput and gradual increase of latency maintains predictable performance for on-going foreground tasks.

Figure 6.2 also shows client throughput when a node is RDn transitioned from 6-of-9 to 7-of-10. There is minor interference during the transition, which can be attributed to the data movement that HDFS performs as a part of decommissioning. The transition requires less work than failed node reconstruction, yet takes longer to complete because Pacemaker limits the transition IO. Eventually, even though 20 Datanodes are running, the throughput is lower by $\approx$5% (one Datanode's throughput). This happens because Pacemaker empties the Datanode before it moves into the new Rgroup, and load-balancing data to newly added Datanodes happens over a longer time-frame. Experiments with RUp transition showed similar results.

6.2.7 Salient features of this architecture

Right level of control and view of the system.

Since the DatanodeManager resides below the block layer, when the data needs to be moved for redundancy adaptations, the logical view of the file remains unaffected. Only the mapping from HDFS blocks to Datanodes gets updated in the inode. The statistics maintained by the DatanodeManager can be used to balance load across Rgroups.

Minimizing changes to the HDFS architecture and maximizing re-purposing of existing HDFS mechanisms

This design obviates the need to change HDFS's block placement policy, since it is implemented at the DatanodeManager level. Block placement policies are notoriously hard to get right. Moreover, block placement decisions are affected by fault domains and network topologies, both of which are orthogonal to the goals of Pacemaker, and thus best left untouched. Likewise, the code for reconstruction of data from a failed Datanode need not be touched, since all of the reads (to reconstruct each lost chunk) and writes (to store it somewhere else) will occur within the set of nodes managed by its DatanodeManager. Existing mechanisms for adding and decommissioning nodes managed by the DatanodeManager can be re-purposed for Pacemaker's Type 1 transitions (described below).

Flexible Rgroup-specific customizations are possible

This design allows for flexibility to add Rgroup-specific functionality in the future. For example, reliability tiering could be performed by allowing sets of Rgroups have different reliability targets. No architectural change would have to be done in order to enable this functionality.

Cost of maintaining multiple DatanodeManagers is small

Each DatanodeManager maintains two threads: a HeartbeatManager and a DatanodeAdminManager. The former tracks and handles heartbeats from each Datanode, and the latter monitors the Datanodes for performing decommissioning and maintenance. The number of DatanodeManager threads in the Namenode will increase from two to $2\times$ the number of Rgroups. Fortunately, even for large clusters, we observe that the number of Rgroups would not exceed the low tens (Section 6.2.6). The Namenode is usually a high-end server compared to the Datanodes, and an additional tens of threads shouldn't affect performance.

File access interface remains unchanged

Pacemaker does not change the file manipulation API or client access paths. But, there is one corner-case related to transitions when file reads can be affected internally. To read a file, a client queries the Namenode for the inode and caches it. Subsequently, the reads are performed directly from the client to the Datanode. If the Datanode transitions to another Rgroup while the file is still being read, the HDFS client may find that that Datanode no longer has the requested data. But, because this design uses existing HDFS decommissioning for transitions, the client software knows to react by re-requesting the updated inode from the Namenode and resuming the read.

6.3 Guidelines for designing future disk-adaptive redundancy systems

In this section, we describe the insights gleaned from our exercise of incorporating Pacemaker into HDFS. These insights are meant to serve as guidelines for designing new cluster storage systems that intend to support disk-adaptive redundancy.

6.3.1 Decoupling the data reliability target from the data redundancy target

Today's cluster storage systems are designed to specify the redundancy scheme for the data in order to achieve the target reliability level. Disk-adaptive redundancy systems require the flexibility of changing the redundancy schemes dynamically while still meeting the target reliability. Therefore, a cluster storage system that intends to support disk-adaptive redundancy should decouple the layer that sets the target reliability from the layer that chooses the desired redundancy scheme. Moreover, applications should be only allowed to specify the target reliability, and the cluster storage system should have the freedom to choose the required redundancy scheme.

6.3.2 Enhanced reliability monitoring mechanisms

Disk-adaptive redundancy described in this dissertation groups disks according to make/model in order to construct a bathtub curve. This grouping is static, and is inspired by prior literature [56, 73] that suggests disk vintage plays an important role in disk failure behavior. But, there could be other parameters that could additionally aid in grouping disks that fail similarly. For example, the disk manufacturing batch, manufacturing facility, firmware version etc. A disk-adaptive redundancy system should ideally look at all such groupings and monitor all of their bathtub curves simultaneously in order to be as safe as possible when making redundancy decisions.

6.3.3 Elevating the role of the redundancy management module

The redundancy management module in current storage clusters is primarily responsible for striping and failed data reconstruction. Its role becomes much more central, and arguably even more critical when supporting disk-adaptive redundancy. It needs to have the components that HeART and Pacemaker have, for instance:

- a change-point detector
- an anomaly detector
- a proactive transition initiator
- a redundancy planner
- a transition executor

In terms of the actions it supports, along with reconstruction and striping, the redundancy management module should keep track of:

- The AFR curves of all disks throughout their lifetimes grouped by different parameters as explained above.
- The different Rgroups and their composition.
- Scheduling the redundancy transition tasks along with the reconstruction tasks.
- Monitoring and building the AFR curve by keeping track of the canary disks.

6.3.4 Maintaining separation between file, block and storage layers

Current HDFS architecture maintains a separation of the file layer (which maintains the namespace of the file system), the block layer (which maintains the logical blocks and their locations on the different Datanodes and the Datanode layer (which maintains all the Datanodes and their vitals). This separation is critical for a seamless implementation of disk-adaptive redundancy in HDFS. In particular, as alluded to in Section 6.2.7, incorporating Rgroups by replicating the DatanodeManager allowed HDFS to observe disk-reliability-heterogeneity seamlessly without the clients requiring any knowledge that HDFS was supporting disk-adaptive redundancy, or changing in their file access interface in any way.

6.3.5 Incorporating disk-adaptive redundancy awareness in existing components

Several existing components of existing cluster storage systems can aid in efficiently performing disk-adaptive redundancy if they are made aware of disk-reliability-heterogeneity. This subsection describes some of these components in detail.

Making data placement aware of changing redundancy

Currently data placement algorithms are orthogonal to the redundancy decisions other than accounting for different fault domains for ensuring data safety. Disk-adaptive redundancy systems built using our design of Pacemaker equipped HDFS can work without requiring any changes to the core placement algorithm. But disk-adaptive redundancy can in fact be made more efficient by making the placement module aware of the redundancy management module. In particular, by placing related data in disks that are of a similar age, if (and when) data gets deleted or moved, disks of a similar age will have more space available in them with minimal data movement. This is advantageous for example in the case of decommissioning, which require disks of a similar age to be emptied together. Another example is in the case of Type 1 transitions; data is moved from the transitioning disk onto other disks of the same Rgroup. By having age-aware data movement, if data is moved from the older disks that are transitioning onto younger disks, a disk-adaptive redundancy system can avoid having to move the same data repeatedly.

Coupling scrubbing with redundancy transitions

HDDs suffer from adjacent track interference, where data written in one track can end up distorting the data on adjacent tracks. This problem is exacerbated in modern HDDs with higher capacity where tracks are packed even closer. Scrubbing is employed to prevent adjacent track interference from causing irrecoverable data loss. Scrubbing is the act of strengthening the signal-to-noise ratio by reading, checking (via checksum) and rewriting data to the same location. Disks in large scale storage clusters are scrubbed every fortnight on average [12].

Pacemaker's proactive-transition-initiator can schedule transitions well in advance of the age that the disks should transition by. Since scrubbing already performs the task of reading data and verifying its contents, if the proactive-transition-initiator has identified that certain disks need to transition to a new redundancy scheme, they can piggyback the reads required for the transitioning with the scrubbing cycle. This will drastically reduce the IO specifically issued for redundancy transitions and yet keep the data adequately reliable. Such an optimization cannot use scrubbing as it currently happens in existing systems, since scrubbing happens on a per-disk basis independent of other disks. For allowing redundancy transitions to utilize scrubbing, there will need to be new coordinated scrubbing algorithms that scrub related data that can be re-encoded.

Incorporating disk-adaptive redundancy into disk deployment

Disks are deployed either as trickle or step (described in Section 4.2.2) as observed in the clusters that are studied as a part of this research. Deployment strategies are currently unaware of disk-adaptive redundancy because today's cluster storage systems do not perform disk-adaptive redundancy. As per our conversations with system administrators, today's disk deployment decisions are largely driven by need (i.e. the capacity or spindle requirement of a cluster) or surplus procurement (i.e. more disks were purchased than were needed, which is driven by financial situations).

Disk deployment patterns can play a crucial role in the smooth functioning of a storage cluster that supports disk-adaptive redundancy as seen in Section 4.2.2. If there is intermingling of trickle-deployed and step-deployed disks of the same make/model, it prevents Pacemaker from using the more IO-efficient Type 2 on all disks of that make/model since all of its disks are not deployed in steps. In addition to whether to deploy disks as trickle or in steps, a disk-adaptive redundancy aware disk deployment strategy should also take into consideration the rate at which disks should be deployed. Spacing out the steps appropriately, whereas having a steady deployment for a trickle-deployed make/model are both decisions that can benefit disk-adaptive redundancy significantly. For example, Type 1 transition moves data from the transitioning disk to another in the same Rgroup. This transitioning method implicitly assumes that, in steady state, disks will always enter the Rgroup at the same rate that disks leave the Rgroup. Suppose a trickle-deployed make/model has an arbitrary deployment schedule, it can lead to Type 1 transitions not finding enough disk space to move data to, causing them to perform the expensive read–re-encode–write operation for performing the redundancy transition.

Chapter 7

Related work

We first talk about the broad category of related works which aim to optimize resources for more efficient redundancy management in distributed storage systems. Erasure coding itself is an optimization over replication [82, 109, 113] as it has a lower storage overhead than replication for the same amount of reliability as explained in Section 2.2. Even within erasure coding, there are works that reduce the cost of reconstruction via (1) reducing the amount of data transfer using techniques such as caching, batching, etc. [14, 23, 63], (2) reducing the amount of data accessed during reconstruction (e.g., [28, 43, 46, 70, 84, 108, 113, 115]) using techniques such as additional parities per stripe, or (3) designing new codes that contact more servers but download less data (e.g., [25, 39, 44, 68, 76, 78, 79, 80, 92, 93, 94, 99, 100, 106].

The closer related works can be classified into disk reliability studies that identify reliability heterogeneity, techniques to predict disk failures using reliability data, systems that reduce excess reliability and systems that automate redundancy scheme selection.

Various systems include support for multiple redundancy schemes, allowing different schemes to be used for different data [27, 33]. Thereska et al. [102] built a self-prediction capability in cluster storage systems to assist in making informed redundancy and data placement decisions by answering *what-if* questions. It differs from disk-adaptive redundancy in that it does not perform and adapt to online analysis of reliability characteristics, relying on pre-knowledge of reliability metrics. Keeton et al. [50] built an optimization framework that automatically provided data dependability solutions to protect against site-level disasters by using information like workload patterns, and cost of recovery. This work also assumes prior knowledge of failure rates. In [15], the authors discuss an inter-file chunk compression mechanism prior to performing redundancy, and choose different redundancy schemes for the different data chunks based on how much data is going to get lost in case a chunk is lost. disk-adaptive redundancy differs from such systems by assuming no prior knowledge of data or disk AFRs (i.e. monitored in-the-field), and focusing on efficiently adapting redundancy to different and time-varying AFRs of disks.

Numerous studies have been conducted to characterize disk failures [12, 26, 42, 47, 56, 72, 73, 85, 86, 87, 95]. Among the studies conducted on large production systems, Shah and Elerath [26, 95], Pinheiro et al. [73] and Ma et al. [56] independently verify that failure rates are highly correlated with disk manufacturers. These studies were conducted on the NetApp, Google and EMC disk fleets, respectively. Schroeder and Gibson also conducted a similar reliability study on disks from a high performance computing environment [85], not only highlighting reliability heterogeneity between disks deployed across systems, but also pointing out that disk datasheet reliability is very different from reliability observed in the field. Recently, Schroeder et al. [88] highlighted the heterogeneity in the reliability of different SSD technologies from four different manufacturers. Also, Schroeder et al. [87] reported heterogeneity of partial disk failures (sector errors) across makes/models for NetApp's disk fleet.

There have been numerous works that predict disk failures [40, 66, 98, 107, 118]. Among the more recent ones, Mahdisoltani et al. [57] use machine learning techniques to predict occurrence of partial disk errors using S.M.A.R.T. data. Anantharaman et al. [6] use random forests and recurrent neural networks to predict remaining useful life for HDDs. Both studies were performed on the Backblaze dataset.

Tempo [97] is a system that proactively creates replicas to ensure high durability in wide-area network distributed systems. It does this economically by allowing the user to specify a maximum maintenance bandwidth, and its design revolves around the efficient use of a distributed hash table. Carbonite [23] is a replica maintenance solution for distributed storage systems spread over the Internet, which makes efficient use of bandwidth in maintaining redundancy in the face of transient failures.

The Recovery Oriented Computing (ROC) project [71] suggests that faster recovery by reducing MTTR may result in requiring lower reliability than what is conventionally used. This in turn will reduce storage cost. Another method of reducing reliability requirement is by having a lower window of vulnerability, for example Byzantine Fault Tolerance [21] or by using innovative data placement techniques [53]. All these methods are static and do not capture, or react to the heterogeneity observed in large-scale cluster storage systems.

Reducing the impact of background IO, such as for data scrubbing, on foreground IO is a common research theme. [5, 8, 54, 55, 67, 89]. Pacemaker converts otherwise-urgent bursts of transition IO into proactive background IO, which could then benefit from these works.

While several works have considered the problem of designing erasure codes that allow transitions using less resources, existing solutions are limited to specific kinds of transitions and hence are not applicable in general. The case of adding parity chunks while keeping the number of data chunks fixed can be viewed [64, 75, 80] as the well-studied reconstruction problem, and hence the codes designed for optimal reconstruction (e.g., [25, 37, 69, 76, 80, 106]) would lead to improved resource usage for this case. Several works have studied the case where the number of data nodes increases while the number of parity nodes remains fixed [45, 74, 111, 116, 119]. In [112], the authors propose two erasure codes designed to undergo a specific transition in parameters.

In [60], the authors propose a general theoretical framework for studying codes that enable efficient transitions for general parameters, called "Convertible Codes". The authors derive lower bounds on the IO cost of transitions as well as describe optimal code constructions for certain specific parameters [60]. However, none of the existing practical code constructions are applicable for the diverse set of transitions needed for disk-adaptive redundancy in real-world storage clusters. There have been more recent theoretical works on convertible codes [59, 61], which seem promising for disk-adaptive redundancy systems. However, the role of recently proposed convertible codes in disk-adaptive redundancy systems remains to be explored.

Chapter 8

Conclusion and future directions

8.1 Conclusions

Disk-adaptive redundancy is the act of dynamically tailoring data redundancy to observed disk failure rates while always meeting a desired reliability target. Current cluster storage systems choose a redundancy scheme based on a static guesstimate of the disk's annualized failure rates (AFR). By assuming all disks fail similarly, the AFR guesstimate is usually a conservative upper bound on the fraction of disks that could fail based off of a combination of specification sheets, historical observations, literature and intuition. Unfortunately, this leads to redundancy schemes that are overly wasteful, but on occasion can also prove inadequate if there is a subset of disks that violates the AFR guesstimate assumptions due to environmental or workload factors, which cannot be determined apriori.

This dissertation takes a closer look at disk AFRs by observing over 5.3 million hard disk drives (HDDs) across three large production environments: Google, NetApp and Backblaze. The first conclusion that our work draws is that different disks fail differently. In particular, we group disks by make/model owing to the manufacturing differences that they are subjected to, and observe that disks from different makes/models have AFRs that differ from each other by over an order of magnitude despite being deployed in the same storage cluster. Additionally, by incorporating the well-studied AFR curve over a disk's lifetime (bathtub curve or hazard curve), this work discards the conventionally used single-number AFR representation. Instead it suggests a rich AFR representation that not only varies by disk make/model but also varies as a function of the disk's age.

Disk-adaptive redundancy utilizes the aforementioned rich AFR representation to design a redundancy orchestrator for cluster storage systems that dynamically tailors data redundancy to the observed AFR differences. A major redesign of a component as core as its redundancy management module (which has matured over the last several decades) requires the benefit of the proposed change to significantly outweigh the cost. In this research we carefully design systems: HeART and Pacemaker and demonstrate that even in storage clusters with several hundred thousand disks, disk-adaptive redundancy systems can provide approximately 20% space-savings. This translates to tens-of-thousands of fewer disks with minimal IO cost (less than 0.1% on average, and less than 5% in the peak) and with no compromise on reliability.

In addition to the substantial space-savings, disk-adaptive redundancy is safer. Today's static redundancy scheme selection process (explained in 2) places an inherent upper bound on the AFR that can be tolerated across all deployed disks. Specifically, the highest AFR tolerated by the most conservative scheme that still meets the target MTTDL acts as the upper bound of the AFR that can be tolerated in that cluster. If a disk make/model violates the AFR upper bound because of a manufacturing defect, or because of a bad firmware upgrade, it causes panic. According to the incidents narrated to us by storage administrators of large-scale cluster storage systems, today's state-of-the-art solution to minimize data loss in case of manufacturing-induced bugs or firmware-induced failures is quick human intervention. A disk-adaptive redundancy system is designed to react to increases in AFR by automatically increasing the redundancy, that too without any human intervention. This is not to say that any AFR rise is tolerable by disk-adaptive redundancy systems, because after some amount of rise (due to the inability to have infinitely many copies), the constraint-driven approach will fail at which point human intervention will be necessary, but this situation is unavoidable no matter how sophisticated the redundancy management techniques are.

One could argue that the constraint-driven system design is too human-dependent, and could lead to disastrous consequences if the constraints aren't correctly specified. While this could occur, we argue that the constraint-based design provides adequate transparency which is necessary for dealing with a component as core, and as important as redundancy management. Since data safety is directly dependent on redundancy, system designers and administrators tend to be paranoid about being able to achieve, and "see" that they can achieve the desired reliability. A constraint-based design provides a window through which the system's designers and administrators can observe the different rules governing the system. In order to prevent catastrophic situations, the constraint-specification for a disk-adaptive redundancy system could afford to have several levels of checks-and-balances since the constraints have to be specified ideally only once and tweaked very rarely.

Disk-adaptive redundancy provides a symbiotic solution for disk manufacturers and disk users. HDDs are incredibly complex hardware devices, and the disk manufacturing research and industry has seen unprecedented innovation to build today's HDD. This complexity makes it virtually impossible for a disk manufacturer to guarantee that there won't be unforeseen failures for a HDD in production. By having an adaptive solution that is designed to meet data reliability targets under changing AFRs, the disk manufacturers have a lower risk angry users complaining about data loss (and more seriously, a lower risk of litigation) due to a higher-than-expected rate of disk failures. On the flip side, the disk users can also heave a sigh of relief with the knowledge that if an unforeseen AFR rise occurs, that the system will react to it automatically to keep data safe. Additionally, it also creates an interesting economic incentive structure for manufacturing HDDs. Since a disk-adaptive redundancy system would require lower redundancy for disks having higher reliability, the reduced cost could be used as an incentive to achieve higher reliability; essentially disks could be priced based on the lowest reliability they can guarantee, while at the same time not facing the risk data loss in case this guarantee is violated.

Finally, we reflect on the impact of the software-only optimization provided by disk-adaptive redundancy in an era where innovation in hardware is leading the path to achieve lower storage cost. Data in large-scale storage clusters is growing at an alarming rate and will continue to do so with large migrations of businesses and data repositories to the cloud [91]. This puts serious space pressure on many (if not all) of the large-scale storage clusters. Furthermore, most of the data being stored is warm or cold data, which is accessed occasionally, but needs to be highly durable. Lowering the storage and energy costs of storing this data without compromising data reliability is one of the main motivations behind public clouds offering low-cost data archival solutions such as Amazon Glacier [1] and Google Cold Storage [36]. These offerings are driven by innovation in hardware via high-density storage devices such as shingled magnetic recording disks (SMR), heat-assisted magnetic recording disks (HAMR) and bit-patterned media recording disks (BPMR). More radical hardware inventions for solving the cold data storage problem (that are not yet commercially available) include projects such as Project Silica that aims to use glass as a high-density storage medium for cold data [7, 22, 81], and DNA storage [16], which aims to store data in synthesized DNA strands. All of these innovations require over a decade of research, with specialized machinery costing billions of dollars, as is evident through recently commercialized technologies such as SMR and HAMR. In contrast, disk-adaptive redundancy is a completely software driven solution for the aforementioned problem that provides space-savings in the same range as SMR disks ($\approx$20% fewer disks; tens-of-thousands of fewer storage devices per cluster). Moreover, through our exercise of incorporating Pacemaker in HDFS, we show that today's distributed storage systems can be easily modified to support disk-adaptive redundancy. We also provide recommendations for re-imagining existing components in order to build a distributed storage system that supports disk-adaptive redundancy out of the box. These recommendations are focused changes and do not require redesigning the entire distributed storage system from scratch. Finally, disk-adaptive redundancy is an optimization technique that is fundamentally applicable to all storage devices currently present, and those that will be invented in the future. Theoretically, it even supports redundancy performed on tiered storage clusters where different storage media are used to service different performance requirements, but the data on any of those tiers has to maintain a target reliability. This makes disk-adaptive redundancy a robust solution for a timely problem.

8.2 Future work

While this thesis has shed light on existing AFR heterogeneity, and how it can be exploited using to attain significant benefits, the exploration of disk-adaptive redundancy is not over by any means. In this section we outline a set of promising future directions that we believe will further enhance disk-adaptive redundancy and make it even more pervasive.

8.2.1 Scheduling background work better

Redundancy transitions can result in substantial IO. Pacemaker through its proactive-transition-initiator and transition-executor has shown ways in which the transition overload can be mitigated. In addition, there are several already existing IO intensive background tasks on which redundancy management tasks can be piggybacked in order to further minimize, or even eliminate the need of explicitly issuing IO for redundancy transitions. Examples of existing background tasks include scrubbing, load-balancing, decommissioning and file system level garbage collection such as segment cleaning for log-structured file systems. As explained in Section 6.3.5, it might require innovating algorithms for these tasks which allow redundancy management to be done along with existing background tasks. Research in this direction will allow for more efficient disk-adaptive redundancy systems.

8.2.2 Deeper understanding of disk failure rates

This thesis has thrown light on the advantages of treating AFR as a dynamically changing quantity as against the current norm of treating it as a static number. With data reliability at stake, and substantial space-savings possible, it is incumbent upon a disk-adaptive redundancy system to have a robust understanding of disk failure rates. In particular, a disk-adaptive redundancy system has to correctly group disks that fail similarly, and have an understanding of how the AFR changes over time. HeART and Pacemaker are built on the current knowledge of disk AFRs, which primarily consider age and make/model as the primary dimensions along with AFR is quantified. Anecdotal evidence and conversations with storage administrators are pointing to environmental metrics such as temperature and vibration, and usage based metrics such as IO workload, seeks, etc. as influential parameters that affect disk AFRs. Understanding effect of these metrics on AFR, along with formulating how these metrics can be combined in order to best group disks that fail similarly will help in extracting the most benefit, while exercising the safest approach for disk-adaptive redundancy.

8.2.3 Incorporating availability in disk-adaptive redundancy

Data is kept redundant for two reasons: durability and availability. This dissertation has explored disk-adaptive redundancy for durability in depth. The purpose of redundancy for availability is to ensure data access even when servers are inaccessible due to events such as software upgrades or network partitioning. The scheme selection process follows a constraint based approach in filtering out infeasible schemes that disks could transition to. In addition to the existing IO and reliability constraints, an availability-aware disk-adaptive redundancy system would also have an availability constraint for scheme selection. One could use different families of codes to achieve the same instead of just tuning the parameters of traditionally used Reed-Solomon codes for example Piggyback codes [80], Regenerating codes [76], Locally Reconstructable Codes [46] etc.

8.2.4 Adaptive redundancy is not restricted to HDDs

The concept of adaptive redundancy transcends HDDs. The obvious extension is to other storage devices such as solid state disks (SSD) and non-volatile memory (NVM). Schroeder et al. [88] recently showed that different Flash SSD makes/models exhibit substantial failure rate differences similar to HDDs. Modeling disk-adaptive redundancy for new device types comes with their own challenges. For example, SSDs have been shown to have a different bathtub curve shape compared to HDDs [62]. We cannot comment on the nature of the bathtub curve for NVMs, since they are still too young for us to know of how their AFR varies over their lifetime. Nevertheless, no matter how the AFR changes, it is highly likely that adaptive redundancy systems can help keep data safe on these devices and provide cost-effective redundancy.

Appendix A

Failure rate estimation details

This section describes how we calculate failure rates for each Dgroup based on the disks' age using empirical data.

In the storage device reliability literature, the failure rate over a period of time is typically expressed in terms of Annualized Failure Rate (AFR), and calculated as:

$$AFR\ (\%) = \frac{d}{E} \times 100, \tag{A.1}$$

where d is the number of observed disk failures, and E is the sum of the exposure time of each disk, measured in years. The exposure time of a disk is the amount of time it was on operation (i.e., deployed and had not failed nor been retired) during the period in consideration, and it is typically measured at the granularity of days.

If the time to failure is exponentially distributed, then Formula A.1 corresponds to the maximum likelihood estimate for the rate parameter of the exponential distribution. Due to the memoryless property of this distribution, such a formula would be appropriate only if we assume that failure rate is constant with respect to time or device age. Thus, Eq. A.1 is useful for estimating AFR over long and stable periods of time, but makes it hard to reason about changes in AFR over time. Therefore, in this work, we estimate AFR using the following approach.

Assume that the lifetime (time from deployment to failure) of each disk is an i.i.d. discrete random variable T with cumulative density function F and probability mass function f. The failure rate (also known as *hazard rate*) [103] of this distribution is given by:

$$h(t) = f(t)/(1 - F(t)). \tag{A.2}$$

The *cumulative hazard* defined as $H(t) = \sum_{i=0}^{t} h(i)$ is commonly estimated using the Nelson-Aalen estimator:

$$\hat{H}(t) = \sum_{i=0}^{t} \frac{d_i}{a_i} \qquad \text{for } t \in \{0, \ldots, m\}, \tag{A.3}$$

where d_i is the number of disks that failed during their i-th day, a_i is the number of disks that were in operation at the start of their i-th day, and m is the age in days of the oldest observed disk drive. An estimate for the failure rate can be obtained by applying the so-called ***kernel method*** [101]:

$$\hat{h}(t) = \sum_{i=0}^{m} \frac{d_i}{a_i} K(t-i), \qquad \text{for } t \in \{0, \dots, m\}, \tag{A.4}$$

where $K(\cdot)$ is a kernel function. Formula A.4 can be considered as a smoothing over the increments of Formula A.3. For our calculations, we utilized an Epanechnikov kernel [41] with a bandwidth of 30 days (the Epanechnikov kernel is frequently used in practice due to its good theoretical properties).

A big advantage of this approach is that it is ***nonparametric***, meaning that it does not assume that the lifetime T follows any particular distribution. This allows Pacemaker to adapt and work effectively with a wide arrange of storage devices with vastly different failure rate behaviors.

Bibliography

[1] Amazon. Amazon Glacier. https://aws.amazon.com/glacier, . 8.1

[2] Amazon. Amazon Simple Storage Service (S3). https://aws.amazon.com/s3, . 2.1

[3] Amazon. Kinesis. https://aws.amazon.com/kinesis, . 3.3.1

[4] Amazon. Robust Random Cut Forest. https://docs.aws.amazon.com/kinesisanalytics/latest/sqlref/sqlrf-random-cut-forest.html, . 3.3.1

[5] George Amvrosiadis, Angela Demke Brown, and Ashvin Goel. Opportunistic storage maintenance. In *ACM Symposium on Operating Systems Principles (SOSP)*, 2015. 7

[6] Preethi Anantharaman, Mu Qiao, and Divyesh Jadav. Large Scale Predictive Analytics for Hard Disk Remaining Useful Life Estimation. In *IEEE International Conference on Big Data*, 2018. 3.2.4, 7

[7] Patrick Anderson, Richard Black, Ausra Cerkauskaite, Andromachi Chatzieleftheriou, James Clegg, Chris Dainty, Raluca Diaconu, Rokas Drevinskas, Austin Donnelly, Alexander L Gaunt, et al. Glass: A new media for a new era? In *USENIX Workshop on Hot Topics in Storage and File Systems (HotStorage)*, 2018. 8.1

[8] Eitan Bachmat and Jiri Schindler. Analysis of methods for scheduling low priority disk drive tasks. In *ACM SIGMETRICS Performance Evaluation Review*, 2002. 7

[9] Backblaze. HDD SMART Stats. https://www.backblaze.com/blog/what-smart-stats-indicate-hard-drive-failures. 3.1.1

[10] Backblaze. Disk Reliability Dataset. https://www.backblaze.com/b2/hard-drive-test-data.html, 2013-2018. (document), 2.2, 3.1.1, 3.3

[11] Backblaze. Erasure coding used by Backblaze. https://www.backblaze.com/blog/reed-solomon/, 2013-2018. 2.2.2

[12] Lakshmi N Bairavasundaram, Garth R Goodson, Shankar Pasupathy, and Jiri Schindler. An analysis of latent sector errors in disk drives. In *ACM SIGMETRICS Performance Evaluation Review*, 2007. 3.1.1, 5.2.4, 5.4.3, 6.3.5, 7

[13] Shimrit Ben-Yair. Updating Google Photos storage policy to build for the future. https://blog.google/products/photos/storage-changes/, 2020. 1

[14] Ranjita Bhagwan, Kiran Tati, Yuchung Cheng, Stefan Savage, and Geoffrey M Voelker. Total recall: System support for automated availability management. In *USENIX Symposium on Networked Systems Design and Implementation (NSDI)*, 2004. 7

[15] Deepavali Bhagwat, Kristal Pollack, Darrell DE Long, Thomas Schwarz, Ethan L Miller, and J-F Pâris. Providing high reliability in a minimum redundancy archival storage system. In *IEEE International Symposium on Modeling, Analysis, and Simulation of Computer and Telecommunications Systems (MASCOTS)*, 2006. 7

[16] James Bornholt, Randolph Lopez, Douglas M Carmean, Luis Ceze, Georg Seelig, and Karin Strauss. A dna-based archival storage system. In *International Conference on Architectural Support for Programming Languages and Operating Systems (ASPLOS)*, 2016. 8.1

[17] Eric Brewer. Spinning Disks and Their Cloudy Future. `https://www.usenix.org/node/194391`, 2018. 1, 2.1.1

[18] Eric Brewer, Lawrence Ying, Lawrence Greenfield, Robert Cypher, and Theodore T'so. Disks for data centers. Technical report, Google, 2016. 1, 2.1.1

[19] Brad Calder, Ju Wang, Aaron Ogus, Niranjan Nilakantan, Arild Skjolsvold, Sam McKelvie, Yikang Xu, Shashwat Srivastav, Jiesheng Wu, Huseyin Simitci, et al. Windows azure storage: a highly available cloud storage service with strong consistency. In *ACM Symposium on Operating Systems Principles (SOSP)*, 2011. 2.1, 5.3.3

[20] Mingming Cao, Suparna Bhattacharya, and Ted Ts'o. Ext4: The next generation of ext2/3 filesystem. In *Linux Storage and Filesystem Workshop*, 2007. 6.1

[21] Miguel Castro and Barbara Liskov. Proactive recovery in a byzantine-fault-tolerant system. In *USENIX Symposium on Operating Systems Design and Implementation (OSDI)*, 2000. 7

[22] Andromachi Chatzieleftheriou, Ioan Stefanovici, Dushyanth Narayanan, Benn Thomsen, and Antony Rowstron. Could cloud storage be disrupted in the next decade? In *USENIX Workshop on Hot Topics in Storage and File Systems (HotStorage)*, 2020. 8.1

[23] Byung-Gon Chun, Frank Dabek, Andreas Haeberlen, Emil Sit, Hakim Weatherspoon, M Frans Kaashoek, John Kubiatowicz, and Robert Morris. Efficient Replica Maintenance for Distributed Storage Systems. In *USENIX Symposium on Networked Systems Design and Implementation (NSDI)*, 2006. 7

[24] Gerry Cole. Estimating drive reliability in desktop computers and consumer electronics systems. *Seagate Technology Paper TP*, 2000. 2.2.3, 3.1.1

[25] Alexandros G. Dimakis, Brighten Godfrey, Yunnan Wu, Martin J. Wainwright, and Kannan Ramchandran. Network coding for distributed storage systems. *IEEE Transactions on Information Theory*, 2010. 7

[26] Jon Elerath. Hard-disk drives: The good, the bad, and the ugly. *Communication of ACM*, 2009. 3.1.2, 7

[27] erasure code ceph documentation. Erasure code Ceph Documentation. `https://docs.ceph.com/docs/master/rados/operations/erasure-code/`, (accessed September 25, 2019). 7

[28] Kyumars Sheykh Esmaili, Lluis Pamies-Juarez, and Anwitaman Datta. Core: Cross-object redundancy for efficient data repair in storage systems. In *IEEE International Conference*

on Big Data, 2013. 7

[29] Facebook. HDFS RAID. `http://www.slideshare.net/ydn/hdfs-raid-facebook`. 1, 2.2.2

[30] Andrew Fikes. Storage architecture and challenges. *Talk at the Google Faculty Summit*, 2010. 2.2.2

[31] Daniel Ford, François Labelle, Florentina I Popovici, Murray Stokely, Van-Anh Truong, Luiz Barroso, Carrie Grimes, and Sean Quinlan. Availability in Globally Distributed Storage Systems. In *USENIX Symposium on Operating Systems Design and Implementation (OSDI)*, 2010. 1, 2.2.2, 2.2.3, 3, 3.1.3, 3.3.2, 5.3.3, 5.4

[32] Apache Software Foundation. HDFS Erasure Coding Phase II – EC with contiguous layout. `https://issues.apache.org/jira/browse/HDFS-8030`, 2016 (accessed November 5, 2020). 6.2.3

[33] Apache Software Foundation. HDFS Erasure Coding. `https://hadoop.apache.org/docs/r3.0.0/hadoop-project-dist/hadoop-hdfs/HDFSErasureCoding.html`, 2017 (accessed November 5, 2020). 1, 5.3.3, 7

[34] S. Ghemawat, H. Gobioff, and S.T. Leung. The Google file system. In *ACM SIGOPS Operating Systems Review*, 2003. 1, 2.1, 2.1.2, 2.2, 6.1

[35] Garth Gibson, Gary Grider, Andree Jacobson, and Wyatt Lloyd. Probe: A thousand-node experimental cluster for computer systems research. *USENIX; login*, 2013. 6.2.6

[36] Google. Google Cold Storage. `https://cloud.google.com/storage/archival`. 8.1

[37] Parikshit Gopalan, Cheng Huang, Huseyin Simitci, and Sergey Yekhanin. On the locality of codeword symbols. *IEEE Transactions on Information Theory*, 2012. 7

[38] Rong Gu, Qianhao Dong, Haoyuan Li, Joseph Gonzalez, Zhao Zhang, Shuai Wang, Yihua Huang, Scott Shenker, Ion Stoica, and Patrick PC Lee. DFS-PERF: A scalable and unified benchmarking framework for distributed file systems. *EECS Dept., Univ. California, Berkeley, Berkeley, CA, USA, Tech. Rep. UCB/EECS-2016-133*, 2016. 6.2.6

[39] Venkatesan Guruswami, Satyanarayana V Lokam, and Sai Vikneshwar Mani Jayaraman. -msr codes: Contacting fewer code blocks for exact repair. *IEEE Transactions on Information Theory*, 2020. 7

[40] Greg Hamerly, Charles Elkan, et al. Bayesian approaches to failure prediction for disk drives. In *International Conference on Machine Learning (ICML)*, 2001. 7

[41] Trevor Hastie, Robert Tibshirani, and Jerome Friedman. Kernel smoothing methods. In *The elements of statistical learning*. Springer, 2009. 2, A

[42] Eric Heien, Derrick Kondo, Ana Gainaru, Dan LaPine, Bill Kramer, and Franck Cappello. Modeling and tolerating heterogeneous failures in large parallel systems. In *ACM / IEEE High Performance Computing Networking, Storage and Analysis (SC)*, 2011. 7

[43] Yuchong Hu, Henry CH Chen, Patrick PC Lee, and Yang Tang. Nccloud: applying network coding for the storage repair in a cloud-of-clouds. In *USENIX File and Storage Technologies (FAST)*, 2012. 7

[44] Yuchong Hu, Patrick PC Lee, and Xiaoyang Zhang. Double regenerating codes for hierarchical data centers. In *IEEE International Symposium on Information Theory (ISIT)*, 2016. 7

[45] Yuchong Hu, Xiaoyang Zhang, Patrick P. C. Lee, and Pan Zhou. Generalized optimal storage scaling via network coding. In *IEEE International Symposium on Information Theory (ISIT)*, 2018. 7

[46] Cheng Huang, Huseyin Simitci, Yikang Xu, Aaron Ogus, Brad Calder, Parikshit Gopalan, Jin Li, Sergey Yekhanin, et al. Erasure Coding in Windows Azure Storage. In *USENIX Annual Technical Conference (ATC)*, 2012. 1, 2.2, 3.1.3, 7, 8.2.3

[47] Weihang Jiang, Chongfeng Hu, Yuanyuan Zhou, and Arkady Kanevsky. Are disks the dominant contributor for storage failures?: A comprehensive study of storage subsystem failure characteristics. *ACM Transactions on Storage (TOS)*, 2008. 7

[48] Saurabh Kadekodi, K V Rashmi, and Gregory R Ganger. Cluster storage systems gotta have HeART: improving storage efficiency by exploiting disk-reliability heterogeneity. In *USENIX File and Storage Technologies (FAST)*, 2019. 1, 1, 5.2.3, 5.4.2

[49] Saurabh Kadekodi, Francisco Maturana, Suhas Jayaram Subramanya, Juncheng Yang, KV Rashmi, and Gregory R Ganger. {PACEMAKER}: Avoiding heart attacks in storage clusters with disk-adaptive redundancy. In *USENIX Symposium on Operating Systems Design and Implementation (OSDI)*, 2020. 1

[50] Kimberly Keeton, Cipriano A Santos, Dirk Beyer, Jeffrey S Chase, John Wilkes, et al. Designing for disasters. In *USENIX File and Storage Technologies (FAST)*, 2004. 7

[51] Larry Lancaster and Alan Rowe. Measuring real-world data availability. 2001. 4.1

[52] Sergey Legtchenko, Hugh Williams, Kaveh Razavi, Austin Donnelly, Richard Black, Andrew Douglas, Nathanaël Cheriere, Daniel Fryer, Kai Mast, Angela Demke Brown, et al. Understanding rack-scale disaggregated storage. In *USENIX Workshop on Hot Topics in Storage and File Systems (HotStorage)*, 2017. 2.1

[53] Witold Litwin and Thomas Schwarz. LH* RS: A high-availability scalable distributed data structure using Reed Solomon codes. In *ACM International Conference on Management of Data (SIGMOD)*, 2000. 7

[54] Christopher R Lumb, Jiri Schindler, Gregory R Ganger, David F Nagle, and Erik Riedel. Towards higher disk head utilization: extracting free bandwidth from busy disk drives. In *USENIX Symposium on Operating Systems Design and Implementation (OSDI)*, 2000. 7

[55] Christopher R Lumb, Jiri Schindler, Gregory R Ganger, et al. Freeblock scheduling outside of disk firmware. In *USENIX File and Storage Technologies (FAST)*, 2002. 7

[56] Ao Ma, Rachel Traylor, Fred Douglis, Mark Chamness, Guanlin Lu, Darren Sawyer, Surendar Chandra, and Windsor Hsu. RAIDShield: characterizing, monitoring, and proactively protecting against disk failures. *ACM Transactions on Storage (TOS)*, 2015. 1, 3.1.1, 3.1.2, 3.2.4, 6.3.2, 7

[57] Farzaneh Mahdisoltani, Ioan Stefanovici, and Bianca Schroeder. Proactive error prediction to improve storage system reliability. In *USENIX Annual Technical Conference (ATC)*,

2017. 3.1.2, 3.2.4, 7

[58] Avantika Mathur, Mingming Cao, Suparna Bhattacharya, Andreas Dilger, Alex Tomas, and Laurent Vivier. The new ext4 filesystem: current status and future plans. In *Linux Symposium*, 2007. 6.1

[59] Francisco Maturana and K. V. Rashmi. Bandwidth cost of code conversions in distributed storage: Fundamental limits and optimal constructions. *arXiv preprint arXiv:2008.12707*, 2020. 7

[60] Francisco Maturana and K. V. Rashmi. Convertible codes: new class of codes for efficient conversion of coded data in distributed storage. In *Innovations in Theoretical Computer Science Conference, (ITCS)*, 2020. 7

[61] Francisco Maturana, V. S. Chaitanya Mukka, and K. V. Rashmi. Access-optimal linear MDS convertible codes for all parameters. In *IEEE International Symposium on Information Theory (ISIT)*, 2020. 7

[62] Justin Meza, Qiang Wu, Sanjev Kumar, and Onur Mutlu. A large-scale study of flash memory failures in the field. *ACM SIGMETRICS Performance Evaluation Review*, 2015. 8.2.4

[63] James W Mickens and Brian D Noble. Exploiting availability prediction in distributed systems. In *USENIX Symposium on Networked Systems Design and Implementation (NSDI)*, 2006. 7

[64] Sara Mousavi, Tianli Zhou, and Chao Tian. Delayed parity generation in MDS storage codes. In *IEEE International Symposium on Information Theory (ISIT)*, 2018. 7

[65] Subramanian Muralidhar, Wyatt Lloyd, Sabyasachi Roy, Cory Hill, Ernest Lin, Weiwen Liu, Satadru Pan, Shiva Shankar, Viswanath Sivakumar, Linpeng Tang, et al. f4: Facebook's warm BLOB storage system. In *USENIX Symposium on Operating Systems Design and Implementation (OSDI)*, 2014. 5.3.3

[66] Joseph F Murray, Gordon F Hughes, and Kenneth Kreutz-Delgado. Hard drive failure prediction using non-parametric statistical methods. In *Springer Artificial Neural Networks and Neural Information Processing (ICANN/CONIP*, 2003. 7

[67] Alina Oprea and Ari Juels. A Clean-Slate Look at Disk Scrubbing. In *USENIX File and Storage Technologies (FAST)*, 2010. 5.2.4, 7

[68] D Papailiopoulos, A Dimakis, and V Cadambe. Repair optimal erasure codes through Hadamard designs. *IEEE Transactions on Information Theory*, 2013. 7

[69] Dimitris S. Papailiopoulos and Alexandros G. Dimakis. Locally repairable codes. *IEEE Transactions on Information Theory*, 2014. 7

[70] D.S. Papailiopoulos and A.G. Dimakis. Locally repairable codes. In *IEEE International Symposium on Information Theory (ISIT)*, 2012. 7

[71] David Patterson, Aaron Brown, Pete Broadwell, George Candea, Mike Chen, James Cutler, Patricia Enriquez, Armando Fox, Emre Kiciman, Matthew Merzbacher, et al. Recovery-oriented computing (roc): Motivation, definition, techniques, and case studies. Technical report, Technical Report UCB//CSD-02-1175, UC Berkeley Computer Science,

2002. 2.1.2, 7

[72] David A Patterson, Garth Gibson, and Randy H Katz. A case for redundant arrays of inexpensive disks (RAID). In *ACM International Conference on Management of Data (SIGMOD)*, 1988. 1, 2.2.3, 7

[73] Eduardo Pinheiro, Wolf-Dietrich Weber, and Luiz André Barroso. Failure Trends in a Large Disk Drive Population. In *USENIX File and Storage Technologies (FAST)*, 2007. 1, 2.2, 3.1.1, 3.1.2, 3.2.4, 6.3.2, 7

[74] Brijesh Kumar Rai, Vommi Dhoorjati, Lokesh Saini, and Amit K. Jha. On adaptive distributed storage systems. In *IEEE International Symposium on Information Theory (ISIT)*, 2015. 7

[75] K. V. Rashmi, Nihar B. Shah, and P. Vijay Kumar. Enabling node repair in any erasure code for distributed storage. In *IEEE International Symposium on Information Theory (ISIT)*, 2011. 7

[76] K. V. Rashmi, Nihar B. Shah, and P. Vijay Kumar. Optimal exact-regenerating codes for distributed storage at the MSR and MBR points via a product-matrix construction. *IEEE Transactions on Information Theory*, 2011. 7, 8.2.3

[77] K V Rashmi, Nihar B Shah, Dikang Gu, Hairong Kuang, Dhruba Borthakur, and Kannan Ramchandran. A Solution to the Network Challenges of Data Recovery in Erasure-coded Distributed Storage Systems: A Study on the Facebook Warehouse Cluster. In *USENIX Workshop on Hot Topics in Storage and File Systems (HotStorage)*, 2013. 1, 2.2, 2.2.2, 2.2.3, 3, 3.1.3, 3.2.3, 3.3.2

[78] K V Rashmi, Nihar B Shah, Dikang Gu, Hairong Kuang, Dhruba Borthakur, and Kannan Ramchandran. A hitchhiker's guide to fast and efficient data reconstruction in erasure-coded data centers. *ACM Special Interest Group on Data Communication (SIGCOMM)*, 2014. 2.2, 2.2.2, 2.2.3, 3, 3.1.3, 3.2.3, 3.3.2, 7

[79] K V Rashmi, Preetum Nakkiran, Jingyan Wang, Nihar B Shah, and Kannan Ramchandran. Having Your Cake and Eating It Too: Jointly Optimal Erasure Codes for I/O, Storage, and Network-bandwidth. In *USENIX File and Storage Technologies (FAST)*, 2015. 7

[80] KV Rashmi, Nihar B Shah, and Kannan Ramchandran. A piggybacking design framework for read-and download-efficient distributed storage codes. *IEEE Transactions on Information Theory*, 2017. 7, 8.2.3

[81] Microsoft Research. Project Silica. `https://www.microsoft.com/en-us/research/project/project-silica`. 8.1

[82] Rodrigo Rodrigues and Barbara Liskov. High availability in dhts: Erasure coding vs. replication. In *Springer International Workshop on Peer-to-Peer Systems (IPTPS)*, 2005. 7

[83] Yasushi Saito, Svend Frølund, Alistair Veitch, Arif Merchant, and Susan Spence. FAB: building distributed enterprise disk arrays from commodity components. In *International Conference on Architectural Support for Programming Languages and Operating Systems (ASPLOS)*, 2004. 3.1.3

[84] Maheswaran Sathiamoorthy, Megasthenis Asteris, Dimitris Papailiopoulos, Alexandros G Dimakis, Ramkumar Vadali, Scott Chen, and Dhruba Borthakur. Xoring elephants: Novel erasure codes for big data. In *International Conference on Very Large Data Bases (VLDB)*, 2013. 2.2, 2.2.2, 3, 3.1.3, 3.3.2, 7

[85] Bianca Schroeder and Garth A Gibson. Disk failures in the real world: What does an MTTF of 1,000,000 hours mean to you? In *USENIX File and Storage Technologies (FAST)*, 2007. 2.1.2, 2.4, 7

[86] Bianca Schroeder and Garth A Gibson. Understanding failures in petascale computers. In *Journal of Physics: Conference Series*. IOP Publishing, 2007. 7

[87] Bianca Schroeder, Sotirios Damouras, and Phillipa Gill. Understanding latent sector errors and how to protect against them. *ACM Transactions on Storage (TOS)*, 2010. 3.1.1, 5.2.4, 7

[88] Bianca Schroeder, Raghav Lagisetty, and Arif Merchant. Flash Reliability in Production: The Expected and the Unexpected. In *USENIX File and Storage Technologies (FAST)*, 2016. 1, 7, 8.2.4

[89] Thomas JE Schwarz, Qin Xin, Ethan L Miller, Darrell DE Long, Andy Hospodor, and Spencer Ng. Disk scrubbing in large archival storage systems. In *IEEE International Symposium on Modeling, Analysis, and Simulation of Computer and Telecommunications Systems (MASCOTS)*, 2004. 7

[90] Seagate. Hard disk drive reliability and MTBF / AFR. `http://knowledge.seagate.com/articles/en_US/FAQ/174791en`. 3.1.1

[91] Seagate. The Digitization of the World From Edge to Core. `https://www.seagate.com/files/www-content/our-story/trends/files/idc-seagate-dataage-whitepaper.pdf`, 2018. 1, 8.1

[92] Nihar B Shah. On minimizing data-read and download for storage-node recovery. *IEEE Communications Letters*, 2013. 7

[93] Nihar B Shah, K Vinayak Rashmi, P Vijay Kumar, and Kannan Ramchandran. Distributed storage codes with repair-by-transfer and nonachievability of interior points on the storage-bandwidth tradeoff. *IEEE Transactions on Information Theory*, 2011. 7

[94] Nihar B Shah, KV Rashmi, P Vijay Kumar, and Kannan Ramchandran. Interference alignment in regenerating codes for distributed storage: Necessity and code constructions. *IEEE Transactions on Information Theory*, 2011. 7

[95] Sandeep Shah and Jon G Elerath. Disk drive vintage and its effect on reliability. In *IEEE Reliability and Maintenance Symposium (RAMS)*, 2004. 7

[96] Konstantin Shvachko, Hairong Kuang, Sanjay Radia, Robert Chansler, et al. The hadoop distributed file system. In *IEEE/NASA Goddard Conference on Mass Storage Systems and Technologies (MSST)*, 2010. 1, 2.1.2, 6, 6.1

[97] Emil Sit, Andreas Haeberlen, Frank Dabek, Byung-Gon Chun, Hakim Weatherspoon, Robert Tappan Morris, M Frans Kaashoek, and John Kubiatowicz. Proactive Replication for Data Durability. In *Springer International Workshop on Peer-to-Peer Systems (IPTPS)*,

2006. 7

[98] Brian D Strom, SungChang Lee, George W Tyndall, and Andrei Khurshudov. Hard disk drive reliability modeling and failure prediction. *IEEE Transactions on Magnetics*, 2007. 7

[99] Itzhak Tamo, Zhiying Wang, and Jehoshua Bruck. Zigzag codes: MDS array codes with optimal rebuilding. *IEEE Transactions on Information Theory*, 2013. 7

[100] Itzhak Tamo, Zhiying Wang, and Jehoshua Bruck. Access versus bandwidth in codes for storage. *IEEE Transactions on Information Theory*, 2014. 7

[101] Martin A. Tanner and Wing Hung Wong. The estimation of the hazard function from randomly censored data by the kernel method. *Annals of Statistics*, 1983. A

[102] Eno Thereska, Michael Abd-El-Malek, Jay J Wylie, Dushyanth Narayanan, and Gregory R Ganger. Informed data distribution selection in a self-predicting storage system. In *IEEE International Conference on Autonomic Computing (ICAC)*, 2006. 7

[103] Kishor Trivedi. *Probability and Statistics with Reliability, Queueing, and Computer Science Applications.* Wiley, 2001. 1, 2.2.3, A

[104] Charles Truong, Laurent Oudre, and Nicolas Vayatis. A review of change point detection methods. In *arXiv:1801.00718v1 [cs.CE]*, 2018. 3.3.1

[105] Charles Truong, Laurent Oudre, and Nicolas Vayatis. ruptures: change point detection in python. In *arXiv:1801.00826v1 [cs.CE]*, 2018. 3.3.1

[106] Myna Vajha, Vinayak Ramkumar, Bhagyashree Puranik, Ganesh Kini, Elita Lobo, Birenjith Sasidharan, P Vijay Kumar, Alexandar Barg, Min Ye, Srinivasan Narayanamurthy, et al. Clay codes: Moulding {MDS} codes to yield an {MSR} code. In *USENIX File and Storage Technologies (FAST)*, 2018. 7

[107] Yu Wang, Eden WM Ma, Tommy WS Chow, and Kwok-Leung Tsui. A two-step parametric method for failure prediction in hard disk drives. *IEEE Transactions on industrial informatics*, 2014. 7

[108] Zhiying Wang, Alexandros G Dimakis, and Jehoshua Bruck. Rebuilding for array codes in distributed storage systems. In *IEEE Globecom Workshops*, 2010. 7

[109] Hakim Weatherspoon and John D Kubiatowicz. Erasure coding vs. replication: A quantitative comparison. In *Springer International Workshop on Peer-to-Peer Systems (IPTPS)*, 2002. 7

[110] Sage A Weil, Scott A Brandt, Ethan L Miller, Darrell DE Long, and Carlos Maltzahn. Ceph: A scalable, high-performance distributed file system. In *USENIX Symposium on Operating Systems Design and Implementation (OSDI)*, 2006. 1

[111] Si Wu, Yinlong Xu, Yongkun Li, and Zhijia Yang. I/O-efficient scaling schemes for distributed storage systems with CRS codes. *IEEE Transactions on Parallel and Distributed Systems*, 2016. 7

[112] Mingyuan Xia, Mohit Saxena, Mario Blaum, and David A. Pease. A tale of two erasure codes in HDFS. In *USENIX File and Storage Technologies (FAST)*, 2015. 7

[113] Liping Xiang, Yinlong Xu, John CS Lui, and Qian Chang. Optimal recovery of single disk failure in rdp code storage systems. *ACM SIGMETRICS Performance Evaluation Review*, 2010. 7

[114] Yong Xu, Kaixin Sui, Randolph Yao, Hongyu Zhang, Qingwei Lin, Yingnong Dang, Peng Li, Keceng Jiang, Wenchi Zhang, Jian-Guang Lou, et al. Improving service availability of cloud systems by predicting disk error. In *USENIX Annual Technical Conference (ATC)*, 2018. 3.2.4

[115] Liuqing Ye, Dan Feng, Yuchong Hu, Xueliang Wei, and Yuzhuo Zhang. STC: Sub-packetization tunable codes for fast recovery. *Journal of Systems Architecture*, 2020. 7

[116] Xiaoyang Zhang, Yuchong Hu, Patrick P. C. Lee, and Pan Zhou. Toward optimal storage scaling via network coding: from theory to practice. In *IEEE Conference on Computer Communications, (INFOCOM)*, 2018. 7

[117] Zhe Zhang, Andrew Wang, Kai Zheng, G Uma Maheswara, and B Vinayakumar. Introduction to hdfs erasure coding in apache hadoop. *blog.cloudera.com*, 2015.

[118] Ying Zhao, Xiang Liu, Siqing Gan, and Weimin Zheng. Predicting disk failures with HMM-and HSMM-based approaches. In *Springer Industrial Conference on Data Mining (ICDM)*, 2010. 7

[119] Weimin Zheng and Guangyan Zhang. Fastscale: accelerate RAID scaling by minimizing data migration. In *USENIX File and Storage Technologies (FAST)*, 2011. 7

[120] Bingpeng Zhu, Gang Wang, Xiaoguang Liu, Dianming Hu, Sheng Lin, and Jingwei Ma. Proactive drive failure prediction for large scale storage systems. In *IEEE/NASA Goddard Conference on Mass Storage Systems and Technologies (MSST)*, 2013. 3.2.4